NOAA Technical Memorandum ERL PMEL-75

A NUMERICAL MODEL FOR THE COMPUTATION OF RADIANCE DISTRIBUTIONS IN NATURAL WATERS WITH WIND-ROUGHENED SURFACES

Curtis D. Mobley
Rudolph W. Preisendorfer

Pacific Marine Environmental Laboratory
Seattle, Washington
January 1988

noaa NATIONAL OCEANIC AND ATMOSPHERIC ADMINISTRATION / Environmental Research Laboratories

NOAA Technical Memorandum ERL PMEL-75

A NUMERICAL MODEL FOR THE COMPUTATION OF RADIANCE DISTRIBUTIONS IN NATURAL WATERS WITH WIND-ROUGHENED SURFACES

Curtis D. Mobley

Joint Institute for Study of Atmosphere and Ocean
University of Washington, AK-40
Seattle, WA 98195

Rudolph W. Preisendorfer

Pacific Marine Environmental Laboratory
Seattle, Washington
January 1988

UNITED STATES DEPARTMENT OF COMMERCE

C.William Verity
Secretary

NATIONAL OCEANIC AND ATMOSPHERIC ADMINISTRATION

Environmental Research Laboratories

Vernon E. Derr,
Director

NOTICE

Mention of a commercial company or product does not constitute an endorsement by NOAA Environmental Research Laboratories. Use for publicity or advertising purposes of information from this publication concerning proprietary products or the tests of such products is not authorized.

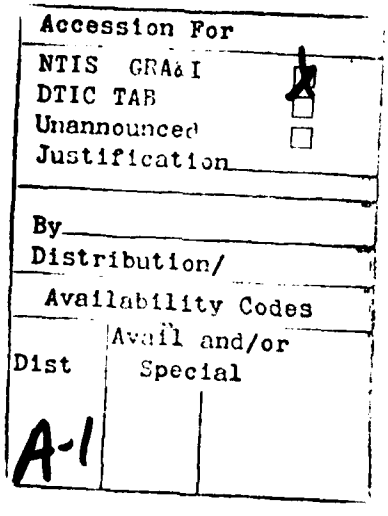

Contribution No. 813 from NOAA/Pacific Marine Environmental Laboratory
Contribution No. 40 from Joint Institute for the Study of the Atmosphere and Ocean

For sale by the National Technical Information Service, 5285 Port Royal Road
Springfield, VA 22161

CONTENTS

LIST OF FIGURES

LIST OF TABLES

A NUMERICAL MODEL FOR THE COMPUTATION OF RADIANCE DISTRIBUTIONS IN NATURAL WATERS WITH WIND-ROUGHENED SURFACES

Curtis D. Mobley
Rudolph W. Preisendorfer

ABSTRACT. This report is a repository of the details of derivation of a numerical procedure to determine the unpolarized radiance distribution as a function of depth, direction, and wavelength, in a natural hydrosol such as a lake or sea. The input to the model consists of (i) the incidence radiance distribution at the air-water surface, (ii) the state of randomness of the air-water surface as a function of wind speed, (iii) the volume scattering and volume attenuation functions of the medium as a function of depth and wavelength, and (iv) the type of bottom boundary.

The fundamental mathematical operation in the development of the numerical model is the discretization over direction space of the continuous radiative transfer equation. The directionally discretized radiances, called quad-averaged radiances, are the averages over a finite set of solid angles of the directionally continuous radiance. The quad-averaged equations are azimuthally decomposed using standard Fourier analysis to obtain equations for the quad-averaged radiance amplitudes. These amplitude equations are then developed in terms of reflectance and transmittance functions. The reflectances and transmittances are continuous functions of depth and are governed by a set of Riccati equations which is easily integrated. The depth-dependent, quad-averaged radiances are assembled from the solution reflectances and transmittances of the water body, in combination with the boundary conditions.

The model has an expandable library of derived quantities that are of use in various applications of optics to natural waters, such as marine biological studies, underwater visual search tasks, remote sensing, and climatology.

1. INTRODUCTION

This report presents a numerical technique for computing the radiance distribution in a natural hydrosol, given the optical properties of the hydrosol itself and appropriate boundary conditions at the surface and bottom of the water body, along with the radiance incident on the water surface. General knowledge of the radiance distribution in a natural hydrosol is a prerequisite for the solution of more specific problems, such as those

occurring in studies of photosynthesis, underwater visibility, remote sensing of the ocean from aircraft or satellites, heating of the upper layers of the medium, and climatology. Our goal is thus the development of a model of some generality and relatively high computational efficiency, rather than the solution of any particular problem. An analogous goal would be the formulation of a numerical model for the general circulation of the atmosphere or oceans. Such a model, once available, can be used as a tool for the solution of many specific problems. Some of the immediate applications of the present model are to study various hypotheses about the behavior of the radiance distribution with depth, direction, and wavelength, and to establish the ranges of validity of simpler light field models that are potentially useful in marine biological studies and in underwater visual search tasks.

Water bodies such as oceans and lakes are well approximated locally as plane parallel media for the purpose of determining the light field within these natural hydrosols. Thus we consider a water body which is laterally homogeneous, although its optical properties may vary arbitrarily with depth. The wind-blown water surface forms the upper boundary of the hydrosol, and a plane of specified radiance reflectance forms the lower boundary. The upper boundary is statistically homogeneous but exhibits a directional anisotropy due to the presence of wind-generated waves. The lower boundary, for example a sandy lake bottom, is less prone to anisotropy. Natural waters are directionally isotropic with respect to the scattering properties of the medium, although the scattering functions may be far from spherical in shape and the optical properties of the water may vary markedly with depth. Moreover, the dominant light sources in the euphotic zones and mixed layers of natural hydrosols are the sun and diffuse sky light, rather than internal sources such as fluorescing chlorophyll in phytoplankton.

a. Assumptions of the Natural Hydrosol Model (NHM)

With these comments in mind, we define in this work a *Natural Hydrosol Model* (NHM) by adopting the following assumptions:

(1) The water body is a plane-parallel medium which

(a) has no internal light sources, and is non-fluorescent

(b) is directionally isotropic,

(c) is laterally homogeneous, but is inhomogeneous with depth.

(2) The upper boundary is the random air-water interface, which is wind-ruffled, laterally homogeneous, and azimuthally anisotropic.

(3) The lower boundary is a surface whose reflectance is azimuthally isotropic. This boundary may be either the physical bottom of an optically shallow water body, or a plane in an optically infinitely deep water body, below which the water is homogeneous with depth.

(4) There is radiant flux incident downward on the upper boundary. There is no radiant flux incident upward on the lower boundary.

(5) The radiance field is monochromatic and unpolarized.

The exact meaning of these assumptions and their mathematical consequences will be clarified in the discussions below.

Section 2 presents the integrodifferential equation which governs the light field under the assumptions of the Natural Hydrosol Model. In §3 we present a technique for the directional discretization of the continuous equations of §2, and this is followed by a review of the Fourier analysis of discrete functions in §4. These analysis formulas are then applied in §5 to the directionally discrete equations of §3, in order to obtain a discrete spectral model. These spectral equations are algebraically reformulated in §6 in order to derive equations which are suitable for numerical solution on a

digital computer. In §7 we show how to solve the model equations for the spectral amplitudes, and then how to reconstitute the desired radiance distribution from those spectral amplitudes. Section 8 discusses the computation of various derived quantities from the computed radiances and the consequences for simple models of the light field in natural hydrosols. Sections 9-11 discuss certain preliminary calculations which are needed in order to set up the desired boundary conditions and inherent optical properties as input to the Natural Hydrosol Model. We close with a section on computer considerations, such as array storage.

Acknowledgments. Author C.D.M. was supported in part by the Oceanic Biology Program of the Office of Naval Research (contract no. N00014-87-K-0525) and in part by the TOGA (Tropical Ocean, Global Atmosphere) Council. Ryan Whitney performed the word processing and Joy Register drew the diagrams.

2. GOVERNING EQUATIONS

In this section we present the equations which govern the light field of the Natural Hydrosol Model. Our starting point is the radiative transfer equation plus equations which describe how light is reflected by and transmitted through the boundaries of the water body. Figure 1 establishes a coordinate system for the expression of these equations.

According to 1c of the Natural Hydrosol Model assumptions, the water body can be represented by extensive horizontal layers of scattering-absorbing material parallel to the upper and lower boundary surfaces. As shown in Fig. 1, a *wind-oriented* spherical coordinate system (y,θ,ϕ) is defined so that

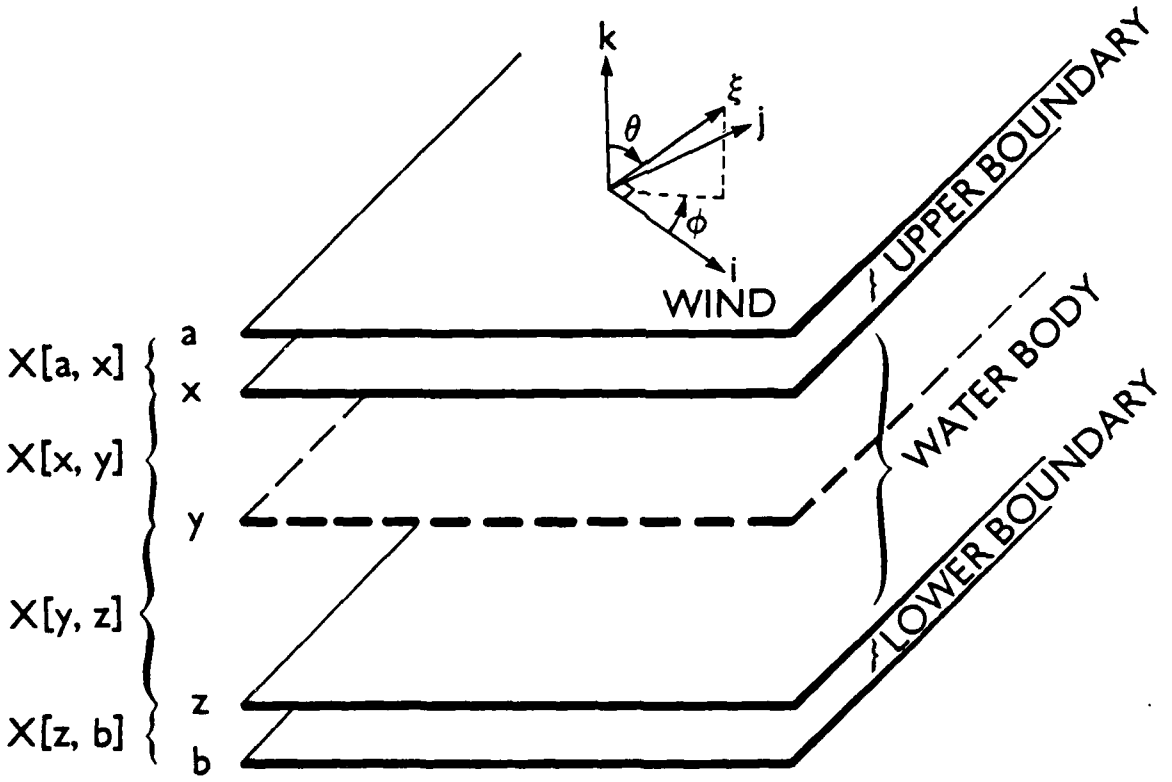

Figure 1.--The geometric setting of the Natural Hydrosol Model and definition of the wind-based coordinate system. The $\underline{i}$ vector is along the wind direction. The $\underline{i},\underline{j},\underline{k}$ vectors form a right-handed system with $\underline{k}$ positive upward.

the downwind direction at the water surface has an azimuthal angle of $\phi \equiv 0$. The azimuthal angle ϕ, $0 \leq \phi < 2\pi$, is measured positive counterclockwise from the downwind direction when looking downward on the water surface from above. The polar (or zenith) angle θ, $0 \leq \theta \leq \pi$, is measured from the unit outward normal $\underline{k}$ (the zenith direction). The normal $\underline{k}$ is perpendicular to the bounding planes of the water body and defines the upward direction. Since the hydrosol is laterally homogeneous, the depth coordinate y is the only relevant spatial coordinate. We take the optical depth y to be a running depth variable, $a \leq y \leq b$, measured positive downward from the upper surface, located at level a, to the lower boundary surface at level b.

We adopt the convention that the two depths a and x seen in Fig. 1 define a region $a \leq y \leq x$, which we call the *upper boundary*. In most applications of the model, this region can be considered infinitesimal in thickness, consisting only of the air-water surface. However, there are situations in which the upper boundary may actually be a composite medium consisting of the infinitesimal air-water surface plus a slab of finite thickness representing, for example, an oil film or a surface layer of relatively great biological activity just below the surface. In either instance the notation is such that "a" denotes a point *in the air* and just above the water surface, while "x" denotes a point *in the water* below the surface. In our basic computations, the upper boundary is always considered to be an infinitesimally thin layer, which merely reflects or transmits light without absorption; in such a case the boundary itself has no internal structure. The lower boundary is defined as a slab of depths y, $z \leq y \leq b$, where b-z may be infinitesimal, finite, or infinite. In any of these cases "z" denotes a depth in the water just above the lower boundary, and "b" denotes the depth of the lower plane of this boundary. The water body itself is the plane parallel region of depths y such

that $x \le y \le z$. We will often use the notation "$X[y_1,y_2]$" to refer to the slab between and including depths y_1 and y_2. Thus the *upper boundary* of the natural hydrosol is the slab $X[a,x]$, the body or *water column* is $X[x,z]$, the *lower boundary* is $X[z,b]$, and so on. The use of two symbols "a" and "x" in $X[a,x]$ helps keep in mind that the top of the air-water surface is at a and the bottom is at x, even though these are infinitesimally close.

The independent variables for the Natural Hydrosol Model are the optical depth y and the direction $\underline{\xi} = \underline{\xi}(\theta,\phi)$, where $\underline{\xi} = (\xi_1,\xi_2,\xi_3)$ is a unit vector, i.e., $\underline{\xi}\cdot\underline{\xi} = 1$. It is often convenient to use $\mu \equiv \cos\theta = \underline{\xi}\cdot\underline{k}$ rather than θ itself; then we can think of $\underline{\xi}$ as specified by μ and ϕ: $\underline{\xi} = \underline{\xi}(\mu,\phi)$, where $-1 \le \mu \le 1$, and $0 \le \phi < 2\pi$. If a wind-oriented cartesian coordinate system $\underline{i}$-$\underline{j}$-$\underline{k}$ is defined in accordance with Fig. 1, with $\underline{i}$ pointed downwind, $\underline{k}$ upward as defined above, and $\underline{j} \equiv \underline{k} \times \underline{i}$ in the crosswind direction (at $\phi = \pi/2$), then $\underline{\xi}(\theta,\phi)$ can be written in any of the forms

$$\begin{aligned}\underline{\xi} &\equiv \xi_1\underline{i} + \xi_2\underline{j} + \xi_3\underline{k} \equiv [\xi_1,\xi_2,\xi_3] \\ &= [\sin\theta\cos\phi,\ \sin\theta\sin\phi,\ \cos\theta] \\ &= [(1-\mu^2)^{\frac{1}{2}}\cos\phi,\ (1-\mu^2)^{\frac{1}{2}}\sin\phi,\ \mu]\ .\end{aligned}$$

The fundamental dependent variable of the Natural Hydrosol Model is the *spectral radiance* $N(y;\underline{\xi};\lambda)$ at depth y in direction $\underline{\xi}$ at wavelength λ. The photons are travelling in direction $\underline{\xi}$. Since the water body is assumed non-fluorescent and the radiance is monochromatic, the wavelength λ is held fixed. We therefore drop "λ" from the explicit notation and write the radiance as $N(y;\underline{\xi};\lambda) \equiv N(y;\underline{\xi}) \equiv N(y;\mu,\phi)$, with units of $W\cdot m^{-2}\cdot sr^{-1}\cdot nm^{-1}$.

In the model to be developed we begin with radiant energy from the sun or sky incident upon the random water surface at y = a. This energy is partly reflected back to the sky and partly transmitted into the water column at y = x and below. The details of this transmission through the random surface are determined by the wave field on the water surface (and hence by the wind speed) and by the directional distribution of the light sources. It is intuitively clear that the time-averaged or ensemble-averaged radiance $N(y;\underline{\xi})$ is thereby determined at each depth y of the entire water column, $x \le y \le z$, and for all directions $\underline{\xi}$, by the absorption and scattering properties of the water and by the interreflections of radiance between the upper and lower boundaries. The analytical basis for this belief rests in the equation governing the radiance field in the body of the water and in the boundary conditions above and below the water body.

a. The Radiative Transfer Equation

The equation for conservation of unpolarized, monochromatic radiance $N(\zeta;\underline{\xi})$ in a source-free optical medium is the *Radiative Transfer Equation* (cf. Preisendorfer, 1965, pp. 65-69):

$$\frac{dN(\zeta;\underline{\xi})}{dr} = -\alpha(\zeta)\, N(\zeta;\underline{\xi}) + \int_{\Xi} N(\zeta;\underline{\xi}')\, \sigma(\zeta;\underline{\xi}';\underline{\xi})\, d\Omega(\underline{\xi}') \qquad (2.1)$$

Here ζ is *geometric depth* measured positive downward, i.e., along the direction $-\underline{k}$. Moreover, r is the geometric distance (always positive) from a point at the geometric depth ζ measured along direction $\underline{\xi}$; r and ζ have units of meters. Ξ is the set of all unit vectors $\underline{\xi}$, i.e. the *unit sphere*, and $d\Omega(\underline{\xi}')$ is an infinitesimal element of solid angle about direction $\underline{\xi}'$. The *volume attenuation function* $\alpha(\zeta)$, with units of m^{-1}, and the *volume scattering*

function $\sigma(\zeta;\underline{\xi};\underline{\xi}')$, with units of $m^{-1}\cdot sr^{-1}$, are considered to be known quantities and are called the *inherent optical properties* of the water.

The integration of any function $f(\underline{\xi}) \equiv f(\theta,\phi) \equiv f(\mu,\phi)$ over all directions $\underline{\xi}$, as in (2.1), is expressible in any of the equivalent forms

$$\int_{\Xi} f(\underline{\xi})\, d\Omega(\underline{\xi}) = \int_0^{\pi}\int_0^{2\pi} f(\theta,\phi)\, \sin\theta d\theta d\phi = \int_{-1}^{1}\int_0^{2\pi} f(\mu,\phi)\, d\mu d\phi \ .$$

We separate the unit sphere Ξ into *upper*, Ξ_+, and *lower*, Ξ_-, *hemispheres* defined by

$$\Xi_+ \equiv \{(\mu,\phi):\ 0 \le \mu \le 1,\ 0 \le \phi < 2\pi\}$$
$$\Xi_- \equiv \{(\mu,\phi):\ -1 \le \mu < 0,\ 0 \le \phi < 2\pi\} \ .$$

In a similar fashion we will often use a "+" or "-" superscript as shorthand notation to indicate quantities whose $\underline{\xi}$ vectors are in the respective Ξ_+ or Ξ_- hemispheres. Thus, for example, we have the *upward* radiance $N^+(y;\underline{\xi}) \equiv N(y;\underline{\xi})$ when $\underline{\xi} \in \Xi_+$ and the *downward* radiance $N^-(y;\underline{\xi}) \equiv N(y;\underline{\xi})$ when $\underline{\xi} \in \Xi_-$.

Equation (2.1) can be placed into a more convenient form for numerical work by noting (from simple plane-parallel medium geometry and our choice of geometric depth ζ as positive downward) that $dr = -d\zeta/\mu$. Here r and ζ are both interpreted as physical distances, in meters. If we define an *increment of optical depth*, dy, as

$$dy \equiv \alpha(\zeta)d\zeta$$

then $dr = -dy/(\alpha\mu)$ and (2.1) can be written

$$-\mu \frac{dN(y;\underline{\xi})}{dy} = -N(y;\underline{\xi}) + \frac{1}{\alpha(y)} \int_{\Xi} N(y;\underline{\xi}') \, \sigma(y;\underline{\xi}';\underline{\xi}) \, d\Omega(\underline{\xi}') \tag{2.2}$$

for $x \le y \le z$ and $\underline{\xi} \in \Xi$. Henceforth the depth variable y will be interpreted as *optical depth*, which is nondimensional. The Natural Hydrosol Model uses the optical depth y as its depth variable, since it is the optical depth which summarizes most efficiently the depth behavior of the light field.

In the absence of scattering, $\sigma = 0$ and (2.2) can be immediately integrated to obtain a simple law of exponential decrease of radiance with optical depth. However, in natural hydrosols, scattering processes are of fundamental importance, and the integral in (2.2), which embodies the phenomenon of "space light" in underwater environs, must be treated with great care. The scattering function $\sigma(y;\underline{\xi}';\underline{\xi})$ describes how strongly photons at depth y initially traveling in direction $\underline{\xi}'$ are scattered into direction $\underline{\xi}$. For directionally isotropic media, the directional dependence of σ rests only on the angle between $\underline{\xi}'$ and $\underline{\xi}$, and not upon their absolute directions. Thus for the Natural Hydrosol Model we have, for various convenient forms of notation:

$$\sigma(y;\underline{\xi}';\underline{\xi}) = \sigma(y;\mu',\phi';\mu,\phi) = \sigma(y;\underline{\xi}'\cdot\underline{\xi}) \equiv \sigma(y;\psi) \, , \tag{2.3}$$

where

$$\cos\psi \equiv \underline{\xi}'\cdot\underline{\xi} = \mu'\mu + (1-\mu'^2)^{\frac{1}{2}} (1-\mu^2)^{\frac{1}{2}} \cos(\phi'-\phi) \tag{2.4}$$

defines the *scattering angle* ψ, $0 \le \psi \le \pi$. This simplification of σ will have an important influence in the choice of numerical solution procedures.

Without loss of generality, and in a convenient contracted notation, we can write σ as the product of the *volume total scattering function*, s(y), and the *phase function*, $p(y;\psi)$:

$$\sigma(y;\psi) \equiv s(y)\, p(y;\psi) \,, \tag{2.5}$$

where we have defined

$$p(y;\psi) \equiv \sigma(y;\psi)/s(y) \qquad (\equiv p(y;\underline{\xi}';\underline{\xi}) = p(y;\underline{\xi}'\cdot\underline{\xi}) = p(y;\mu',\phi';\mu,\phi))$$

and where the volume total scattering function is defined by

$$s(y) \equiv 2\pi \int_0^{\pi} \sigma(y;\psi) \sin\psi \, d\psi \qquad \left(= \int_{\Xi} \sigma(y;\underline{\xi}';\underline{\xi})\, d\Omega(\underline{\xi})\right) . \tag{2.6}$$

It follows from (2.6) that the phase function must satisfy

$$2\pi \int_0^{\pi} p(y;\psi) \sin\psi \, d\psi = 1 \qquad \text{for any } y,$$

or returning to the full (μ,ϕ) notation,

$$\int_{-1}^{1} \int_0^{2\pi} p(y;\mu',\phi';\mu,\phi)\, d\mu d\phi = 1 \qquad \left(= \int_{\Xi} p(y;\underline{\xi}';\underline{\xi})\, d\Omega(\underline{\xi})\right) \tag{2.7}$$

for any y, μ' and ϕ'. The volume total scattering function s(y) thus is a measure of the overall *amount* of scattering, and the phase function $p(y;\psi)$ contains the information about the *shape* of the scattering function.

Substituting (2.3) and (2.5) into (2.2) gives

$$-\mu \frac{dN(y;\underline{\xi})}{dy} = -N(y;\underline{\xi}) + \omega(y) \int_{\Xi} N(y;\underline{\xi}')\, p(y;\underline{\xi}';\underline{\xi})\, d\Omega(\underline{\xi}') \tag{2.8}$$

$x \le y \le z$

$\underline{\xi} \in \Xi$

where $\omega(y) \equiv s(y)/\alpha(y)$ is the *scattering-attenuation ratio* or *albedo of single scattering*. This ratio satisfies $0 \leq \omega(y) \leq 1$ and is a measure of the relative importance of scattering and absorption processes in the water. Equation (2.8) is the basic equation of the Natural Hydrosol Model.

b. Boundary Conditions at the Water Surface

At the random upper boundary of the water, downward radiance incident from the sky onto the water surface is partially reflected back to the sky and partially transmitted through the surface into the water. Moreover, upward radiance incident from the water onto the underside of the water surface is partially reflected back to the water and partially transmitted through the surface into the air. These processes, after time or ensemble averaging, are expressed by the pair of equations (cf., Preisendorfer, 1965, p. 123, Eq. II):*

$$N(x;\underline{\xi}) = \int_{\Xi_-} N(a;\underline{\xi}')\, t(a,x;\underline{\xi}';\underline{\xi})\, d\Omega(\underline{\xi}') + \int_{\Xi_+} N(x;\underline{\xi}')\, r(x,a;\underline{\xi}';\underline{\xi})\, d\Omega(\underline{\xi}') \quad , \quad \underline{\xi} \in \Xi_- \tag{2.9}$$

and

$$N(a;\underline{\xi}) = \int_{\Xi_+} N(x;\underline{\xi}')\, t(x,a;\underline{\xi}';\underline{\xi})\, d\Omega(\underline{\xi}') + \int_{\Xi_-} N(a,\underline{\xi}')\, r(a,x;\underline{\xi}';\underline{\xi})\, d\Omega(\underline{\xi}') \quad , \quad \underline{\xi} \in \Xi_+ \, . \tag{2.10}$$

* Equations (2.9) and (2.10) are instances of the interaction principle for surfaces of plane parallel media. Eq. II of the cited reference allows us to write down (2.9) and (2.10) in general, on the grounds of linearity of radiative transfer processes. However, in any specific application of Eq. II, one must actually determine the numerical values of the r and t functions. This is the task of the procedure in §9, below.

The r and t functions describe in averaged form how radiance is reflected and transmitted by the boundary.* In particular, in the first term on the right hand side of (2.9), $t(a,x;\underline{\xi}';\underline{\xi})$ determines how much of the downward radiance $N(a;\underline{\xi}')$, incident on the upper surface at $y = a$ along direction $\underline{\xi}' \in \Xi_-$, is transmitted through the surface into the water at $y = x$ along direction $\underline{\xi} \in \Xi_-$. Likewise, the second term on the right side of (2.9) shows how much of the upward radiance $N(x;\underline{\xi}')$, incident on the lower side of the surface at $y = x$ along direction $\underline{\xi}' \in \Xi_+$, is reflected back into the water along direction $\underline{\xi} \in \Xi_-$. Similar comments hold for the terms of (2.10), where now upward radiance is being transmitted through the surface from the water side to the air side. Note the reversed (x,a) notation in $t(x,a;\underline{\xi}';\underline{\xi})$ and the reversed hemispheres of $\underline{\xi}'$ and $\underline{\xi}$, relative to the transmission term of (2.9). Likewise in the second term of (2.10), downward radiance from the sky is being reflected back to the sky by the water surface. The order of the (a,x) and (x,a) arguments identifies the four distinct r and t functions of (2.9) and (2.10), which shows our use of the depth conventions of Fig. 1.

When computing the light field in the hydrosol, these reflectance and transmittance functions must be known. For certain special cases, such as that of a perfectly calm sea surface, the r's and t's are available in analytic form. However, in the general case of a wind-ruffled, anisotropic sea surface, the linear interaction principle notwithstanding, the determination of the r's and t's is a relatively difficult task. Later in this study we will show (in §9) how the reflectance and transmittance functions can be numerically estimated for wind-blown water surfaces using

* For an alternate approach to the random surface's effect on the light field at and below the surface of a natural hydrosol, see H.O., Vol. VI, secs. 12.10-12.17.

geometrical optics, quad averaging, and suitable constructions of random surfaces.

c. Boundary Conditions at the Water Bottom

A pair of equations analogous to (2.9) and (2.10) can be written for an arbitrary lower boundary. However, the assumptions of the Natural Hydrosol Model lead to lower boundary conditions which are much simpler than those of the surface. Since there are no light sources below the lower boundary, there is no radiance incident on the lower boundary from below, and therefore the transmission term may be omitted. Thus we have only

$$N(z;\underline{\xi}) = \int_{\Xi_-} N(z;\underline{\xi}')\, r(z,b;\underline{\xi}';\underline{\xi})\, d\Omega(\underline{\xi}') \quad , \quad \xi \in \Xi_+ \, , \tag{2.11}$$

which shows how downward radiance incident on the lower boundary is reflected back upward into the water. There is no need for an equation giving $N(b;\underline{\xi})$, $\xi \in \Xi_-$, corresponding to (2.10), since we are not concerned with finding the light field below the bottom (although we will find the emergent light field above the surface via (2.10)).

Either of two types of bottom boundaries can be modeled by the Natural Hydrosol Model. The first is a *matte bottom*, which represents for example a sandy or silty lake bottom. For a matte surface, the reflectance function is (H.O., Vol. II, p. 215):

$$r(z,b;\underline{\xi}';\underline{\xi}) = r(z,b;\underline{\mu}',\underline{\phi}';\underline{\mu},\underline{\phi}) = -\frac{r_-}{\pi}\,\mu' \, , \tag{2.12}$$

where r_- is the irradiance reflectance of the matte surface, $0 \le r_- \le 1$. Note that $\mu' < 0$ since $\underline{\xi}' \in \Xi_-$ in (2.11). We see from (2.12) that radiance

incident on the matte bottom is equally reflected into all directions $\underline{\xi} = \underline{\xi}(\mu,\phi)$, independent of the incident azimuthal angle ϕ', in accordance with our assumption of an isotropic lower boundary.

The second type of bottom boundary is a plane at level z. Below this plane is an optically infinitely deep water body, in which the optical properties of the water have a specified variation with depth. In this case $r(z,b;\underline{\xi}';\underline{\xi})$ gives the reflectance at depth z of the water body due to the upward scattering of downward radiance at all depths in the entire water body below level z. An appropriate form of this reflectance is developed in §10.

d. Discretization of the Model Equations

Equation (2.8) and boundary conditions (2.9)-(2.11) constitute the *continuous geometrical* form of the Natural Hydrosol Model (NHM). The word "continuous" refers to the formulation of the model as an integrodifferential equation in which the direction variables θ and ϕ may take any real values in their allowed ranges, and the term "geometrical" refers to the setting of the equations in the physical space suggested by the plane-parallel geometry of the water body. However, in order to solve the NHM equations on a digital computer (with finite storage capacity), we have decided to discretize the equations so that only a finite number of radiance directions need be computed. This discretization process is the subject of the next section; the result is termed the *discrete geometrical* form of the NHM. Furthermore, it is numerically advantageous, for the reason explained below, to recast the discrete geometrical NHM into a spectral form, termed the *discrete spectral* NHM. This final formulation of the NHM is solved for a finite set of discrete spectral amplitudes. These amplitudes are then used to compute the discrete geometrical radiances, which are the final output of the numerical model. In

the limit of infinitely fine resolution in our chosen discretization process, these discrete geometrical radiances approach the continuous geometrical radiances which are in turn the solutions of the continuous geometrical equations. Note that the word "spectral" now, and henceforth, refers to the Fourier decomposition of the azimuthal angle, and not to the wavelength of light.

Before proceeding with the discretization operations, it is worthwhile considering the theoretical and numerical implications of two available paths which lead to discretized model equations. The path briefly sketched above is shown as the right hand branch in Fig. 2. The discretization process consists of first partitioning the unit sphere Ξ into a finite number of subsets bounded by lines of constant μ and constant ϕ. These subsets are termed *quads* and can be visualized as regions bounded by latitude and longitude lines on a globe (cf. Fig. 3 below).* After defining these quads, the discretization process consists of integrating all model equations over the various quads, where "integration over a quad" means integrating over all directions $\underline{\xi}$ such that $\underline{\xi}$ is within the solid angle subtended by that quad. The discretization is thus a *directional averaging* of the continuous equations, after which, for example, a continuous radiance $N(y;\underline{\xi})$ is replaced by a discrete radiance $N(y;u,v)$, where (u,v) are the discrete integer indices labeling quad Q_{uv}. $N(y;u,v)$ is the average of $N(y;\underline{\xi})$ as $\underline{\xi}$ varies over Q_{uv}. The model equations of level 2 in the right-hand branch of Fig. 2 turn out to be a set of coupled

* This intuitively simple procedure generalizes the classical partition of the unit sphere Ξ into just two subsets Ξ_+ and Ξ_-, the upper and lower hemispheres of directions about each point of the environment, and which yielded the classical two-flow theory of light. For an initial exploration of this generalization see H.O., Vol. V, pp. 57-61 and H.O., Vol. IV, pp. 97-103. It is perhaps of interest to note that this procedure returns to and completes a numerical solution program outlined along the present lines 20 years ago (cf. Preisendorfer, 1965, footnote, p. 204). Modern computers now allow that program to be completed and widely applied.

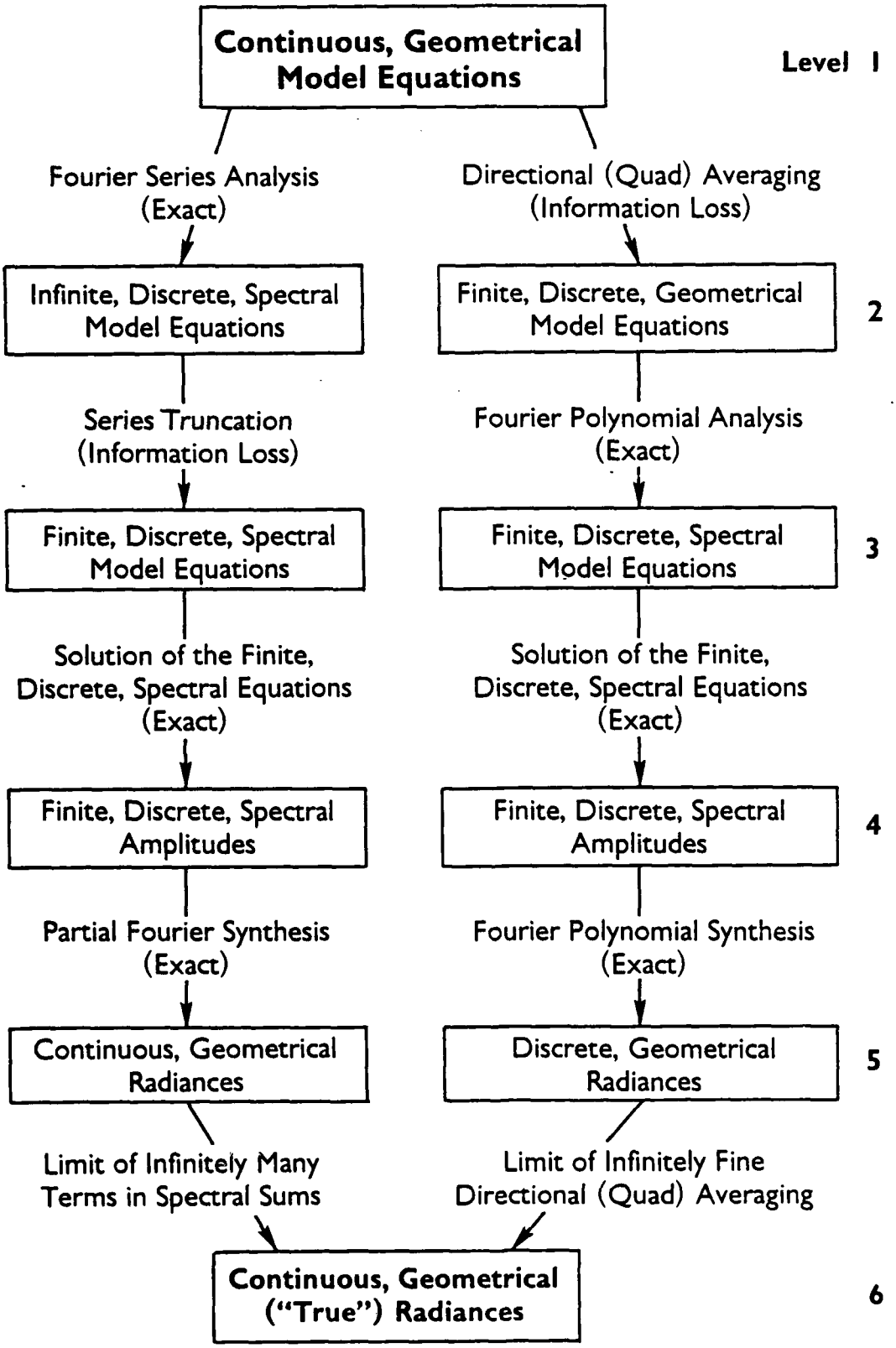

Figure 2.--Two paths leading to a discrete spectral model. The NHM takes the right-hand path.

ordinary differential equations with respect to depth y for a finite number of discrete, or quad-averaged, radiances. It is important to note that any loss of resolution, or realism, of the present numerical model when compared to nature, occurs in the quad-averaging level of the discretization procedure. The Fourier polynomial analysis leads to an uncoupling of the equations over azimuth space, without loss of information. This permits a savings in computational effort when handling reflectance and transmittance matrices. The remaining steps of the solution procedure eventually yield a set of discrete geometrical radiances which are *exact* solutions of the *discrete* geometrical model equations. How closely these solution radiances correspond to the "true" solutions of the continuous equations depends only on how fine is the original partitioning of the unit sphere Ξ into quads. The loss of model accuracy thus has an easily visualized, geometrical origin, and the discrete solution radiances are readily interpreted as averages of the "true" continuous radiances.

An alternate approach to obtaining a finite set of model equations is shown as the left hand branch of Fig. 2. In this approach, which goes back to the early work of Eddington and of Jeans (1917), the continuous geometrical model equations are first Fourier analyzed over direction space using spherical harmonics to find an infinite set of equations for the discrete spectral radiance amplitudes. No loss of accuracy occurs in this level of the reformulation. However, the infinite series in these spectral equations must be truncated at some finite value in order to obtain a finite set of coupled ordinary differential equations for the spectral amplitudes that is amenable to numerical solution. It is this truncation which introduces a loss of accuracy into the numerical model, particularly in the hydrologic optics setting which has volume scattering functions that are highly peaked in the

forward direction; a faithful representation of $\sigma(y;\underline{\xi}';\underline{\xi})$ requires very many spherical harmonics to be retained by the model. The solution radiances of level 5 on the left branch in Fig. 2 are *now exact* solutions of the *truncated* model equations; these radiances themselves are continuous functions of the azimuthal angle ϕ. How closely the solution radiances correspond to the true radiances depends only on how many terms were included in the truncated series. Although the solution radiances are easily interpreted as approximations of the true radiances, the loss of model accuracy due to series truncation at the spectral equation level is not as easily visualized. It is for this reason that in this study we adopt and explore the potentialities of the right hand path of Fig. 2 as our solution procedure. The primary goal is the form of the local interaction equations, (5.29), below).

It may be noted that the left branch of Fig. 2 can also lead to local interaction equations of precisely the form (5.29). This means that the solution procedures of §6 and 7 are also available for exploration of the numerical road starting out along the Eddington-Jeans (i.e., the left) path of Fig. 2. Indeed, the first rudimentary form of this approach is due to Chandrasekhar (1950) building on an insight of Ambarzumian (1943).

The next several sections of this report give the mathematical details of the various steps outlined above and in the right branch of Fig. 2.

3. DIRECTIONAL DISCRETIZATION OF THE MODEL EQUATIONS

We now address the mathematical details of the directional, or quad, averaging of the model equations.

a. Partitioning the Unit Sphere

For our purposes we partition the unit sphere of directions, Ξ, into quadrilateral domains called *quads*, and into *polar caps*. A quad is bounded by circular arcs of constant μ (or θ) and circular arcs of constant ϕ. The polar caps are circular domains centered on the two poles of the sphere. Figure 3 illustrates a partitioning of Ξ by means of 9 circles of constant μ (4 in the upper hemisphere, 4 in the lower hemisphere, and the equator) and by 20 semicircles of constant ϕ. Thus there are $4 \times 20 + 4 \times 20 = 160$ quads, and two polar caps. The notation "Q_{pq}" denotes the quad indexed by the p^{th} μ band and the q^{th} ϕ band, where p and q are numbered from a reference quad chosen for convenience. We are free to center the $q = 1$ row of quads on the $\phi = 0$, or downwind, direction as shown by the wind-oriented $\underline{i}$-$\underline{j}$-$\underline{k}$ coordinate system in Fig. 3. The figure also shows two directions, $\underline{\xi}'$ and $\underline{\xi}$, respectively belonging to two different quads, $Q_{rs} = Q_{1,4}$ in Ξ_- and $Q_{uv} = Q_{3,5}$ in Ξ_+. Note that the solid angles Ω_{rs} and Ω_{uv} associated with quads Q_{rs} and Q_{uv} are in general unequal in size.

Let the number of quads in the μ-direction be M (counting polar caps) and let the number in the ϕ-direction be N (we have $M = 10$ and $N = 20$ in Fig. 3). Furthermore, let M and N be even, i.e., of the form $M \equiv 2m$ and $N \equiv 2n$ and, as will be convenient later (cf. paragraph f, below), let n itself be even. This restriction to even M and n values represents no significant loss of generality in the numerical model, but greatly simplifies the analysis formulas. We also require that non-polar cap quads have equal angular widths $\Delta\phi$ in the ϕ-direction, thus

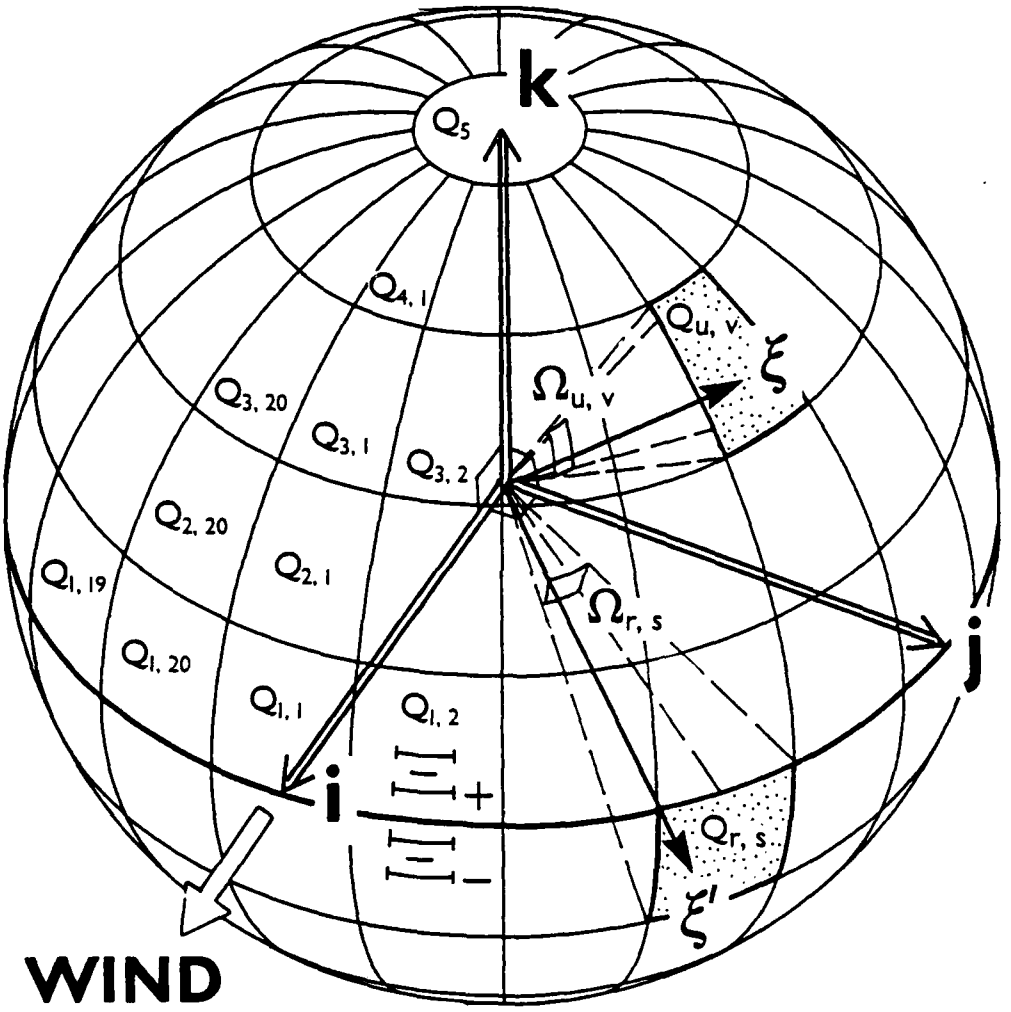

Figure 3.--An example partitioning of the unit sphere into quads, for the case of m = 5, n = 10. The origin of the wind-oriented $\underline{i}$-$\underline{j}$-$\underline{k}$ coordinate system is at the center of the unit sphere Ξ, and $\underline{\xi}'$ and $\underline{\xi}$ are unit vectors.

$$\Delta\phi = \frac{2\pi}{N} = \frac{\pi}{n} .$$

Then the centers of the non-polar quads Q_{uv} have the ϕ values

$$\phi_v = (v-1)\Delta\phi \quad , \quad v = 1,\ldots,2n . \tag{3.1}$$

The azimuthal angle ϕ_v is not defined for the polar cap quads (just as ϕ is not defined at the poles, $\theta = 0$ and $\theta = \pi$, in a spherical coordinate system).

The angular size $\Delta\mu$ (or $\Delta\theta$) of the quads in the μ direction can be fixed as desired. There is no requirement that the quads in different μ-bands defined by pairs of neighboring μ circles have equal $\Delta\mu$ values. One simple scheme for defining the μ-bands is to let $\Delta\mu_u = \Delta\mu = 1/m$, and thus have quads of equal μ-size and hence of equal solid angle (except for the polar cap quads) $\Omega_{uv} = \Delta\mu_u\Delta\phi_v = \Delta\mu\Delta\phi$, since $\Delta\phi_v = \pi/n$. With this choice there are $2(m-1)2n$ non-polar quads of size $\Omega_{uv} = (1/m)(\pi/n)$ and two polar cap quads of size $\Omega_m = (1/m)(2\pi)$, which total to the required 4π steradians in Ξ. If we set

$$\Delta\mu_u \equiv \frac{2n}{(m-1)2n+1} = \Delta\mu \quad \text{for } u = 1,\ldots,m-1$$

and

$$\Delta\mu_m = \frac{\Delta\mu}{2n} \quad \text{for the polar cap, } u = m,$$

then all quads, including the polar caps, have the same solid angle $\Delta\Omega_{uv} = \Delta\Omega = 2\pi/[(m-1)2n+1]$. This equal solid angle partition is shown in Fig. 4a for $m = 10$, $n = 12$.

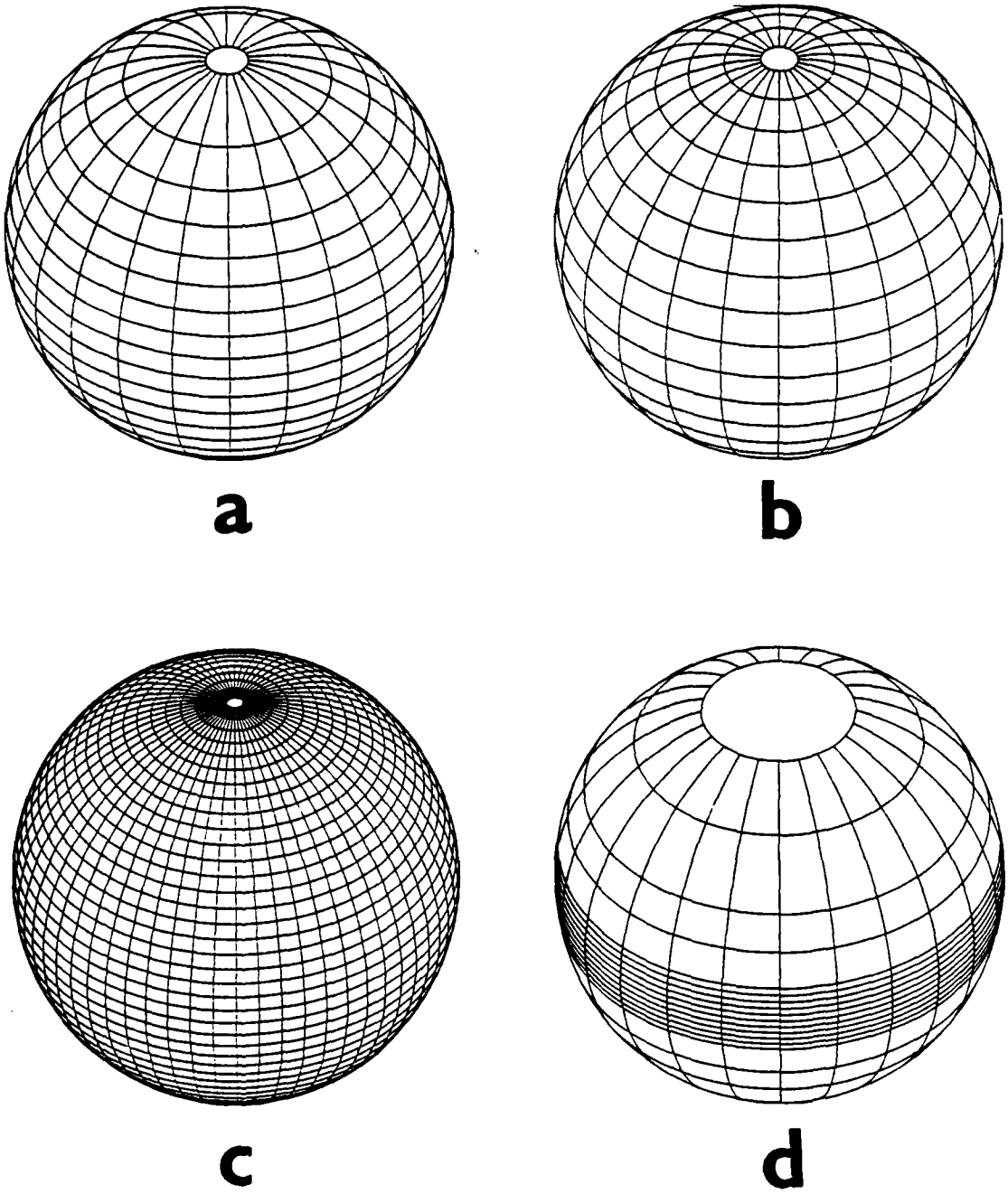

Figure 4.--Further examples of partitions of the unit sphere into quads. (a) m = 10 μ-bands and n = 12 φ-bands, with all solid angles Ω_{pq} and Ω_m equal. (b) m = 10 and n = 12, with all Δθ values equal. (c) m = 23, n = 30 with equal Δθ values, so that Δθ = 4° and Δφ = 6°. (d) m = 10, n = 12 with an ad hoc selection of the Δθ values.

The equal solid angle partition may be inconvenient for some applications, since the quads near the pole cover a large θ range and thus, for example, may cause an unacceptable loss of θ-resolution for solar positions near the zenith or lines of sight directed at the nadir. Another convenient choice of μ-bands is to use equal $\Delta\theta$ values, as shown in Fig. 4b for m = 10, n = 12. Here the θ-resolution is the same everywhere (the polar caps have a half-angle of $\Delta\theta/2$), but of course the quads in different μ-bands have different solid angles Ω_{uv}. A quad resolution of m ~ 10, n ~ 12 has been found to be reasonable for use in debugging and in production model runs where extreme accuracy is not required.

Some applications of the Natural Hydrosol Model may require even finer directional resolution. For example, changing the sun's elevation by only a few degrees may have a large effect on the subsurface light field when the sun is near the horizon. Figure 4c shows a higher resolution, equal $\Delta\phi$ partition of Ξ with m = 23 and n = 30, so that $\Delta\theta = 4°$ and $\Delta\phi = 6°$. Grids of this resolution are currently (1988) at the limit of computational feasibility. Figure 4d shows an m = 10, n = 12 grid with an ad hoc $\Delta\theta$ selection which gives $\Delta\theta = 2°$ near the horizon and $\Delta\theta = 20°$ near the poles.

It can be noted that a grid for which the solar disk, which subtends an angle of about 0.5°, fills one quad of size $\Delta\theta = \Delta\phi = 0.5°$ would require m = 180, n = 360. Since computation and storage requirements of the model are generally proportional to m^2n^2, such a grid would require nearly 300,000 times the computer effort relative to the m = 10, n = 12 grid. Such resolution is far beyond current general-purpose computer capacities (1988). Such resolution would, however, at present not be beyond the capacity of dedicated

computers that could be constructed for specific radiative transfer integration tasks (cf., H.O., Vol. 1, p. 208).*

In our later development we shall have frequent need to evaluate sums of discrete functions, f(p,q), defined on the quads Q_{pq} of Ξ. Thus "$\sum_p \sum_q f(p,q)$" will denote a sum of f(p,q) over all quads and polar caps in the unit sphere Ξ. Henceforth, unless otherwise noted, the polar caps will be considered as special quads. We shall also occasionally write sums over all quads as separate sums over Ξ_+ and Ξ_-, and we shall sometimes add a "+" or "-" superscript to the summand as a reminder of which hemisphere is referenced by the sum, as for example in

$$\sum_p \sum_q f(p,q) = \sum_p \sum_q f^+(p,q) + \sum_p \sum_q f^-(p,q) \,.$$

$$(Q_{pq} \text{ in } \Xi) \qquad (Q_{pq} \text{ in } \Xi_+) \qquad (Q_{pq} \text{ in } \Xi_-)$$

Here "(Q_{pq} in Ξ)" means "all quads Q_{pq} of Ξ are to be summed over." "(Q_{pq} in Ξ_+)" is interpreted as "all quads Q_{pq} of Ξ_+ are to be summed over", etc. For ease of indexing in the computer code, we also let p = 1,2,...,m label the μ-bands of the quads Q_{pq}, regardless of whether Q_{pq} is in Ξ_+ or Ξ_-; p = 1 is the row of quads nearest the "equator" and p = m refers to the polar cap quads. Since there is no ϕ dependence for the polar caps, these "quads" are always special cases. The value of f(p,q) at a polar cap will then be denoted by "$f^{\pm}(m,\cdot)$". Thus we write

* Another possibility would be to produce a variable-grid partition of Ξ around directions where there exists a high radiance gradient. In this way the grid would be fine around the sun direction and become progressively less fine away from that direction. This would, however, require a revision of the spectral decomposition of the present method.

$$\sum_{p}\sum_{q} f(p,q) = \sum_{p=1}^{m-1}\sum_{q=1}^{2n} f^{+}(p,q) + f^{+}(m,\cdot) + \sum_{p=1}^{m-1}\sum_{q=1}^{2n} f^{-}(p,q) + f^{-}(m,\cdot) \ . \qquad (3.2)$$

$(Q_{pq} \text{ in } \Xi)$

Sums over Ξ or $\Xi_{\pm}$ will always be computed as shown by the explicit notation of (3.2).

b. Quad-Averaging

Let "$F(y;\underline{\xi})$" denote any function of depth y and direction $\underline{\xi}$. The *quad-average* of $F(y;\underline{\xi})$ over any quad Q_{uv} in Ξ is defined by

$$F(y;u,v) \equiv \frac{1}{\Omega_{uv}} \int_{Q_{uv}} F(y;\underline{\xi})\, d\Omega(\underline{\xi}) = \frac{1}{\Omega_{uv}} \iint_{Q_{uv}} F(y;\mu,\phi)\, d\mu d\phi \ . \qquad (3.3)$$

$a \le y \le b$

Q_{uv} in Ξ

The quad-averaged quantities are the fundamental building blocks of the numerical Natural Hydrosol Model. Owing to the "smearing out" of the continuous $F(y;\underline{\xi})$ by the directional averaging in (3.3), the numerical model cannot resolve features of the radiance distribution which subtend solid angles smaller than Ω_{uv}. In a manner of speaking, the quad-averaging process replaces the clear unit sphere (with perfect resolution) by a polyhedron of frosted glass windows; each window (i.e., quad or polar cap) homogenizes the radiance distribution within that window. Note, however, that the Natural Hydrosol Model is capable of arbitrarily fine resolution in the vertical direction down through the body of water, so long as the number of depths y, where a solution is desired, remains finite.

The basic step of the quad-averaging procedure can be represented as the formal replacement of a function $F(y;\mu,\phi)$, defined on the unit sphere Ξ, by the following linear combination $\overline{F}(y;\mu,\phi)$ of its quad averages $F(y;p,q)$:

$$\boxed{\begin{aligned}&\bar{F}(y;\mu,\phi) \equiv \sum_p \sum_q \chi_{pq}(\mu,\phi)\, F(y;p,q)\ , \\ &a \le y \le b \\ &(\mu,\phi) \in \Xi\end{aligned}} \tag{3.4}$$

where

$$\chi_{pq}(\mu,\phi) \equiv \begin{cases} 1 \text{ if } (\mu,\phi) \in Q_{pq} \\ 0 \text{ if } (\mu,\phi) \notin Q_{pq}\ , \end{cases}$$

and where $\sum''_p \sum''_q$ denotes a sum over all quads and caps Q_{pq} in the unit sphere Ξ, evaluated as shown explicitly in (3.2). Observe that $\bar{F}(y;\mu,\phi)$ is constant as (μ,ϕ) varies over Q_{pq}, and is of magnitude $F(y;p,q)$, even though the original $F(y;\mu,\phi)$ in (3.3) may have varied over Q_{pq}. This follows from our interpretation of $F(y;u,v)$ as an average and emphasizes the consequence of the directional averaging operation. This same quad average over Q_{uv}, namely $F(y;u,v)$, is obtained from (3.3) if $\bar{F}(y;\mu,\phi)$ is used in place of $F(y;\mu,\phi)$. That the *step function* form $\bar{F}(y;\mu,\phi)$ of $F(y;\mu,\phi)$, given by (3.4) is consistent with (3.3) in this sense, is verified by direct substitution of (3.4) into (3.3). Thus (3.3) becomes

$$\frac{1}{\Omega_{uv}} \iint_{Q_{uv}} \bar{F}(y;\mu,\phi)\, d\mu d\phi = \frac{1}{\Omega_{uv}} \iint_{Q_{uv}} \left[\sum_p \sum_q \chi_{pq}(\mu,\phi)\, F(y;p,q) \right] d\mu d\phi$$

$$= \sum_p \sum_q F(y;p,q)\, \frac{1}{\Omega_{uv}} \iint_{Q_{uv}} \chi_{pq}(\mu,\phi)\, d\mu d\phi\ .$$

$$= F(y;u,v)$$

That is, we have

$$F(y;u,v) = \frac{1}{\Omega_{uv}} \iint_{Q_{uv}} \overline{F}(y;\mu,\phi)\, d\mu d\phi \qquad (3.5)$$

$a \le y \le b$

Q_{uv} in Ξ

The interchange of summation and integration in the derivation of (3.5) is possible since only $\chi_{pq}(\mu,\phi)$ depends on (μ,ϕ). But $\chi_{pq}(\mu,\phi)$ is non-zero (namely of unit magnitude) only when $(\mu,\phi) \in Q_{pq}$, so the integral over Q_{uv} is non-zero only when quad Q_{pq} is quad Q_{uv}. In terms of the Kroneker delta symbol,

$$\delta_k \equiv \begin{cases} 1 \text{ if } k = 0 \\ 0 \text{ if } k \neq 0 \end{cases}, \qquad (3.6)$$

the second line of the derivation leading to (3.5) becomes

$$\sum_p \sum_q F(y;p,q)\, \frac{1}{\Omega_{uv}}\, \delta_{p-u}\, \delta_{q-v} \iint_{Q_{uv}} d\mu d\phi$$

$$= F(y;u,v)\, \frac{1}{\Omega_{uv}} \cdot \Omega_{uv} = F(y;u,v) ,$$

where we have noted that the solid angle of quad Q_{uv} is just

$$\Omega_{uv} = \iint_{Q_{uv}} d\mu d\phi . \qquad (3.7)$$

Thus (3.5) and (3.4) constitute a transform pair which respectively carry a function of (μ,ϕ) into a function of (u,v), and conversely.

c. Discretization of the Radiative Transfer Equation

We are now prepared to apply the quad-averaging operator (3.3) to the entire radiative transfer equation (2.8); the result will be the quad-averaged version of the equation. Eq. (2.8) written in terms of (μ,ϕ) is

$$-\mu \frac{dN(y;\mu,\phi)}{dy} = -N(y;\mu,\phi) + \omega(y) \int_{\Xi} d\mu' d\phi' \; N(y;\mu',\phi') \; p(y;\mu',\phi';\mu,\phi) \quad (3.8)$$

where $x \le y \le z$ and $(\mu,\phi) \in \Xi$. Let us now consider, term by term, the effect on (3.8) of quad-averaging.

(i) The derivative term

On the left hand side of (3.8) we have

$$\frac{1}{\Omega_{uv}} \iint_{Q_{uv}} \left[-\mu \frac{dN(y;\mu,\phi)}{dy}\right] d\mu d\phi = \frac{1}{\Omega_{uv}} \int_{\Delta\mu_u} d\mu \int_{\Delta\phi_v} d\phi \left[-\mu \frac{dN(y;\mu,\phi)}{dy}\right]$$

$$= \frac{1}{\Omega_{uv}} \int_{\mu_u(1)}^{\mu_u(2)} d\mu \int_{\phi_v(1)}^{\phi_v(2)} d\phi \left[-\mu \frac{dN(y;\mu,\phi)}{dy}\right], \quad (3.9)$$

where $\mu_u(1)$, $\mu_u(2)$ and $\phi_v(1)$, $\phi_v(2)$ are the bounding μ and ϕ values, respectively, of quad Q_{uv}. Thus $\Delta\mu_u = \mu_u(2) - \mu_u(1)$ and $\Delta\phi_v = \phi_v(2) - \phi_v(1)$. The continuous radiance $N(y;\mu,\phi)$ is replaced by its approximating step function form using (3.4), so that (3.9) becomes

$$\frac{1}{\Omega_{uv}} \int_{\mu_u(1)}^{\mu_u(2)} d\mu \int_{\phi_v(1)}^{\phi_v(2)} d\phi \left[-\mu \sum_p \sum_q \chi_{pq}(\mu,\phi) \frac{dN(y;p,q)}{dy} \right]$$

$$= -\frac{1}{\Omega_{uv}} \frac{dN(y;u,v)}{dy} \Delta\phi_v \int_{\mu_u(1)}^{\mu_u(2)} \mu \, d\mu$$

$$= -\frac{1}{\Omega_{uv}} \frac{dN(y;u,v)}{dy} \Delta\phi_v \, \tfrac{1}{2}[\mu_u^2(2) - \mu_u^2(1)]$$

Now $\Omega_{uv} = \Delta\mu_u \Delta\phi_v$ and

$$\tfrac{1}{2}[\mu_u^2(2) - \mu_u^2(1)] = \tfrac{1}{2}[\mu_u(2) + \mu_u(1)][\mu_2(2) - \mu_u(1)] \equiv \bar{\mu}_u \Delta\mu_u \ ,$$

where the overbar denotes the average μ value over the quad or polar cap. Thus we have the result

$$\frac{1}{\Omega_{uv}} \iint_{Q_{uv}} \left[-\mu \frac{dN(y;\mu,\phi)}{dy} \right] d\mu d\phi = -\bar{\mu}_u \frac{dN(y;u,v)}{dy} \ . \tag{3.10}$$

Henceforth we will drop the overbar, and "μ_u" will always denote the average μ value over the Q_{uv} quad or polar cap. Observe that at this stage of the developments μ_u can take on negative as well as positive values, just as can its continuous counterpart μ. Thus if Q_{uv} is in Ξ_-, then $\mu_u < 0$, and if Q_{uv} is in Ξ_+, then $\mu_u > 0$. Observe that the μ_u's come in signed pairs by virtue of the same decompositions of Ξ_+ and Ξ_- into quads. (Later, in (5.2) and beyond, the μ_u will be restricted to their positive subset.)

(ii) The attenuation term

The first term on the right hand side of (3.8) yields, by definition, the quad-averaged radiance, $-N(y;u,v)$.

(iii) The scattering term

The integral on the right side of (3.8) is quad-averaged as follows:

$$\frac{1}{\Omega_{uv}} \iint_{Q_{uv}} \left[\omega(y) \iint_{\Xi} N(y;\mu',\phi')\, p(y;\mu',\phi';\mu,\phi)\, d\mu' d\phi' \right] d\mu d\phi$$

$$= \frac{\omega(y)}{\Omega_{uv}} \iint_{Q_{uv}} d\mu d\phi \left\{ \sum_r \sum_s \iint_{Q_{rs}} d\mu' d\phi'\, N(y;\mu',\phi')\, p(y;\mu',\phi';\mu,\phi) \right\}$$

$$= \frac{\omega(y)}{\Omega_{uv}} \iint_{Q_{uv}} d\mu d\phi \left\{ \sum_r \sum_s \iint_{Q_{rs}} d\mu' d\phi' \left[\sum_p \sum_q \chi_{pq}(\mu',\phi')\, N(y;p,q) \right] p(y;\mu',\phi';\mu,\phi) \right\}.$$

In the first step above, the μ'-ϕ' integration over all directions Ω has been rewritten as a sum of integrations over all quads comprising the unit sphere. In the second step, the radiance has been replaced by its approximate step function form over each quad. Owing to the step function $\chi_{pq}(\mu',\phi')$, we have a contribution to the μ'-ϕ' integral only when $(p,q) = (r,s)$, which leaves just

$$\frac{\omega(y)}{\Omega_{uv}} \iint_{Q_{uv}} d\mu d\phi \sum_r \sum_s N(y;r,s) \iint_{Q_{rs}} d\mu' d\phi'\, p(y;\mu',\phi';\mu,\phi)$$

$$= \omega(y) \sum_r \sum_s N(y;r,s) \frac{1}{\Omega_{uv}} \iint_{Q_{uv}} d\mu d\phi \iint_{Q_{rs}} d\mu' d\phi'\, p(y;\mu',\phi';\mu,\phi)$$

$$= \omega(y) \sum_r \sum_s N(y;r,s)\, p(y;r,s|u,v)\ ,$$

where we have defined the *quad-averaged phase function* as

$$p(y;r,s|u,v) \equiv \frac{1}{\Omega_{uv}} \iint_{Q_{uv}} d\mu d\phi \iint_{Q_{rs}} d\mu' d\phi' \; p(y;\mu',\phi';\mu,\phi) \qquad (3.11)$$

$x \le y \le z$

Q_{rs} and Q_{uv} in Ξ_+ or Ξ_-

$r,u = 1,\ldots,m$

$s,v = 1,\ldots,2n$

Note that $p(y;r,s|u,v)$ is well defined even if Q_{rs} or Q_{uv} is a polar quad. Although the discrete azimuthal angles ϕ_s and ϕ_v are not defined for the polar quads, the continuous azimuthal angles ϕ' and ϕ are defined within the polar caps, except at the poles themselves ($\mu' = \pm 1$, $\mu = \pm 1$), so that the integrations shown in (3.11) can be performed. Following the notational convention for polar cap values in (3.7), if Q_{rs} or Q_{uv} are polar caps, we write $p(y;r,s|u,v)$ respectively as "$p(y;m,\cdot|u,v)$" or "$p(y;r,s|m,\cdot)$". If Q_{rs} and Q_{uv} are both polar caps, we write* "$p(y;m,\cdot|m,\cdot)$".

Collecting the results of (i)-(iii) above, we obtain the *quad-averaged radiative transfer equation*:

$$-\mu_u \frac{dN(y;u,v)}{dy} = -N(y;u,v) + \omega(y) \sum_r \sum_s N(y;r,s)\, p(y;r,s|u,v) \qquad (3.12)$$

$x \le y \le z$

Q_{uv} in Ξ_+ or Ξ_-

$(-1 \le \mu_u \le 1)$

$u = 1,\ldots,m$

$v = 1,\ldots,2n$

* How these singular cases are handled in a computer program is explained in §12.

where $\sum_r \sum_s$ represents a sum over all quads Q_{rs} in Ξ, evaluated as in (3.2). We now have a finite set of ordinary differential equations with respect to optical depth y for the finite number of quad-averaged, or discrete, radiances N(y;u,v). Equation (3.12) is thus the discrete geometric form of the continuous geometric eq. (2.8).

d. Symmetries of the Phase Function

As discussed in §2a above, the isotropic volume scattering function and hence the phase function $p(y;\mu',\phi';\mu,\phi)$ depends at each y only on the angle between the directions (μ',ϕ') and (μ,ϕ). The basic symmetry of $p(y;\mu',\phi';\mu,\phi) \equiv p(y;\underline{\xi}';\underline{\xi})$ is then given by the following equality

$$p(y;\underline{\xi}';\underline{\xi}) = p(y;\underline{\xi}_0';\underline{\xi}_0) \tag{3.13}$$

which holds whenever

$$\underline{\xi}'\cdot\underline{\xi} = \underline{\xi}_0'\cdot\underline{\xi}_0$$

where, as in (2.4)

$$\underline{\xi}'\cdot\underline{\xi} = \mu'\mu + (1-\mu'^2)^{\frac{1}{2}}\,(1-\mu^2)^{\frac{1}{2}}\cos(\phi'-\phi)\ .$$

There are four immediate corollaries of (3.13) which are useful in practice. Thus we have for $p(y;\underline{\xi}';\underline{\xi})$,

1) Invariance under interchange of μ',μ:

$$p(y;\mu',\phi';\mu,\phi) = p(y;\mu,\phi';\mu',\phi) \tag{3.13a}$$

2) Invariance under interchange of ϕ', ϕ:

$$p(y;\mu',\phi';\mu,\phi) = p(y;\mu',\phi;\mu,\phi') \tag{3.13b}$$

3) Invariance under simultaneous sign changes of μ', μ:

$$p(y;\mu',\phi';\mu,\phi) = p(y;-\mu',\phi';-\mu,\phi) \tag{3.13c}$$

4) Invariance under simultaneous shifts of ϕ', ϕ; i.e., for all angles a,

$$p(y;\mu',\phi';\mu,\phi) = p(y;\mu',\phi'+a;\mu,\phi+a) \tag{3.13d}$$

As a special case of 4), set $a = -\phi'$. Then with the help of 2),

$$\begin{aligned} p(y;\mu',\phi';\mu,\phi) &= p(y;\mu',0;\mu,\phi-\phi') \\ &= p(y;\mu',0;\mu,-(\phi-\phi')) \end{aligned} \tag{3.13e}$$

This shows that for fixed y, μ', and μ, $p(y;\mu',0;\mu,\phi-\phi')$ is an even function of $\phi-\phi'$. This observation is a basis for the cosine representation of $p(y;\mu',\phi';\mu,\phi)$ (cf. (4.11), (3.13k), below, and (5.5a)) which we shall use in the reduction of the equation of transfer to spectral form.

In what follows we shall use properties 2)-4) to reduce the complexity of the spectral form of the equation of transfer. The only property not used is 1) which is a form of reciprocity property (full reciprocity is obtained by combining 1) and 2)).

The preceding symmetries are inherited by the quad-averaged form of the phase function. To show these symmetries succinctly we adopt the following conventions. If Q_{rs} is in Ξ_+ or Ξ_-, with $r = 1,\ldots,m$, then $Q_{-r,s}$ is in Ξ_- or Ξ_+, respectively. More precisely, $Q_{-r,s}$ is the quad that is the mirror image, in the equatorial plane of Ξ, of the quad Q_{rs}. Finally, shifting the azimuthal index s in Q_{rs} by an arbitrary integer a produces a new quad $Q_{r,s+a}$ which is the quad Q_{rq} where $q \equiv (s+a) \bmod(2n)$. In other words we find q by dividing s+a by 2n and taking the remainder. A zero remainder is identified with 2n. Hence it follows that $-s = (-s+2n) \bmod(2n)$ (see Fig. 5b, below, for the case n = 12. Check, for example, that $s+a = 22+4 = 26 \bmod 24 = 2$ and that $-s = -2 = (-2+24) \bmod(24) = 22$.) With these preliminaries, the preceding symmetries of $p(y;u',\phi';u,\phi)$ take the following forms in the quad-averaged context of the phase function. Each of the following symmetries may be proved by using the corresponding property 1)-4) in (3.11) and reducing the result to the desired form.

Thus we have for $p(y;r,s|u,v)$,

1)' Invariance under interchange of r,u:

$$p(y;r,s|u,v) = p(y;u,s|r,v) \tag{3.13f}$$

2)' Invariance under interchange of s,v:

$$p(y;r,s|u,v) = p(y;r,v|u,s) \tag{3.13g}$$

3)' Invariance under simultaneous sign changes of r,u:

$$p(y;r,s|u,v) = p(y;-r,s|-u,v) \tag{3.13h}$$

4)' Invariance under simultaneous shifts of s,v, i.e., for all integers a,

$$p(y;r,s|u,v) = p(y;r,s+a|u,v+a) \tag{3.13i}$$

From 4)' and 2)' we find

$$\begin{aligned} p(y;r,s|u,v) &= p(y;r,0|u,v-s) \\ &= p(y;r,0|u,-(v-s)) \end{aligned} \tag{3.13j}$$

Since the working range of s and v is 1,...,2n, we can either replace 0 by 2n in (13.3j) or using 4)' again, write the preceding equalities as

$$\begin{aligned} p(y;r,s|u,v) &= p(y;r,1|u,(v-s)+1) \\ &= p(y;r,1|u,(s-v)-1) \end{aligned} \tag{3.13k}$$

e. Discretization of the Surface Boundary Equations

The surface boundary conditions (2.9) and (2.10) on the radiance field are discretized in the same manner as the radiative transfer equation. Consider, for example, (2.9):

$$\begin{aligned} N(x;\mu,\phi) = &\int_{\Xi_-} N(a;\mu',\phi')\, t(a,x;\mu',\phi';\mu,\phi)\, d\mu' d\phi' \\ &+ \int_{\Xi_+} N(x;\mu',\phi')\, r(x,a;\mu',\phi';\mu,\phi)\, d\mu' d\phi' \quad , \quad (\mu,\phi) \in \Xi_- \ . \end{aligned} \tag{3.14}$$

The left side of (3.14), when quad-averaged, yields by definition the quad-averaged radiance. The first term of the right side of (3.14) becomes

$$\frac{1}{\Omega_{uv}} \iint\limits_{Q_{uv}} d\mu d\phi \left\{ \int\limits_{\Xi_-} N(a;\mu',\phi')\ t(a,x;\mu',\phi';\mu,\phi)\ d\mu' d\phi' \right\}$$

$$= \frac{1}{\Omega_{uv}} \iint\limits_{Q_{uv}} d\mu d\phi \left\{ \sum_r \sum_s \iint\limits_{Q_{rs}} d\mu' d\phi' \left[\sum_p \sum_q \chi_{pq}(\mu',\phi')\ N(a;p,q) \right] t(a,x;\mu',\phi';\mu,\phi) \right\}$$

after rewriting the integral over Ξ_- as a sum of integrals over all quads Q_{rs} in Ξ_-, and after replacing $N(a;\mu',\phi')$ by its approximate step function form (3.4). The last expression can be reordered to get

$$\sum_r \sum_s \sum_p \sum_q N(a;p,q) \left\{ \frac{1}{\Omega_{uv}} \iint\limits_{Q_{uv}} d\mu d\phi \left[\iint\limits_{Q_{rs}} d\mu' d\phi'\ \chi_{pq}(\mu',\phi')\ t(a,x;\mu',\phi';\mu,\phi) \right] \right\}.$$

Observe that the μ'-ϕ' integral involving χ_{pq} integrated over Q_{rs} is non-zero only if $(p,q) = (r,s)$; so we have left just

$$\sum_r \sum_s N(a;r,s) \left\{ \frac{1}{\Omega_{uv}} \iint\limits_{Q_{uv}} d\mu d\phi \iint\limits_{Q_{rs}} d\mu' d\phi'\ t(a,x;\mu',\phi';\mu,\phi) \right\}$$

$$= \sum_r \sum_s N(a;r,s)\ t(a,x;r,s|u,v)\ , \qquad (3.15)$$

after defining the quantity in braces to be the *quad-averaged transmittance*:

$$t(a,x;r,s|u,v) \equiv \frac{1}{\Omega_{uv}} \iint\limits_{Q_{uv}} d\mu d\phi \iint\limits_{Q_{rs}} d\mu' d\phi'\ t(a,x;\mu',\phi';\mu,\phi) \qquad (3.16)$$

Q_{rs} in Ξ_-

Q_{uv} in Ξ_-.

This transmittance is therefore for the downward quad-averaged radiance incident at level a of boundary X[a,x]. The second term on the right side of (3.14) is treated in an exactly analogous manner to obtain a result corresponding to (3.15). Collecting these results, we have the *discrete geometric* boundary condition at level x of boundary X[a,x]:

$$N(x;u,v) = \sum_r \sum_s N(a;r,s)\, t(a,x;r,s|u,v) + \sum_r \sum_s N(x;r,s)\, r(x,a;r,s|u,v) \tag{3.17}$$

which holds at level x of X[a,x] for all quads Q_{uv} in Ξ_-. Note how the order of a,x in t(a,x;r,s|u,v), for example, shows that the (r,s) pairs in the first sum are over Q_{rs} in Ξ_-, while Q_{rs} varies over Ξ_+ in the second sum. A similar equation is obtained from (2.10), namely

$$N(a;u,v) = \sum_r \sum_s N(x;r,s)\, t(x,a;r,s|u,v) + \sum_r \sum_s N(a;r,s)\, r(a,x;r,s|u,v) \tag{3.18}$$

which holds at level a of X[a,x] for all quads Q_{uv} in Ξ_+.

Just as in the continuous equations (2.9) and (2.10), the four transmittance and reflectance functions in (3.17) and (3.18) are considered known as regards the solution procedure for the radiative transfer equation. We shall consider in §9 the numerical computation of these quantities.

We observe that the continuous transmittance and reflectance functions in (2.9) and (2.10) have units of steradian^{-1}, whereas their discrete forms seen in (3.17) and (3.18) are dimensionless. The continuous r's and t's are *densities*, showing how much incident radiance is reflected or transmitted *per steradian*. The discrete r's and t's are integrated densities, showing how much quad-averaged radiance is reflected or transmitted between particular

quads Q_{rs} and Q_{uv}. The magnitudes of the discrete forms depend explicitly on the solid angles of the quads, as is evident from the defining equation (3.16).

The quad-averaged phase function of (3.11) and the quad-averaged surface reflectances and transmittances of (3.16) all have the same mathematical form, namely $f(r,s|u,v)$ where we write in analogy to (3.11):

$$f(r,s|u,v) \equiv \frac{1}{\Omega_{uv}} \iint_{Q_{uv}} d\mu d\phi \iint_{Q_{rs}} d\mu' d\phi' \; f(\mu',\phi';\mu,\phi) \qquad (3.19)$$
$$Q_{rs},\ Q_{uv} \text{ in } \Xi$$

Here $f(\mu',\phi';\mu,\phi)$ is any phase, surface reflectance or surface transmittance function. Corresponding to $f(\mu',\phi';\mu,\phi)$, there is a step function $\bar{f}(\mu',\phi';\mu,\phi)$, which we use formally to replace $f(\mu',\phi';\mu,\phi)$, namely

$$\bar{f}(\mu',\phi';\mu,\phi) \equiv \sum_r \sum_s \sum_u \sum_v \chi_{rs}(\mu',\phi')\, \chi_{uv}(\mu,\phi)\, \frac{f(r,s|u,v)}{\Omega_{rs}} \qquad (3.20)$$
$$(\mu',\phi'),(\mu,\phi) \in \Xi$$

As can be verified, substituting $\bar{f}(\mu',\phi';\mu,\phi)$ into (3.19) we obtain $f(r,s|u,v)$. This is comparable to the verification of (3.3). Therefore, relations (3.19) and (3.20) are a transform pair which carry a function of two directions back and forth between the discrete and continuous representations.

Note that for any directions (μ',ϕ') in Q_{rs} and (μ,ϕ) in Q_{uv}, (3.20) implies that

$$\bar{f}(\mu',\phi';\mu,\phi) = \frac{f(r,s|u,v)}{\Omega_{rs}} \qquad (3.21)$$

for all (μ',ϕ') in Q_{rs} and (μ,ϕ) in Q_{uv}. This result is also obtained approximately from (3.19) if Ω_{rs} and Ω_{uv} are sufficiently small so that $f(\mu',\phi';\mu,\phi)$ can be taken as constant over the quads Q_{rs} and Q_{uv}. Once again we see the implications of the quad-averaging operation on the directional resolution of a physical quantity. Note also that if we wish to numerically compare any two-directional quad-averaged quantity (e.g. $r(a,x;r,s|u,v)$) with its continuous counterpart (in this case, $r(a,x;\mu',\phi';\mu,\phi)$ for (μ',ϕ') in Q_{rs} and (μ,ϕ) in Q_{uv}), then the rule in (3.21) says we must first convert the dimensionless, quad-averaged quantity $f(r,s|u,v)$ into its approximate, dimensional, continuous counterpart by dividing $f(r,s|u,v)$ by Ω_{rs}.

f. Symmetries of the Surface Boundary

The discussion of the previous section is valid for completely arbitrary r and t functions. However the actual model of a wind-blown sea surface which we adopt for the natural hydrosol model is based on a two-dimensional probability distribution of the wave slopes in the form (cf., H.O., Vol. VI, p. 148):

$$p(\zeta_u,\zeta_c) = (2\pi\sigma_u\sigma_c)^{-1} \exp\left[-\tfrac{1}{2}\left(\frac{\zeta_u^2}{\sigma_u^2} + \frac{\zeta_c^2}{\sigma_c^2}\right)\right] . \tag{3.22}$$

Here ζ_u and ζ_c are the wave slopes in the upwind and crosswind directions, respectively; and $\sigma_u^2 = a_u U$ and $\sigma_c^2 = a_c U$ are the variances of ζ_u and ζ_c, where U is the wind speed. $p(\zeta_u,\zeta_c)$ is the probability density of occurrence of a wave facet with slopes ζ_u and ζ_c. For unequal proportionality constants, $a_u \neq a_c$, the wave slope distribution is anisotropic. Measurements indicate that $a_u = 3.16 \times 10^{-3}$ sec m^{-1} and $a_c = 1.92 \times 10^{-3}$ sec m^{-1}, so $a_u/a_c = 1.65$. With $\phi = 0$ chosen as in Fig. 1 to be the downwind direction, the distribution

(3.22) displays the azimuthal symmetry of an ellipse with its major axis in the upwind-downwind direction and its minor axis in the crosswind direction.

In order to exploit the elliptical symmetry of the water surface, recall from §2 that a direction $\underline{\xi} = (\xi_1,\xi_2,\xi_3)$ has the components $\xi_1 = (1-\mu^2)^{\frac{1}{2}} \cos\phi$, $\xi_2 = (1-\mu^2)^{\frac{1}{2}} \sin\phi$, $\xi_3 = \mu$ in the wind-based coordinate system. If a downward directed light ray $\underline{\xi}'$ is reflected by a wave facet into the upward direction $\underline{\xi}$, then it follows from the laws of geometrical optics that the wave facet must have the slopes

$$\zeta_u = -(\xi_1-\xi_1')/(\xi_3-\xi_3')$$
$$\zeta_c = -(\xi_2-\xi_2')/(\xi_3-\xi_3').$$

(See Preisendorfer and Mobley, 1985 for a detailed development of these relations.) Then the argument of the exponential in (3.22) can be written

$$\frac{\zeta_u^2}{\sigma_u^2} + \frac{\zeta_c^2}{\sigma_c^2} = \frac{1}{\sigma_u^2} \cdot \frac{(\xi_1-\xi_1')^2}{(\xi_3-\xi_3')^2} + \frac{1}{\sigma_c^2} \cdot \frac{(\xi_2-\xi_2')^2}{(\xi_3-\xi_3')^2}$$

$$= \frac{1}{(\mu-\mu')^2} \left\{ (1-\mu^2)\left(\frac{\cos^2\phi}{\sigma_u^2} + \frac{\sin^2\phi}{\sigma_c^2}\right) + (1-\mu'^2)\left(\frac{\cos^2\phi'}{\sigma_u^2} + \frac{\sin^2\phi'}{\sigma_c^2}\right) \right.$$

$$\left. - 2(1-\mu^2)^{\frac{1}{2}}(1-\mu'^2)^{\frac{1}{2}}\left(\frac{\cos\phi\,\cos\phi'}{\sigma_u^2} + \frac{\sin\phi\,\sin\phi'}{\sigma_c^2}\right) \right\}$$

$$\equiv q(\mu',\phi';\mu,\phi)$$

This function clearly has the symmetries

$$q(\mu',\phi';\mu,\phi) = q(\mu',2\pi-\phi';\mu,2\pi-\phi) \tag{3.23a}$$

$$= q(\mu',\pi-\phi';\mu,\pi-\phi) \tag{3.23b}$$

$$= q(\mu',\pi+\phi';\mu,\pi+\phi) \tag{3.23c}$$

for $-1 \le \mu' \le 1$ and $-1 \le \mu \le 1$, and for the azimuthal arguments in the ranges $0 \le \phi' < 2\pi$ and $0 \le \phi < 2\pi$. These symmetries are associated with the symmetries of an ellipse and are illustrated in Fig. 5a.

Since the symmetry properties of the reflected radiance are entirely determined by the symmetry properties of the water surface itself, via the underlying wave-slope distribution (3.22), it follows that $r(a,x;\mu',\phi';\mu,\phi)$ also obeys the elliptical symmetries of (3.23). Similar examination of the other three possibilities for reflected and transmitted light leads to the same elliptical symmetry properties of the ϕ',ϕ variables in $r(x,a;\mu',\phi';\mu,\phi)$, $t(a,x;\mu',\phi';\mu,\phi)$ and $t(x,a;\mu',\phi';\mu,\phi)$.

The symmetries of (3.23) in turn imply that the quad-averaged reflectances and transmittances given by (3.19) obey the corresponding symmetries

$$f(r,s|u,v) = f(r,2n+2-s|u,2n+2-v) \tag{3.24a}$$

$$= f(r,n+2-s|u,n+2-v) \tag{3.24b}$$

$$= f(r,n+s|u,n+v) \ . \tag{3.24c}$$

for all Q_{rs} and Q_{uv} in Ξ and specifically for $r,u = 1,\ldots,m$ and $s,v = 1,\ldots,2n$. The azimuthal arguments in (3.24) are computed modulo 2n, on the range $1,\ldots,2n$. Figure 5b illustrates the symmetries (3.24) for the case of $2n = 24$ azimuthal quad divisions. The indexing of (3.24) is not as lucid

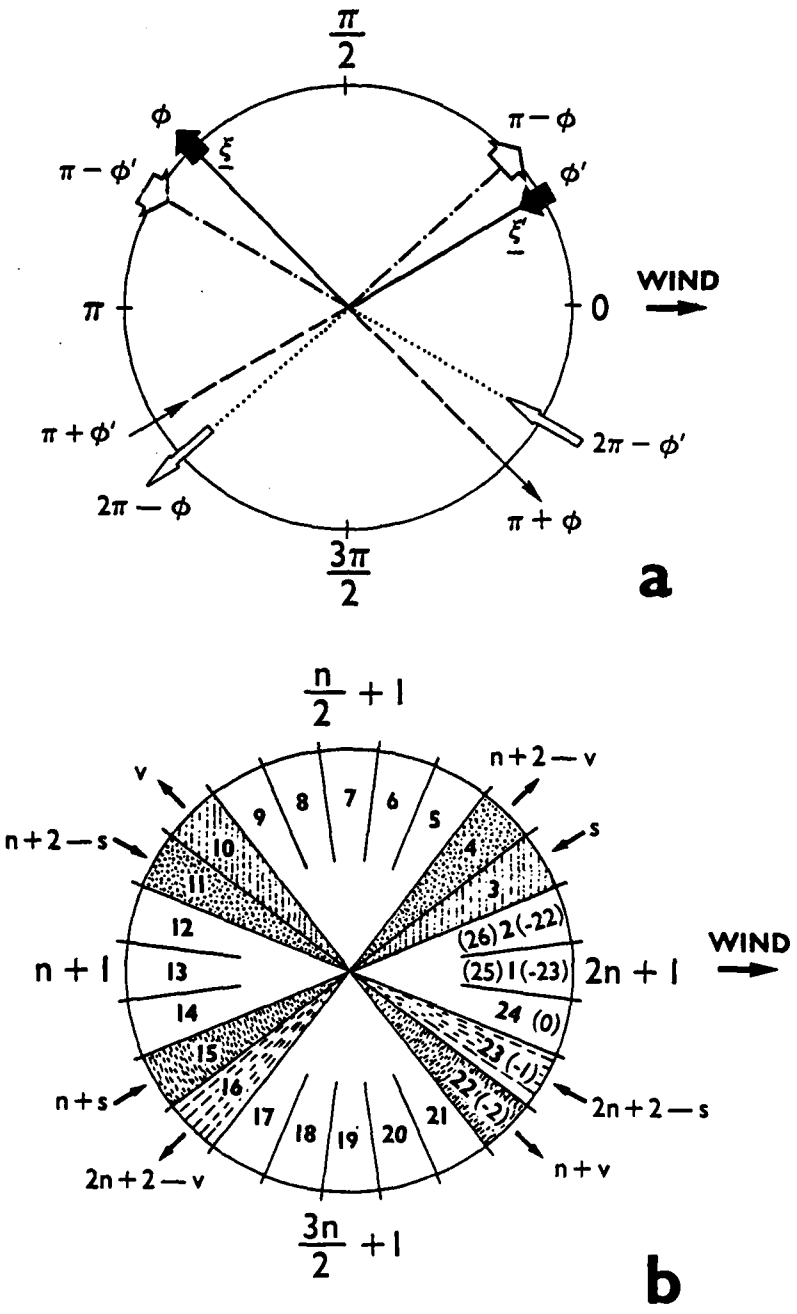

Figure 5.--Azimuthal symmetries of the reflectance and transmittance functions looking downward at the air-water surface. Panel a represents the continuous case, whose symmetries are expressed by (3.23). $\underline{\xi}'$ at ϕ' represents an incoming light ray, and $\underline{\xi}$ at ϕ represents the reflected or transmitted ray. The four pairs of similarly drawn vectors all have the same reflectance and transmittance. Panel b represents the discrete case for $2n = 24$. The symmetries are expressed by (3.24). s represents a quad Q_{rs} containing incoming radiance $N(y;r,s)$ and v represents the quad Q_{uv} receiving the reflected or transmitted radiance $N(y;u,v)$. The four pairs of similarly shaded Q_{rs},Q_{uv} quads all have the same quad-averaged reflectances and transmittances.

as the arguments of (3.23), owing to the azimuthal numbering of quads from 1 to 2n (instead of from 0 to 2n-1).* Nevertheless, a quad indexed by 2n+v is the same as the quad indexed by v. For example, the quad indexed by 1 is the same as that indexed by 2n+1. A moment's contemplation of Fig. 5b, moreover, shows that quad s, centered at ϕ_s, is the symmetric partner, about the wind direction, of quad 2n+2-s, centered at $\phi_{2n+2-s} = 2\pi - \phi_s$.

We also note in Fig. 5b that the directions $\phi_s = \pi/2$ (s = n/2 + 1) and $\phi_s = 3\pi/2$ (s = 3n/2 + 1) are located at quad centers. Having quads centered on the directions at right angles to the wind (at $\phi_1 = 0$) enables us, in applications of the NHM, to place the sun (or other incident light source) at right angles to the wind if we wish to compare, say, the differences in the radiance distributions generated by incoming solar rays parallel to and perpendicular to the wind direction. This is our reason for choosing n even. If n is odd, then the directions at $\pi/2$ and $3\pi/2$ lie on the boundary between two quads, which is not as convenient.

The symmetries of (3.24) imply that the quad-averaged reflectance and transmittance functions need be computed and stored for Q_{rs} only in the "first quadrant" of the unit sphere, i.e., for azimuthal indexes s = $1,2,\ldots,\frac{n}{2}+1$ only (here is where it is convenient to have n even) and for r = 1,...,m: all other possible values can be obtained from symmetry, as is easily seen in Fig. 5b. Thus the elliptical symmetry of the wave slope distribution (3.22) gives a factor of four reduction in the computation and storage requirements involved with processing the r and t functions. However, as seen in (3.24), the discrete indexing conventions are somewhat cumbersome. We therefore

* The numbering of quad azimuth indexes from 1 to 2n instead of from 0 to 2n-1 (as would be instinctively done by a mathematician) was dictated by Fortran programming language restrictions at the time the associated computer code was written.

choose to retain the general notation "f(r,s|u,v)", with s and v running over their full ranges s = 1,...,2n and v = 1,...,2n, in equations such as (3.17) or (3.18). The symmetry relations (3.24) will, however, be used at the appropriate time to introduce simplifications in the spectral model.

g. Discretization of the Bottom Boundary Equations

The bottom boundary condition (2.11), or

$$N(z;\mu,\phi) = \int_{\Xi_-} d\mu' d\phi' \; N(z;\mu',\phi') \; r(z,b;\mu',\phi';\mu,\phi) \quad , \quad (\mu,\phi) \in \Xi_+ \; ,$$

is discretized in the same manner as the surface boundary conditions to obtain the following result which holds at level z of X[z,b] for all Q_{uv} in Ξ_+:

$$\boxed{N(z;u,v) = \sum_r \sum_s N(z;r,s) \; r(z,b;r,s|u,v) \; .} \qquad (3.25)$$

For a matte bottom, r(z,b;μ',φ';μ,φ) is given in analytic form by (2.12) which, when substituted into (3.19), gives

$$r(z,b;r,s|u,v) = \frac{1}{\Omega_{uv}} \iint_{Q_{uv}} d\mu d\phi \iint_{Q_{rs}} d\mu' d\phi' \left[-\frac{r_-}{\pi} \mu' \right]$$

$$= -\frac{r_-}{\pi} \frac{1}{\Omega_{uv}} \Omega_{uv} \Delta\phi'_s \int_{\mu_r(1)}^{\mu_r(2)} \mu' d\mu'$$

$$= -\frac{r_-}{\pi} \Delta\phi'_s \tfrac{1}{2} \left[\mu_r^2(2) - \mu_r^2(1) \right]$$

$$= -\frac{r_-}{\pi} \Delta\phi'_s \tfrac{1}{2} \left[\mu_r(2) + \mu_r(1) \right] \left[\mu_r(2) - \mu_r(1) \right]$$

$$= -\frac{r_-}{\pi} \Delta\phi'_s \mu_r \Delta\mu'_r$$

Therefore,

$$r(z,b;r,s|u,v) = -\frac{r_-}{\pi} \mu_r \Omega_{rs} , \tag{3.26}$$

for Q_{rs} in Ξ_- and Q_{uv} in Ξ_+. It is to be noted that $\mu_r < 0$ since Q_{rs} in Ξ_-. Thus the matte reflectance is a positive-valued function, the magnitude of which depends explicitly on the quad solid angle Ω_{rs}.

The matter of the evaluation of the air-water surface transfer functions is considerably more complex than the bottom transfer function and will be taken up in §9. Moreover, the reflectance of the lower boundary of a medium resting on an infinitely deep water layer will be considered in §10.

We have now arrived at level 2 of Fig. 2, in that we have developed a finite set of discrete geometrical model equations for the quad-averaged radiances.

4. FOURIER POLYNOMIAL ANALYSIS

In order to recast the discrete geometrical equations into a discrete spectral form, we need several results from the theory of Fourier analysis of discrete functions. This section collects the needed formulas; they will be applied in §5.

a. Discrete Orthogonality Relations

We first present several formulas involving trigonometric functions whose arguments are the discrete azimuthal angles ϕ_v defined in (3.1). Let $k,\ell = 0,\ldots,n$. Then

$$\sum_{v=1}^{2n} \cos(k\phi_v)\cos(\ell\phi_v) = \begin{cases} 0 \text{ if } k \neq \ell \\ 2n \text{ if } k = \ell = 0 \text{ or } n \\ n \text{ if } k = \ell,\ \ell = 1,\ldots,n-1. \end{cases}$$

Using the Kronecker delta symbol (3.6), these results can be condensed as

$$\sum_{v=1}^{2n} \cos(k\phi_v)\cos(\ell\phi_v) = n(\delta_{k+\ell} + \delta_{k-\ell} + \delta_{k+\ell-2n}). \tag{4.1}$$

Likewise we have

$$\sum_{v=1}^{2n} \sin(k\phi_v)\sin(\ell\phi_v) = \begin{cases} 0 \text{ if } k \neq \ell \\ 0 \text{ if } k = \ell = 0 \text{ or } n \\ n \text{ if } k = \ell\ ,\ \ell = 1,\ldots,n-1 \end{cases}$$

which can be written

$$\sum_{v=1}^{2n} \sin(k\phi_v)\sin(\ell\phi_v) = n(\delta_{k-\ell} - \delta_{k+\ell} - \delta_{k+\ell-2n}). \tag{4.2}$$

Finally we note that, for all $k,\ell = 0,\ldots,n$,

$$\sum_{v=1}^{2n} \cos(k\phi_v) \sin(\ell\phi_v) = 0 \ . \tag{4.3}$$

After application of trigonometric identities and (4.1)-(4.3), we obtain the following formulas for $k,\ell = 0,\ldots,n-1$:

$$\sum_{v=1}^{2n} \cos(k\phi_v) \cos\ell(\phi_s-\phi_v) = n(\delta_{k+\ell} + \delta_{k-\ell} + \delta_{k+\ell-2n}) \cos(\ell\phi_s) \tag{4.4}$$

and

$$\sum_{v=1}^{2n} \sin(k\phi_v) \cos\ell(\phi_s-\phi_v) = n(\delta_{k-\ell} - \delta_{k+\ell} - \delta_{k+\ell-2n}) \sin(\ell\phi_s) \ . \tag{4.5}$$

b. Fourier Polynomial Formulas

Let $f_v \equiv f(\phi_v)$ be any *discrete* function of the azimuthal angle ϕ, where the ϕ_v, $v = 1,\ldots,2n$, are given by (3.1). Then f_v has the Fourier polynomial representation

$$f_v = \sum_{\ell=0}^{n} [\hat{f}_1(\ell) \cos(\ell\phi_v) + \hat{f}_2(\ell) \sin(\ell\phi_v)] \ , \quad v = 1,\ldots,2n \tag{4.6}$$

where $\hat{f}_1(\ell)$ and $\hat{f}_2(\ell)$ are the *spectral amplitudes*, which we shall determine below. This is the formula by which we will transform the discrete geometrical Natural Hydrosol Model into discrete spectral form. We shall see that the number of values of the discrete function f_v (namely 2n) is determined exactly by n+1 generally nonzero cosine terms and n-1 generally nonzero sine terms in (4.6). The $\cos(\ell\phi_v)$ term with $\ell = 0$ gives a

constant, $\hat{f}_1(0)$, which is the average of f_v over v = 1,...,2n. Moreover, the $\cos(n\phi_v)$ term gives the "two-point oscillation," the wavelength of which is $2\Delta\phi = 2\pi/n$. This shows that the shortest resolvable wave in the Fourier representation is directly determined by the fineness of the directional resolution $\Delta\phi$ in the quad-averaging. Using the representation (4.6) for f_v, which exactly reproduces f_v, will introduce no further loss of radiance detail in the azimuthal direction when N(y;u,v) replaces f_v. Since $\sin(\ell\phi_v)$ is identically zero if $\ell = 0$, or $\ell = n$, the amplitudes $\hat{f}_2(0)$ and $\hat{f}_2(n)$ may be arbitrarily chosen. We therefore will define $\hat{f}_2(0) \equiv \hat{f}_2(n) \equiv 0$, which will be convenient for bookkeeping purposes in the computer code.

The *cosine amplitudes* $\hat{f}_1(\ell)$ are determined by multiplying (4.6) by $\cos(k\phi_v)$ and summing over v to find

$$\sum_{v=1}^{2n} f_v \cos(k\phi_v) = \sum_{\ell=0}^{n} \hat{f}_1(\ell)\left[\sum_{v=1}^{2n} \cos(\ell\phi_v)\cos(k\phi_v)\right] + \sum_{\ell=0}^{n} \hat{f}_2(\ell)\left[\sum_{v=1}^{2n} \sin(\ell\phi_v)\cos(k\phi_v)\right].$$

Applying the orthogonality relations (4.1) and (4.3) yields

$$\sum_{v=1}^{2n} f_v \cos(k\phi_v) = \sum_{\ell=0}^{n} \hat{f}_1(\ell) n[\delta_{k+\ell} + \delta_{k-\ell} + \delta_{k+\ell-2n}]$$

$$= \hat{f}_1(k) n[\delta_{2k} + 1 + \delta_{2k-2n}].$$

Replacing the index k by ℓ and defining

$$\varepsilon_\ell \equiv n(1 + \delta_{2\ell} + \delta_{2\ell-2n}) = \begin{cases} 2n \text{ if } \ell = 0 \text{ or } \ell = n \\ n \text{ if } \ell = 1,\ldots,n-1 \end{cases} \tag{4.7}$$

we can write

$$\hat{f}_1(\ell) \equiv \frac{1}{\varepsilon_\ell} \sum_{v=1}^{2n} f_v \cos(\ell\phi_v) \qquad (4.8)$$
$$\ell = 0,\ldots,n$$

Expanding (4.8) gives

$$\hat{f}_1(0) = \frac{1}{2n} \sum_{v=1}^{2n} f_v \qquad \text{(the average of } f_v\text{)}$$

$$\hat{f}_1(\ell) = \frac{1}{n} \sum_{v=1}^{2n} f_v \cos(\ell\phi_v) \qquad \text{if } \ell = 1,\ldots,n-1$$

$$\hat{f}_1(n) = \frac{1}{2n} \sum_{v=1}^{2n} (-1)^v f_v \,.$$

The generally non-zero *sine amplitudes* $\hat{f}_2(\ell)$ are determined for $\ell = 1,\ldots,n-1$ in a like manner by multiplying $\sin(k\phi_v)$ into (4.6), summing over v, and using (4.2) and (4.3) to find

$$\hat{f}_2(\ell) \equiv \frac{1}{\gamma_\ell} \sum_{v=1}^{2n} f_v \sin(\ell\phi_v) \qquad (4.9)$$
$$\ell = 1,2,\ldots,n-1.$$

Here γ_ℓ is defined similarly to ε_ℓ in (4.7):

$$\gamma_\ell \equiv n(1 - \delta_{2\ell} - \delta_{2\ell-2n}) = \begin{cases} 0 \text{ if } \ell = 0 \text{ or } \ell = n \\ n \text{ if } \ell = 1,\ldots,n-1 \end{cases} \qquad (4.10)$$

Note that $\gamma_0 = \gamma_n = 0$ and that these values, which will be of use in later developments, do not occur in (4.9). Moreover, in the allowed range of ℓ in (4.9), we have $\gamma_\ell = \varepsilon_\ell = n$. Expanding (4.9) and recalling our decision to set $\hat{f}_2(0) \equiv \hat{f}_2(n) \equiv 0$, gives

$$\hat{f}_2(0) = 0$$

$$\hat{f}_2(\ell) = \frac{1}{n} \sum_{v=1}^{2n} f_v \sin(\ell\phi_v) \qquad \text{if } \ell = 1,\ldots,n-1$$

$$\hat{f}_2(n) = 0 \ .$$

Equations (4.6)-(4.10) bear a resemblance to the well known Fourier series representation of a continuous function of ϕ, although the two-point amplitudes $\hat{f}_1(n)$ and $\hat{f}_2(n)$ are peculiar to the discrete case.

Consider next a function that is a linear combination of $\cos\ell(\phi_s-\phi_v)$ terms:

$$g_{sv} \equiv g[\cos(\phi_s-\phi_v)] = \sum_{\ell=0}^{n} \hat{g}(\ell) \cos\ell(\phi_s-\phi_v) \ . \tag{4.11}$$

This form is motivated on the basis of (3.13k). Upon multiplying g_{sv} by $\cos(k\phi_v)$, summing over v, applying (4.4) and recalling (4.7), the amplitudes $\hat{g}(\ell)$ of g_{sv} are defined to be

$$\hat{g}(\ell) \equiv \frac{1}{\epsilon_\ell \cos(\ell\phi_s)} \sum_{v=1}^{2n} g_{sv} \cos(\ell\phi_v) \ . \tag{4.12}$$

Since g_{sv} depends only on the difference $\phi_s-\phi_v$ rather than on ϕ_s and ϕ_v separately, we can, for example, anchor $\phi_s-\phi_v$ to $\phi_1 = 0$, i.e., set s = 1 in (4.12). This will be done later in (5.5b).

We finally consider the representation of an arbitrary discrete function of two direction variables ϕ_s and ϕ_v. Let $h_{sv} \equiv h(\phi_s,\phi_v)$; s,v = 1,...,2n. Then we expect that h_{sv} is of the form

$$
\begin{aligned}
h_{sv} = & \sum_{k=0}^{n} \sum_{\ell=0}^{n} \hat{h}_{11}(k,\ell) \cos(k\phi_s) \cos(\ell\phi_v) \\
& + \sum_{k=0}^{n} \sum_{\ell=0}^{n} \hat{h}_{12}(k,\ell) \cos(k\phi_s) \sin(\ell\phi_v) \\
& + \sum_{k=0}^{n} \sum_{\ell=0}^{n} \hat{h}_{21}(k,\ell) \sin(k\phi_s) \cos(\ell\phi_v) \\
& + \sum_{k=0}^{n} \sum_{\ell=0}^{n} \hat{h}_{22}(k,\ell) \sin(k\phi_s) \sin(\ell\phi_v) \, .
\end{aligned}
\tag{4.13}
$$

To find the amplitudes $\hat{h}_{11}(k,\ell)$, for example, we multiply (4.13) by $\cos(k'\phi_s) \cos(\ell'\phi_v)$ and sum over s and v to obtain

$$
\sum_{s=1}^{2n} \sum_{v=1}^{2n} h_{sv} \cos(k'\phi_s) \cos(k'\phi_v) =
$$

$$
\sum_{k=0}^{n} \sum_{\ell=0}^{n} \hat{h}_{11}(k,\ell) \left[\sum_{s=1}^{2n} \cos(k\phi_s) \cos(k'\phi_s) \right] \left[\sum_{v=1}^{2n} \cos(\ell\phi_v) \cos(\ell'\phi_v) \right]
$$

+ 3 other similar terms.

Using (4.1)-(4.3) formally yields the first of the following defining equations:

$$
\left.
\begin{aligned}
\hat{h}_{11}(k,\ell) &\equiv \frac{1}{\varepsilon_k \varepsilon_\ell} \sum_{s=1}^{2n} \sum_{v=1}^{2n} h_{sv} \cos(k\phi_s) \cos(\ell\phi_v) \\
\hat{h}_{12}(k,\ell) &\equiv \frac{1}{\varepsilon_k \gamma_\ell} \sum_{s=1}^{2n} \sum_{v=1}^{2n} h_{sv} \cos(k\phi_s) \sin(\ell\phi_v) \\
\hat{h}_{21}(k,\ell) &\equiv \frac{1}{\gamma_k \varepsilon_\ell} \sum_{s=1}^{2n} \sum_{v=1}^{2n} h_{sv} \sin(k\phi_s) \cos(\ell\phi_v) \\
\hat{h}_{22}(k,\ell) &\equiv \frac{1}{\gamma_k \gamma_\ell} \sum_{s=1}^{2n} \sum_{v=1}^{2n} h_{sv} \cos(k\phi_s) \sin(\ell\phi_v)
\end{aligned}
\right\}
\tag{4.14}
$$

Analogous operations readily yield similar formulas for the remaining three amplitudes as shown in (4.14). The pattern of the formulas follows from and builds precisely on the one-dimensional case: see (4.8) and (4.9) for the allowed ranges of k and ℓ. Note that cosine amplitudes have ε_ℓ, while sine amplitudes have γ_ℓ normalizers, and that $\varepsilon_\ell = \gamma_\ell = n$ in the common allowed ranges ($k,\ell = 1,\ldots,n-1$). The arbitrary zero amplitudes $\hat{f}_2(0)$, $\hat{f}_2(n)$ now have their counterparts in $\hat{h}_{12}(k,\ell) = \hat{h}_{21}(k,\ell) = \hat{h}_{22}(k,\ell) = 0$ for k and ℓ equal to 0 or n, as the "2" subscript on $\hat{h}$ requires. Thus, for future reference we summarize these singular values as

$$\begin{aligned} &\hat{h}_{12}(k,0) = \hat{h}_{12}(k,n) = 0 \qquad , \quad k = 0,\ldots,n \\ &\hat{h}_{21}(0,\ell) = \hat{h}_{21}(n,\ell) = 0 \qquad , \quad \ell = 0,\ldots,n \\ &\hat{h}_{22}(0,0) = \hat{h}_{22}(n,n) = 0 \\ &\hat{h}_{22}(n,0) = \hat{h}_{22}(0,n) = 0 \end{aligned} \tag{4.14a}$$

It will turn out that when (4.14) and (4.14a) are applied to the air-water surface's transfer functions in §5b below, the amplitudes $\hat{h}_{12}(k,\ell)$ and $\hat{h}_{21}(k,\ell)$ will be identically zero owing to certain symmetries of the surface.

We now have at our disposal all of the tools necessary for converting the discrete geometrical Natural Hydrosol Model into a discrete spectral form.

c. Rayleigh's Equality

A check on the spectral parts of the computer code can be made using a Rayleigh-type equality, which relates the squares of the values f_v to the squares of their amplitudes $\hat{f}_1(\ell)$ and $\hat{f}_2(\ell)$. To derive the present form of Rayleigh's equality, we evaluate $\sum_v f_v^2$ in terms of the amplitudes, as follows:

$$\sum_{v=1}^{2n} f_v^2 = \sum_{v=1}^{2n} \left\{ \sum_{k=0}^{n} \left[\hat{f}_1(k) \cos(k\phi_v) + \hat{f}_2(k) \sin(k\phi_v) \right] \right\} \times$$

$$\times \left\{ \sum_{\ell=0}^{n} \left[\hat{f}_1(\ell) \cos(\ell\phi_v) + \hat{f}_2(\ell) \sin(\ell\phi_v) \right] \right\}$$

$$= \sum_{k=0}^{n} \sum_{\ell=0}^{n} \hat{f}_1(k)\, \hat{f}_1(\ell) \sum_{v=1}^{2n} \cos(k\phi_v) \cos(\ell\phi_v)$$

$$+ 3 \text{ similar terms.}$$

The sums over v are evaluated by (4.1)-(4.3). The four preceding summation terms reduce to two:

$$\sum_{v=1}^{2n} f_v^2 = \sum_{k=0}^{n} \sum_{\ell=0}^{n} \hat{f}_1(k)\, \hat{f}_1(\ell)\, n(\delta_{k+\ell} + \delta_{k-\ell} + \delta_{k+\ell-2n})$$

$$+ \sum_{k=0}^{n} \sum_{\ell=0}^{n} \hat{f}_2(k)\, \hat{f}_2(\ell)\, n(\delta_{k-\ell} - \delta_{k+\ell} - \delta_{k+\ell-2n}) .$$

Only the $k=\ell$ terms remain, and thereby we find the desired form of Rayleigh's equality:

$$\sum_{v=1}^{2n} f_v^2 = \sum_{\ell=0}^{n} \left[\varepsilon_\ell\, \hat{f}_2^2(\ell) + \gamma_\ell\, \hat{f}_2^2(\ell) \right] . \tag{4.15}$$

Expanding (4.15) and explicitly evaluating ε_ℓ and γ_ℓ gives an alternate useful form

$$\frac{1}{2n} \sum_{v=1}^{2n} f_v^2 = \hat{f}_1^2(0) + \frac{1}{2} \sum_{\ell=1}^{n-1} \left[\hat{f}_1^2(\ell) + \hat{f}_2^2(\ell) \right] + \hat{f}_1^2(n) . \tag{4.16}$$

A Rayleigh's equality can be derived for the two-dimensional case by evaluating $\sum_s \sum_v h_{sv}^2$. The result corresponding to (4.15) is

$$\sum_{s=1}^{2n}\sum_{v=1}^{2n} h_{sv}^2 = \sum_{k=0}^{n}\sum_{\ell=0}^{n}\Big[\varepsilon_k\varepsilon_\ell\,\hat{h}_{11}^2(k,\ell) + \varepsilon_k\gamma_\ell\,\hat{h}_{12}^2(k,\ell) + \gamma_k\varepsilon_\ell\,\hat{h}_{21}^2(k,\ell) + \gamma_k\gamma_\ell\,\hat{h}_{22}^2(k,\ell)\Big]\,. \tag{4.17}$$

5. THE NATURAL HYDROSOL MODEL IN DISCRETE SPECTRAL FORM

a. Transforming the Radiative Transfer Equation to Spectral Form: The Local Interaction Equations

The discrete geometric transfer equation shown in (3.12) can be rewritten as separate equations for *upward radiances*, $N^{+}(y;u,v)$ where Q_{uv} is in Ξ_{+}, and for *downward radiances*, $N^{-}(y;u,v)$ where Q_{uv} is in Ξ_{-}. The + and - superscripts are now added to the radiances to denote which hemisphere, Ξ_{+} or Ξ_{-}, contains Q_{uv} (recall the discussion leading to (3.2)). In a similar fashion, a general function of (r,s) and (u,v) would require two superscripts. Thus for the phase function $p(y;r,s|u,v)$ we would write

$$\text{"}p^{++}(y;r,s|u,v)\text{"} \quad \text{for } p(y;r,s|u,v) \quad \text{if } Q_{rs} \text{ in } \Xi_{+} \text{ and } Q_{uv} \text{ in } \Xi_{+},$$
$$\text{"}p^{+-}(y;r,s|u,v)\text{"} \quad \text{for } p(y;r,s|u,v) \quad \text{if } Q_{rs} \text{ in } \Xi_{+} \text{ and } Q_{uv} \text{ in } \Xi_{-},$$
$$\text{"}p^{-+}(y;r,s|u,v)\text{"} \quad \text{for } p(y;r,s|u,v) \quad \text{if } Q_{rs} \text{ in } \Xi_{-} \text{ and } Q_{uv} \text{ in } \Xi_{+},$$
$$\text{"}p^{--}(y;r,s|u,v)\text{"} \quad \text{for } p(y;r,s|u,v) \quad \text{if } Q_{rs} \text{ in } \Xi_{-} \text{ and } Q_{uv} \text{ in } \Xi_{-}.$$

The isotropy of the phase function as expressed by (3.13h) implies that

$$p^{++}(y;r,s|u,v) = p^{--}(y;r,s|u,v)$$

and

$$p^{+-}(y;r,s|u,v) = p^{-+}(y;r,s|u,v).$$

Thus only a single superscript is needed, and we shall write

$$\text{"}p^{+}(y;r,s|u,v)\text{"} \quad \text{for} \quad p^{++}(y;r,s|u,v) \; (= p^{--}(y;r,s|u,v))$$
and (5.1)
$$\text{"}p^{-}(y;r,s|u,v)\text{"} \quad \text{for} \quad p^{+-}(y;r,s|u,v) \; (= p^{-+}(y;r,s|u,v)),$$

where we have recalled the azimuthal symmetry of the quad-averaged phase function. With the superscripted notation, the quad-averaged radiative transfer equation of (3.12) takes its two-flow form:

$$\mp\mu_u \frac{dN^{\pm}(y;u,v)}{dy} = -N^{\pm}(y;u,v) + \omega(y) \sum_r \sum_s N^{+}(y;r,s)\, p^{\pm}(y;r,s|u,v) + \omega(y) \sum_r \sum_s N^{-}(y;r,s)\, p^{\mp}(y;r,s|u,v) \tag{5.2}$$

where now $\mu_u > 0$ and

$x \le y \le z$

$u,r = 1,\ldots,m$

$v,s = 1,\ldots,2n$

and "$\sum_r \sum_s$" represents sums over hemispheres indicated by the superscript on N.

Equation (5.2) is a coupled pair of differential equation systems. The *upward system* is obtained by taking all upper signs together. This system describes the evolution with depth y of the upward radiances $N^{+}(y;u,v)$. The *downward system* is obtained by taking all lower signs together, and describes the evolution of downward radiances $N^{-}(y;u,v)$. Note particularly that $\mu_u > 0$ for $u = 1,\ldots,m$ for both upward and downward systems; the negative values of μ_u seen in (3.12) are now incorporated in the $\mp\mu_u$ notation of (5.2).

The system (5.2) is in the form of the *local interaction principles* or the *local form* of the *principles of invariance*. See Preisendorfer (1965, p. 103) and H.O., Vol. III, p. 4; Vol. II, p. 295. This pair of systems of differential equations can be solved as it stands using boundary conditions (3.17), (3.18) and (3.25) and applying the general tools and procedures of §6 and §7, below, leading to the various reflectance and transmittance matrices of the body of the

water mass. However, as noted in our introductory remarks, the computation and storage loads accompanying (5.2) can be cut considerably by first resolving the $N^{\pm}(y;u,v)$ into their azimuthal spectral amplitudes, and finding the spectral counterparts of (5.2).

The derivation of the spectral form of (5.2) begins by noting that, for fixed y and u values, $N^{\pm}(y;u,v)$ as a function of v can be represented by a trigonometric polynomial of the form (4.6)*:

$$N^{\pm}(y;u,v) \equiv \sum_{\ell=0}^{n} [A_1^{\pm}(y;u;\ell)\cos(\ell\phi_v) + A_2^{\pm}(y;u;\ell)\sin(\ell\phi_v)] \quad . \tag{5.3}$$

$$a \le x \le y \le z \le b$$

$$u = 1,\ldots,m$$

$$v = 1,\ldots,2n$$

We have added arguments (y;u) to the *cosine amplitudes* for radiance, $A_1^{\pm}(y;u;\ell)$, and to the *sine amplitudes* for radiance, $A_2^{\pm}(y;u;\ell)$, in order to show their full functional form as needed in the computations. These amplitudes, for fixed y and u, are computed from equations (4.8) and (4.9) given the v-dependence of $N^{\pm}(y;u,v)$. Specifically, we have, for the case of quads:

$$A_1^{\pm}(y;u;\ell) = \frac{1}{\varepsilon_\ell}\sum_{v=1}^{2n} N^{\pm}(y;u,v)\cos\ell\phi_v \quad , \quad \ell = 0,\ldots,n;\ u = 1,\ldots,m-1 \tag{5.3a}$$

$$A_2^{\pm}(y;u;\ell) = \frac{1}{\gamma_\ell}\sum_{v=1}^{2n} N^{\pm}(y;u,v)\sin\ell\phi_v \quad , \quad \ell = 1,\ldots,n-1;\ u = 1,\ldots,m-1 \tag{5.3b}$$

---

* Theoretical works on radiative transfer theory (e.g., Preisendorfer, 1965 or 1976) sometimes use the notation "$A_p(y,\pm;u;\ell)$" instead of "$A_p^{\pm}(y;u;\ell)$", that is, they try to keep a basic symbol such as A_p free of avoidable superscripts. The present notation is chosen so that the arguments of a function, here y, u and ℓ, show *only* those independent variables which the associated FORTRAN computer code references in DO-loops.

Of particular interest is the $\ell=0$ case for the cosine amplitude. This will serve to define a generalization of the classic two-flow irradiance model (in §8). In this case (5.3a) reduces to

$$A_1^{\pm}(y;u;0) = \frac{1}{\Omega(Z_u)} \int_{Z_u} N^{\pm}(y;\underline{\xi})\, d\Omega(\underline{\xi}) \qquad (5.3c)$$
$$u = 1,\ldots,m$$

where Z_u is the zone comprising all quads Q_{uv}, $v = 1,\ldots,2v$ for $u = 1,\ldots,m-1$; and $\Omega(Z_u)$ is the solid angle content of Z_u, namely $\Omega(Z_u) = 2n\ \Omega_{uv}$. For $u = m$, Z_m is the polar cap. Thus $A_1^{\pm}(y;u;0)$ is then simply the zonally averaged radiance for zone Z_u, or cap Z_m. The classic two-flow irradiance model has only one "zone": the upper or lower hemisphere of Ξ. Hence the system of zero-mode equations (5.23) below will serve to check the accuracy of the classic irradiance model. For the polar cap case in general, where $u = m$, there is by definition no dependence of radiance on the azimuthal angle ϕ_v, and an expansion like (5.3) is formally trivial. To retain the useful notation in (5.3), however, we recall the notational convention in (3.2) and define

$$A_1^{\pm}(y;m;0) \equiv N^{\pm}(y;m,\cdot)\ \left(= \frac{1}{\Omega(Z_m)} \int_{Z_m} N^{\pm}(y;\underline{\xi})\, d\Omega(\underline{\xi}) \quad , \text{ as in (5.3c)}\right)$$

$$A_1^{\pm}(y;m;\ell) \equiv 0 \quad , \quad \ell = 1,\ldots,n \qquad (5.4)$$

and

$$A_2^{\pm}(y;m;\ell) \equiv 0 \quad , \quad \ell = 0,\ldots,n\ .$$

Therefore Eq. (5.3) may be regarded as holding for all quads and caps, if we remember that *all amplitudes for polar caps are by definition zero, except the cosine amplitude for the zero azimuthal wave number.*

Continuing the preliminary observations leading to the spectral form of (5.2), we note that, for fixed y, r and u, where $r \neq m$ and $u \neq m$, the quad-averaged phase functions $p^{\pm}(y;r,s|u,v)$ can, by the isotropy conditions (3.13e,k), be written as linear combinations of $\cos\ell(\phi_s-\phi_v)$, $s,v = 1,\ldots,2n$. Thus $p^{\pm}(y;r,s|u,v)$ can be represented by a series of the form (4.11), namely

$$p^{\pm}(y;r,s|u,v) = \sum_{\ell=0}^{n} \hat{p}^{\pm}(y;r,u;\ell)\cos\ell(\phi_s-\phi_v) \qquad (5.5a)$$

$x \leq y \leq z$

$r,u = 1,\ldots,m$

$s,v = 1,\ldots,2n.$

The amplitudes $\hat{p}^{\pm}(y;r,u;\ell)$ are defined by an equation of the form (4.12), namely

$$\hat{p}^{\pm}(y;r,u;\ell) \equiv \frac{1}{\varepsilon_\ell \cos(\ell\phi_s)} \sum_{v=1}^{2n} p^{\pm}(y;r,s|u,v)\cos\ell(\phi_s-\phi_v) \; . \qquad (5.5b)$$

We next consider the four cases which occur in numerical computations of the amplitudes $\hat{p}^{\pm}(y;r,u;\ell)$. Each of these cases is evaluated by specializing the form of (5.5b). They are as follows:

1) *Quad-to-Quad Case* ($u,r = 1,\ldots,m-1$). With $s = 1$, (5.5b) becomes

$$\hat{p}^{\pm}(y;r,u;\ell) \equiv \frac{1}{\varepsilon_\ell} \sum_{v=1}^{2n} p^{\pm}(y;r,1|u,v)\cos(\ell\phi_v) \qquad (5.6a)$$

$\ell = 0,\ldots,n$

2) *Cap-to-Quad Case* ($r = m$; $u = 1,\ldots,m-1$). Then (5.5b) becomes

$$\hat{p}^{\pm}(y;m,u;0) \equiv p^{\pm}(y;m,\cdot|u,1)$$
$$\hat{p}^{\pm}(y;m,u;\ell) \equiv 0 \quad , \quad \ell = 1,\ldots,n \tag{5.6b}$$

3) *Quad-to-Cap Case* (r = 1,...,m-1; u = m). Then (5.5b) becomes

$$\hat{p}^{\pm}(y;r,m;0) \equiv p^{\pm}(y;r,1|m,\cdot)$$
$$\hat{p}^{\pm}(y;r,m;\ell) \equiv 0 \quad , \quad \ell = 1,\ldots,n \tag{5.6c}$$

4) *Cap-to-Cap Case* (r = m, u = m). Then (5.5b) becomes

$$\hat{p}^{\pm}(y;m,m;0) \equiv p^{\pm}(y;m,\cdot|m,\cdot)$$
$$\hat{p}^{\pm}(y;m,m;\ell) \equiv 0 \quad , \quad \ell = 1,\ldots,n \tag{5.6d}$$

Observe in (5.6a,b,c) that s or v has been set to 1, as the case may be. This is permissible by virtue of the dependence of $p^{\pm}(y;r,s|u,v)$ on v-s rather than on v and s separately (see (3.13k)).

We turn next to the decomposition of (5.2) into its spectral components. We split the task into two main parts: (i) the case of a non-polar-quad output radiance $N^{\pm}(y;u,v)$, u = 1,...,m-1; and (ii) the case of the polar cap radiances $N^{\pm}(y;m,\cdot)$.

For case (i), we now use the radiances and phase functions from (5.3) and (5.5a) to substitute into (5.2). The sum over quads in (5.2) must now be explicitly evaluated as in (3.2). For the present case of a non-polar output quad, i.e., u = 1,...,m-1, the radiative transfer equation (5.2) becomes

$$\mp\mu_u \frac{d}{dy}\left\{\sum_{\ell=0}^{n}\left[A_1^{\pm}(y;u;\ell)\cos(\ell\phi_v) + A_2^{\pm}(y;u;\ell)\sin(\ell\phi_v)\right]\right\} =$$

$$-\sum_{\ell=0}^{n}\left[A_1^{\pm}(y;u;\ell)\cos(\ell\phi_v) + A_2^{\pm}(y;u;\ell)\sin(\ell\phi_v)\right] \qquad (5.7)$$

$$+\omega(y)\sum_{r=1}^{m-1}\sum_{s=1}^{2n}\sum_{\ell=0}^{n}\left[A_1^{+}(y;r;\ell)\cos(\ell\phi_s) + A_2^{+}(y;r;\ell)\sin(\ell\phi_s)\right]\left[\sum_{k=0}^{n}\hat{p}^{\pm}(y;r,u;k)\cosk(\phi_s-\phi_v)\right]$$

$$+\omega(y)\,A_1^{+}(y;m;0)\,\hat{p}^{\pm}(y;m,u;0)$$

$$+\omega(y)\sum_{r=1}^{m-1}\sum_{s=1}^{2n}\sum_{\ell=0}^{n}\left[A_1^{-}(y;r;\ell)\cos(\ell\phi_s) + A_2^{-}(y;r;\ell)\sin(\ell\phi_s)\right]\left[\sum_{k=0}^{n}\hat{p}^{\mp}(y;r,u;k)\cosk(\phi_s-\phi_v)\right]$$

$$+\omega(y)\,A_1^{-}(y;m,0)\,\hat{p}^{\mp}(y;m,u;0)\ .$$

The second and fourth terms on the right side of (5.7) each have the form

$$\omega(y)\sum_{r=1}^{m-1}\sum_{\ell=0}^{n}\sum_{k=0}^{n}A_1(y;r;\ell)\,\hat{p}(y;r,u;k)\left[\sum_{s=1}^{2n}\cos(\ell\phi_s)\cosk(\phi_s-\phi_v)\right]$$

$$+\omega(y)\sum_{r=1}^{m-1}\sum_{\ell=0}^{n}\sum_{k=0}^{n}A_2(y;r;\ell)\,\hat{p}(y;r,u;k)\left[\sum_{s=1}^{2n}\sin(\ell\phi_s)\cosk(\phi_s-\phi_v)\right]\ . \qquad (5.8)$$

Application of (4.4) and (4.5) to the sums over s gives

$$\omega(y)\sum_{r=1}^{m-1}\sum_{\ell}\sum_{k}A_1(y;r;\ell)\,\hat{p}(y;r,u;k)\,n(\delta_{k+\ell}+\delta_{k-\ell}+\delta_{k+\ell-2n})\cos(\ell\phi_v)$$

$$+\omega(y)\sum_{r=1}^{m-1}\sum_{\ell}\sum_{k}A_2(y;r;\ell)\,\hat{p}(y;r,u;k)\,n(\delta_{k-\ell}-\delta_{k+\ell}-\delta_{k+\ell-2n})\sin(\ell\phi_v)$$

$$=\omega(y)\sum_{r=1}^{m-1}\sum_{\ell}A_1(y;r;\ell)\,\hat{p}(y;r,u;\ell)\,n(1+\delta_{2\ell}+\delta_{2\ell-2n})\cos(\ell\phi_v)$$

$$+\omega(y)\sum_{r=1}^{m-1}\sum_{\ell}A_2(y;r;\ell)\,\hat{p}(y;r,u;\ell)\,n(1-\delta_{2\ell}-\delta_{2\ell-2n})\sin(\ell\phi_v)\ .$$

Thus (5.7) becomes

$$\mp\mu_u \sum_{\ell=0}^{n}\left[\frac{dA_1^{\pm}(y;u;\ell)}{dy}\cos(\ell\phi_v) + \frac{dA_2^{\pm}(y;u;\ell)}{dy}\sin(\ell\phi_v)\right] =$$

$$- \sum_{\ell=0}^{n}\left[A_1^{\pm}(y;u;\ell)\cos(\ell\phi_v) + A_2^{\pm}(y;u;\ell)\sin(\ell\phi_v)\right] \qquad (5.9)$$

$$+ \omega(y) \sum_{\ell=0}^{n}\sum_{r=1}^{m-1} A_1^{+}(y;r;\ell)\,\hat{p}^{\pm}(y;r,u;\ell)\,n(1+\delta_{2\ell}+\delta_{2\ell-2n})\cos(\ell\phi_v)$$

$$+ \omega(y)\,A_1^{+}(y;m;0)\,\hat{p}^{\pm}(y;m,u;0)$$

$$+ \omega(y) \sum_{\ell=0}^{n}\sum_{r=1}^{m-1} A_2^{+}(y;r;\ell)\,\hat{p}^{\pm}(y;r,u;\ell)\,n(1-\delta_{2\ell}-\delta_{2\ell-2n})\sin(\ell\phi_v)$$

$$+ \omega(y) \sum_{\ell=0}^{n}\sum_{r=1}^{m-1} A_1^{-}(y;r;\ell)\,\hat{p}^{\mp}(y;r,u;\ell)\,n(1+\delta_{2\ell}+\delta_{2\ell-2n})\cos(\ell\phi_v)$$

$$+ \omega(y)\,A_1^{-}(y;m;0)\,\hat{p}^{\mp}(y;m,u;0)$$

$$+ \omega(y) \sum_{\ell=0}^{n}\sum_{r} A_2^{-}(y;r;\ell)\,\hat{p}^{\mp}(y;r,u;\ell)\,n(1-\delta_{2\ell}-\delta_{2\ell-2n})\sin(\ell\phi_v)\,.$$

The polar quad terms are coefficients of $\cos(\ell\phi_v)$ for $\ell = 0$, and as such they can be incorporated into the other summations. Now recalling ε_ℓ of (4.7) and γ_ℓ of (4.10), the preceding equation can be written

$$\mp\mu_n \sum_{\ell=0}^{n} \left[\frac{dA_1^{\pm}(y;u;\ell)}{dy} \cos(\ell\phi_v) + \frac{dA_2^{\pm}(y;u;\ell)}{dy} \sin(\ell\phi_v) \right] =$$

$$- \sum_{\ell=0}^{n} \left[A_1^{\pm}(y;u;\ell) \cos(\ell\phi_v) + A_2^{\pm}(y;u;\ell) \sin(\ell\phi_v) \right] \qquad (5.10)$$

$$+ \omega(y) \sum_{\ell=0}^{n} \left[\sum_{r=1}^{m-1} A_1^{+}(y;r;\ell)\, \hat{p}^{\pm}(y;r,u;\ell)\, \varepsilon_\ell + A_1^{+}(y;m;\ell)\, \hat{p}^{\pm}(y;m,u;\ell)\delta_\ell \right] \cos(\ell\phi_v)$$

$$+ \omega(y) \sum_{\ell=0}^{n} \left[\sum_{r=1}^{m-1} A_2^{+}(y;r;\ell)\, \hat{p}^{\pm}(y;r,u;\ell)\gamma_\ell \right] \sin(\ell\phi_v)$$

$$+ \omega(y) \sum_{\ell=0}^{n} \left[\sum_{r=1}^{m-1} A_1^{-}(y;r;\ell)\, \hat{p}^{\mp}(y;r,u;\ell)\, \varepsilon_\ell + A_1^{-}(y;m;\ell)\, \hat{p}^{\mp}(y;m,u;\ell)\delta_\ell \right] \cos(\ell\phi_v)$$

$$+ \omega(y) \sum_{\ell=0}^{n} \left[\sum_{r=1}^{m-1} A_2^{-}(y;r;\ell)\, \hat{p}^{\mp}(y;r,u;\ell)\gamma_\ell \right] \sin(\ell\phi_v) \,.$$

We now take advantage of the linear independence of $\cos(\ell\phi_v)$ and $\sin(\ell\phi_v)$ to observe that this last equation must hold true for each ℓ value $\ell = 0,\ldots,n$ for the A_1 and for $\ell = 1,\ldots,n-1$ for the A_2 amplitudes separately. Accordingly, collecting together and equating coefficients of $\cos(\ell\phi_v)$ in (5.10) gives

$$\mp\mu_u \frac{d}{dy} A_1^{\pm}(y;u;\ell) = -A_1^{\pm}(y;u;\ell)$$

$$+ \omega(y)\, \varepsilon_\ell \sum_{r=1}^{m-1} A_1^{+}(y;r;\ell)\, \hat{p}^{\pm}(y;r,u;\ell) + \omega(y)\, \delta_\ell\, A_1^{+}(y;m;\ell)\, \hat{p}^{\pm}(y;m,u;\ell)$$

$$+ \omega(y)\, \varepsilon_\ell \sum_{r=1}^{m-1} A_1^{-}(y;r;\ell)\, \hat{p}^{\mp}(y;r,u;\ell) + \omega(y)\, \delta_\ell\, A_1^{-}(y;m;\ell)\, \hat{p}^{\mp}(y;m,u;\ell) \qquad (5.11)$$

where $x \le y \le z$

$u = 1,\ldots,m-1$

$\ell = 0,\ldots,n$

and $\mu_u > 0$.

Collecting together and equating coefficients of $\sin(\ell\phi_v)$ on each side of (5.10) for $\ell = 1,\ldots,n-1$ in (5.10) gives a similar equation for the sine amplitudes:

$$\mp\mu_u \frac{d}{dy} A_2^{\pm}(y;u;\ell) = -A_2^{\pm}(y;u;\ell)$$

$$+ \omega(y)\, \gamma_\ell \sum_{r=1}^{m-1} A_2^{+}(y;r;\ell)\, \hat{p}^{\pm}(y;r,u;\ell) \qquad (5.12)$$

$$+ \omega(y)\, \gamma_\ell \sum_{r=1}^{m-1} A_2^{-}(y;r;\ell)\, \hat{p}^{\mp}(y;r,u;\ell)$$

where $x \le y \le z$

$u = 1,\ldots,m-1$

$\ell = 1,\ldots,n-1$

and $\mu_u > 0$.

Since $A_2^{\pm}(y;u;\ell) \equiv 0$ when $\ell = 0$ or $\ell = n$ (recall Eq. (4.9) and the comments following (4.6)), we can regard (5.12) as formally holding for the full range of ℓ values, $\ell = 0,1,\ldots,n$.

We now return to (5.2) and consider case (ii), namely the case of the polar cap radiances $N^{\pm}(y;m,\cdot)$. Once again our goal is the appropriate spectral decomposition of (5.2). Setting $u = m$ in (5.2) and recalling the procedure in (3.2) we obtain

$$\mp \mu_m \frac{d}{dy} N^{\pm}(y;m,\cdot) = -N^{\pm}(y;m,\cdot) \qquad \text{(a)}$$

$$+ \omega(y) \sum_{r=1}^{m-1} \sum_{s=1}^{2n} N^{+}(y;r,s)\, p^{\pm}(y;r,s|m,\cdot) \qquad \text{(b)}$$

$$+ \omega(y)\, N^{+}(y;m,\cdot)\, p^{\pm}(y;m,\cdot|m,\cdot) \qquad \text{(c)} \qquad (5.13)$$

$$+ \omega(y) \sum_{r=1}^{m-1} \sum_{s=1}^{2n} N^{-}(y;r,s)\, p^{\mp}(y;r,s|m,\cdot) \qquad \text{(d)}$$

$$+ \omega(y)\, N^{-}(y;m,\cdot)\, p^{\mp}(y,m,\cdot|m,\cdot) \qquad \text{(e)}$$

Now $N^{\pm}(y;m,\cdot)$ in line (a) of (5.13) is reduced to spectral form by (5.4). Indeed, we see at once that in the present case (of $u = m$) there will be only one up-down pair of nonzero spectral radiance amplitudes, namely $A_1^{\pm}(y;m;0)$. Thus (5.13) should reduce to a nontrivial pair of coupled equations describing the depth rate of change of $A_1^{+}(y;m;0)$ and $A_1^{-}(y;m;0)$. The reduction of term (b) in (5.13) is made via (5.3) and the quad-to-cap case (5.6c) for $p^{\pm}(y;r,s|m,\cdot)$. From the latter we see that the only nonzero term in (5.5a) is that for $\ell = 0$. Hence term (b) in (5.13) becomes

$$\omega(y) \sum_{r=1}^{m-1} \sum_{s=1}^{2n} \left\{ \sum_{\ell=0}^{n} [A_1^+(y;r;\ell) \cos(\ell\phi_s) + A_2^+(y;r;\ell) \sin(\ell\phi_s)] \right\} \hat{p}^{\pm}(y;r,m;0) \tag{b}$$

Moving the sum-over-s operator inward to the trigonometric functions we see that (b) in (5.13) reduces to

$$\omega(y)\ \varepsilon_0 \sum_{r=1}^{m-1} A_1^+(y;r;0)\ \hat{p}^{\pm}(y;r,m;0) \tag{b}$$

In like manner, (c) in (5.13) becomes

$$\omega(y)\ A_1^+(y;m;0)\ \hat{p}^{\pm}(y;m,m;0) \tag{c}$$

Also in like manner, (d) and (e) in (5.13), respectively, become

$$\omega(y)\ \varepsilon_0 \sum_{r=1}^{m-1} A_1^-(y;r;0)\ \hat{p}^{\mp}(y;r,m;0) \tag{d}$$

and

$$\omega(y)\ A_1^-(y;m;0)\ \hat{p}^{\mp}(y;m,m;0)\ . \tag{e}$$

Assembling these results (5.13) becomes

$$
\begin{aligned}
\mp \mu_m \frac{d}{dy} A_1^{\pm}(y;m;0) &= -A_1^{\pm}(y;m;0) \\
&+ \omega(y)\, \varepsilon_0 \sum_{r=1}^{m-1} A_1^{+}(y;r,0)\, \hat{p}^{\pm}(y;r,m;0) + \omega(y)\, A_1^{+}(y;m;0)\, \hat{p}^{\pm}(y;m,m;0) \\
&+ \omega(y)\, \varepsilon_0 \sum_{r=1}^{m-1} A_1^{-}(y;r;0)\, \hat{p}^{\mp}(y;r,m;0) + \omega(y)\, A_1^{-}(y;m;0)\, \hat{p}^{\mp}(y;m,m;0)
\end{aligned}
\tag{5.14}
$$

This is the desired spectral form of (5.2) for the polar cap case u = m.

As they stand, the set of coupled equations (5.11), (5.12) and (5.14) constitute the spectral form of (5.2). However, unlike (5.2), the physics they describe is obscured by being spread over a variety of different terms. Nor is there a suggestion as to any solution procedure other than an unceremonial dumping of the equation set into some prepackaged numerical subroutine for solution of coupled ordinary differential equations. (This will not work unless the subroutine has provisions for solving a two-point boundary value problem and unless this two-point problem is specified with care.) However, by a regrouping of the various terms in (5.11), (5.12) and (5.14) we can package them in a form of some heuristic value, both physical and mathematical, which will suggest the solution procedure for the complete boundary value problem.

The two equations of (5.11), written separately and rearranged, become

$$-\frac{d}{dy}A_1^+(y;u;\ell) = \sum_{r=1}^{m-1} A_1^+(y;r;\ell)\left[\frac{\omega(y)\,\varepsilon_\ell\,\hat{p}^+(y;r,u;\ell)}{\mu_u} - \frac{\delta_{r-u}}{\mu_u}\right]$$

$$+ A_1^+(y;m;\ell)\left[\frac{\omega(y)\,\delta_\ell\,\hat{p}^+(y;m,u;\ell)}{\mu_u}\right]$$

$$+ \sum_{r=1}^{m-1} A_1^-(y;r;\ell)\left[\frac{\omega(y)\,\varepsilon_\ell\,\hat{p}^-(y;r,u;\ell)}{\mu_u}\right]$$

$$+ A_1^-(y;m;\ell)\left[\frac{\omega(y)\,\delta_\ell\,\hat{p}^-(y;m,u;\ell)}{\mu_u}\right] \qquad (5.15)$$

for $u = 1,\ldots,m-1$ and $\ell = 0,\ldots,n$, and moreover

$$\frac{d}{dy}A_1^-(y;u;\ell) = \sum_{r=1}^{m-1} A_1^+(y;r;\ell)\left[\frac{\omega(y)\,\varepsilon_\ell\,\hat{p}^-(y;r,u;\ell)}{\mu_u}\right]$$

$$+ A_1^+(y;m;\ell)\left[\frac{\omega(y)\,\delta_\ell\,\hat{p}^-(y;m,u;\ell)}{\mu_u}\right]$$

$$+ \sum_{r=1}^{m-1} A_1^-(y;r;\ell)\left[\frac{\omega(y)\,\varepsilon_\ell\,\hat{p}^+(y;r,u;\ell)}{\mu_u} - \frac{\delta_{r-u}}{\mu_u}\right]$$

$$+ A_1^-(y;m;\ell)\left[\frac{\omega(y)\,\delta_\ell\,\hat{p}^+(y;m,u;\ell)}{\mu_u}\right] \qquad (5.16)$$

for $u = 1,\ldots,m-1$, and $\ell = 0,\ldots,n$.

The two equations of (5.12) written separately and rearranged, become

$$-\frac{d}{dy} A_2^+(y;u;\ell) = \sum_{r=1}^{m-1} A_2^+(y;r;\ell) \left[\frac{\omega(y)\ \gamma_\ell\ \hat{p}^+(y;r,u;\ell)}{\mu_u} - \frac{\delta_{r-u}}{\mu_u} \right]$$

$$+ \sum_{r=1}^{m-1} A_2^-(y;r;\ell) \left[\frac{\omega(y)\ \gamma_\ell\ \hat{p}^-(y;r,u;\ell)}{\mu_u} \right] \qquad (5.17)$$

$$\frac{d}{dy} A_2^-(y;u;\ell) = \sum_{r=1}^{m-1} A_2^+(y;r;\ell) \left[\frac{\omega(y)\ \gamma_\ell\ \hat{p}^-(y;r,u;\ell)}{\mu_u} \right]$$

$$+ \sum_{r=1}^{m-1} A_2^-(y;r;\ell) \left[\frac{\omega(y)\ \gamma_\ell\ \hat{p}^+(y;r,u;\ell)}{\mu_u} - \frac{\delta_{r-u}}{\mu_u} \right] \qquad (5.18)$$

for $u = 1,\ldots,m-1$; and $\ell = 1,\ldots,n-1$.

Next, the two equations of (5.14) written separately and rearranged, become

$$-\frac{d}{dy} A_1^+(y;m;0) = \sum_{r=1}^{m-1} A_1^+(y;r;0) \left[\frac{\omega(y)\ \varepsilon_0\ \hat{p}^+(y;r,m;0)}{\mu_m} \right]$$

$$+ A_1^+(y;m;0) \left[\frac{\omega(y)\ \hat{p}^+(y;m,m;0)}{\mu_m} - \frac{1}{\mu_m} \right]$$

$$+ \sum_{r=1}^{m-1} A_1^-(y;r;0) \left[\frac{\omega(y)\ \varepsilon_0\ \hat{p}^-(y;r,m;0)}{\mu_m} \right]$$

$$+ A_1^-(y;m;0) \left[\frac{\omega(y)\ \hat{p}^-(y;m,m;0)}{\mu_m} \right] \qquad (5.19)$$

and finally

$$\frac{d}{dy} A_1^-(y;m;0) = \sum_{r=1}^{m-1} A_1^+(y;r;0) \left[\frac{\omega(y)\ \varepsilon_0\ \hat{p}^-(y;r,m;0)}{\mu_m} \right]$$

$$+ A_1^+(y;m;0) \left[\frac{\omega(y)\ \hat{p}^-(y;m,m;0)}{\mu_m} \right]$$

$$+ \sum_{r=1}^{m-1} A_1^-(y;r;0) \left[\frac{\omega(y)\ \varepsilon_0\ \hat{p}^+(y;r,m;0)}{\mu_m} - \frac{1}{\mu_m} \right]$$

$$+ A_1^-(y;m;0) \left[\frac{\omega(y)\ \hat{p}^+(y;m,m;0)}{\mu_m} \right] \qquad (5.20)$$

The quantities in the square brackets of the preceding equations are the local reflectance and transmittance functions for the radiance field amplitudes $A_1^{\pm}(y;u,\ell)$. We shall now define them formally in the usual four-case analysis regarding quad and polar cap directions (cf. (5.6)). Our goal is the construction of the m×m *local reflectance matrix* $\underline{\hat{\rho}}(y;\ell)$ and the m×m *local transmittance matrix* $\underline{\hat{\tau}}(y;\ell)$ for each azimuthal mode $\ell = 0,\ldots,n$ and for all depths y, $x \le y \le z$. Let the elements in the r^{th} row and u^{th} column of these matrices be denoted by "$[\underline{\hat{\rho}}(y;\ell)]_{ru}$" and "$[\underline{\hat{\tau}}(y;\ell)]_{ru}$". Moreover, observe (cf. (4.7), (4.10)) that in the range $\ell = 1,\ldots,n-1$, we have $\gamma_\ell = \varepsilon_\ell = n$. Then we make the definitions as follows:

1) *Quad-to-Quad Case* (u,r = 1,...,m-1)

$$\left.\begin{aligned} [\underline{\hat{\tau}}(y;\ell)]_{ru} &\equiv [\varepsilon_\ell\ \omega(y)\ \hat{p}^+(y;r,u;\ell) - \delta_{r-u}]/\mu_u \\ [\underline{\hat{\rho}}(y;\ell)]_{ru} &\equiv \varepsilon_\ell\ \omega(y)\ \hat{p}^-(y;r,u;\ell)/\mu_u \end{aligned}\right\} \qquad (5.20b)$$

$\ell = 0,\ldots,n$

2) *Cap-to-Quad Case* (r = m; u = 1,...,m-1)

$$\left.\begin{aligned} [\underline{\hat{\tau}}(y;\ell)]_{mu} &\equiv \delta_{\ell}\ \omega(y)\ \hat{p}^{+}(y;m;u;\ell)/\mu_{u} \\ [\underline{\hat{\rho}}(y;\ell)]_{mu} &\equiv \delta_{\ell}\ \omega(y)\ \hat{p}^{-}(y;m,u;\ell)/\mu_{u} \end{aligned}\right\} \qquad (5.20c)$$

$$\ell = 0,\ldots,n$$

3) *Quad-to-Cap Case* (r = 1,...,m-1; u = m)

$$\left.\begin{aligned} [\underline{\hat{\tau}}(y;0)]_{rm} &\equiv \varepsilon_{0}\ \omega(y)\ \hat{p}^{+}(y;r,m;0)/\mu_{m} \\ [\underline{\hat{\tau}}(y;\ell)]_{rm} &\equiv 0 \quad \text{for } \ell = 1,\ldots,n \\ [\underline{\hat{\rho}}(y;0)]_{rm} &\equiv \varepsilon_{0}\ \omega(y)\ \hat{p}^{-}(y;r,m;0)/\mu_{m} \\ [\underline{\hat{\rho}}(y;\ell)]_{rm} &\equiv 0 \quad \text{for } \ell = 1,\ldots,n \end{aligned}\right\} \qquad (5.20d)$$

4) *Cap-to-Cap Case* (r = m; u = m)

$$\left.\begin{aligned} [\underline{\hat{\tau}}(y;0)]_{mm} &\equiv [\omega(y)\ \hat{p}^{+}(y;m,m;0) - 1]/\mu_{m} \\ [\underline{\hat{\tau}}(y;\ell)]_{mm} &\equiv 0 \quad \text{for } \ell = 1,\ldots,n \\ [\underline{\hat{\rho}}(y;0)]_{mm} &\equiv \omega(y)\ \hat{p}^{-}(y;m,m;0)/\mu_{m} \\ [\underline{\hat{\rho}}(y;\ell)]_{mm} &\equiv 0 \quad \text{for } \ell = 1,\ldots,n. \end{aligned}\right\} \qquad (5.20e)$$

With these definitions, (5.15) and (5.16) become

$$\begin{cases} -\frac{d}{dy} A_1^+(y;u;\ell) = \sum_{r=1}^{m} A_1^+(y;r;\ell)\,[\underline{\hat{\tau}}(y;\ell)]_{ru} + \sum_{r=1}^{m} A_1^-(y;r;\ell)\,[\underline{\hat{\rho}}(y;\ell)]_{ru} \end{cases} \tag{5.15a}$$

$$\begin{cases} \frac{d}{dy} A_1^-(y;u;\ell) = \sum_{r=1}^{m} A_1^+(y;r;\ell)\,[\underline{\hat{\rho}}(y;\ell)]_{ru} + \sum_{r=1}^{m} A_1^-(y;r;\ell)\,[\underline{\hat{\tau}}(y;\ell)]_{ru} \end{cases} \tag{5.16a}$$

valid for $\ell = 0,\ldots,n$ and $u = 1,\ldots,m-1$.

Equations (5.17) and (5.18) become, on recalling that $\varepsilon_\ell = \gamma_\ell$ for $\ell = 1,\ldots,n-1$,

$$\begin{cases} -\frac{d}{dy} A_2^+(y;u;\ell) = \sum_{r=1}^{m} A_2^+(y;r;\ell)\,[\underline{\hat{\tau}}(y;\ell)]_{ru} + \sum_{r=1}^{m} A_2^-(y;r;\ell)\,[\underline{\hat{\rho}}(y;\ell)]_{ru} \end{cases} \tag{5.17a}$$

$$\begin{cases} \frac{d}{dy} A_2^-(y;u;\ell) = \sum_{r=1}^{m} A_2^+(y;r;\ell)\,[\underline{\hat{\rho}}(y;\ell)]_{ru} + \sum_{r=1}^{m} A_2^-(y;r;\ell)\,[\underline{\hat{\tau}}(y;\ell)]_{ru} \end{cases} \tag{5.18a}$$

valid for $\ell = 1,\ldots,n-1$ and $u = 1,\ldots,m-1$.

Equations (5.19) and (5.20) become

$$\begin{cases} -\frac{d}{dy} A_1^+(y;m;0) = \sum_{r=1}^{m} A_1^+(y;r;0)\,[\underline{\hat{\tau}}(y;0)]_{rm} + \sum_{r=1}^{m} A_1^-(y;r;0)\,[\underline{\hat{\rho}}(y;0)]_{rm} \end{cases} \tag{5.19a}$$

$$\begin{cases} \frac{d}{dy} A_1^-(y;m;0) = \sum_{r=1}^{m} A_1^+(y;r;0)\,[\underline{\hat{\rho}}(y;0)]_{rm} + \sum_{r=1}^{m} A_1^-(y;r;0)\,[\underline{\hat{\tau}}(y;0)]_{rm} \end{cases} \tag{5.20a}$$

valid for $u = m$ only.

We next examine these systems of equations for the two naturally occurring cases of azimuth index values $\ell = 0,\ldots,n$. These are the case for $\ell = 0$ and the case of all remaining values $\ell = 1,\ldots,n$.

For the case of $\ell = 0$, (5.15a), (5.16a), (5.19a) and (5.20a) form a system of 2m coupled ordinary differential equations in the 2m unknowns $A_1^{\pm}(y;u;0)$, $u = 1,\ldots,m$. It will be useful to write out the m×m matrices $\underline{\hat{\tau}}(y;0)$ and $\underline{\hat{\rho}}(y;0)$ for inspection. For example,

$$\underline{\hat{\tau}}(y;0) = \begin{bmatrix} [\underline{\hat{\tau}}(y;0)]_{1,1} & [\underline{\hat{\tau}}(y;0)]_{1,2} & \cdots & [\underline{\hat{\tau}}(y;0)]_{1,m-1} & [\underline{\hat{\tau}}(y;0)]_{1,m} \\ \vdots & \vdots & & \vdots & \vdots \\ [\underline{\hat{\tau}}(y;0)]_{m-1,1} & [\underline{\hat{\tau}}(y;0)]_{m-1,2} & \cdots & [\underline{\hat{\tau}}(y;0)]_{m-1,m-1} & [\underline{\hat{\tau}}(y;0)]_{m-1,m} \\ [\underline{\hat{\tau}}(y;0)]_{m,1} & [\underline{\hat{\tau}}(y;0)]_{m,2} & \cdots & [\underline{\hat{\tau}}(y;0)]_{m,m-1} & [\underline{\hat{\tau}}(y;0)]_{m,m} \end{bmatrix} \tag{5.21}$$

The matrix $\underline{\hat{\rho}}(y;0)$ has a similar appearance; just replace "τ" by "ρ". The zero-mode cosine amplitudes can then be assembled into a 1×m vector by defining

$$\underline{A}_1^{\pm}(y;0) \equiv [A_1^{\pm}(y;1,0),\ldots,A_1^{\pm}(y;m;0)] \tag{5.22}$$

Thus the system (5.15a), (5.16a), (5.19a) and (5.20a) for the case $\ell = 0$ can be written

$$\mp \frac{d}{dy}\, \underline{A}_1^{\pm}(y;0) = \underline{A}_1^{\pm}(y;0)\, \underline{\hat{\tau}}(y;0) + \underline{A}_1^{\mp}(y;0)\, \underline{\hat{\rho}}(y;0) \tag{5.23}$$

$$x \le y \le z$$

It is interesting to note that this system by itself, for large enough m, is sufficient to accurately compute all the quantities needed in the two-flow irradiance model discussed in §8.

Next we consider the same system (5.15a), (5.16a), (5.19a), and (5.20a) for the case where $\ell = 1,\ldots,n$. By (5.4) we have $A_1^{\pm}(y;m;\ell) = 0$ for ℓ in this range. Moreover, by examining the definitions of $[\underline{\hat{\tau}}(y;\ell)]_{ru}$ and $[\underline{\hat{\rho}}(y;\ell)]_{ru}$ in the four cases above, we see that the bottom (the m^{th}) rows and right-most (the m^{th}) columns of these matrices are filled with zeros. This suggests defining two $(m-1)\times(m-1)$ matrices $\underline{\hat{\tau}}(y;\ell)$ and $\underline{\hat{\rho}}(y;\ell)$ for the case $\ell = 1,\ldots,n$ where, for example

$$\hat{\tau}(y;\ell) = \begin{bmatrix} [\underline{\hat{\tau}}(y;\ell)]_{1,1} & [\underline{\hat{\tau}}(y;\ell)]_{1,2} & \cdots & [\underline{\hat{\tau}}(y;\ell)]_{1,m-1} \\ \vdots & \vdots & & \vdots \\ [\underline{\hat{\tau}}(y;\ell)_{m-1,1} & [\underline{\hat{\tau}}(y;\ell)]_{m-1,2} & \cdots & [\underline{\hat{\tau}}(y;\ell)]_{m-1,m-1} \end{bmatrix} \tag{5.24}$$

The $(m-1)\times(m-1)$ matrix $\underline{\hat{\rho}}(y;\ell)$, $\ell = 1,\ldots,n$ has a similar appearance; just replace "τ" by "ρ" in (5.24).

The non-trivial zero-mode cosine amplitudes for the case $\ell = 1,\ldots,n$ can then be assembled into a $1\times(m-1)$ vector by writing

$$\underline{A}_1^{\pm}(y;\ell) \equiv [A_1^{\pm}(y;1;\ell),\ldots,A_1^{\pm}(y;m-1;\ell)] \tag{5.25}$$

Thus the system (5.15a), (5.16a), (5.19a), and (5.20a) for the case $\ell = 1,\ldots,n$ can be written

$$\boxed{\mp \frac{d}{dy}\,\underline{A}_1^{\pm}(y;\ell) = \underline{A}_1^{\pm}(y;\ell)\,\underline{\hat{\tau}}(y;\ell) + \underline{A}_1^{\mp}(y;\ell)\,\underline{\hat{\rho}}(y;\ell) \qquad x \le y \le z \;\; ; \;\; \ell = 1,\ldots,n} \tag{5.26}$$

The equation set (5.17a) and (5.18a) for the sine amplitudes $A_2^{\pm}(y;u;\ell)$, $u = 1,\ldots,m-1$, $\ell = 1,\ldots,n-1$, can be assembled into matrix form also. We now

use the (m-1)×(m-1) matrices $\underline{\hat{t}}(y;\ell)$ and $\underline{\hat{\rho}}(y;\ell)$ defined in (5.24), and for the non-trivial sine amplitude 1×(m-1) vectors, we write

$$\underline{A}_2^{\pm}(y;\ell) \equiv [A_2^{\pm}(y;1;\ell),\ldots,A_2^{\pm}(y;m-1;\ell)] \tag{5.27}$$

Then we obtain from (5.17a) and (5.18a):

$$\boxed{\mp \frac{d}{dy}\,\underline{A}_2^{\pm}(y;\ell) = \underline{A}_2^{\pm}(y;\ell)\,\underline{\hat{t}}(y;\ell) + \underline{A}_2^{\mp}(y;\ell)\,\underline{\hat{\rho}}(y;\ell)} \tag{5.28}$$

$$x \le y \le z \quad ; \quad \ell = 1,\ldots,n-1$$

Equation systems (5.26) and (5.28) give all the required azimuthal information needed to study the shapes of radiance distributions in natural hydrosols; while as already noted, (5.23) contains the information on scalar irradiances and horizontal irradiances.

Observe that the sets of equations (5.23), (5.26), and (5.28) govern *individual* azimuthal modes $\ell = 0,\ldots,n$. This permits a considerable savings in storage requirements during a computation of the amplitudes for each mode; and in fact this is the reason for going from the relatively aesthetic set (5.2) to the total collection of amplitude equations, above. We note that the total number of nontrivial radiances in (5.2) is $2(m-1)2n + 2 = 4mn - 4n + 2$, where the "$2(m-1)2n$" term tallies the quads and the "2" is for the polar caps (for which the v index is unneeded). These $4mn - 4n + 2$ radiance equations must be solved simultaneously. Equation (5.23) governs $2m$ amplitudes, (5.26) governs $2(m-1)n$ amplitudes, and (5.28) governs $2(m-1)(n-1)$ amplitudes, for a total of $4mn - 4n + 2$ amplitudes. Thus the "information content" is the same for either the "radiance" or the "amplitude" formulations but, as just noted, the amplitude equations can be solved as a sequence of smaller systems of equations.

Much of our discussions below and, indeed, even the programming of the theory, will be materially simplified if we cast (5.23), (5.26), and (5.28) into a commonly dimensioned algebraic mold. Moreover, we recover a measure of beauty lost while spectrally decomposing (5.2). This simply entails filling out the $1\times(m-1)$ vectors $\underline{A}_p^{\pm}(y;\ell)$ in (5.25) and (5.27) to become $1\times m$ vectors with zero m^{th} components. Moreover the $(m-1)\times(m-1)$ matrices in (5.24) receive an m^{th} row and an m^{th} column of zeros compatible with their four-case definitions, above. When this is done, (5.23), (5.26), and (5.28) become expressible in the unified form

$$\mp \frac{d}{dy}\,\underline{A}_p^{\pm}(y;\ell) = \underline{A}_p^{\pm}(y;\ell)\,\underline{\hat{\tau}}(y;\ell) + \underline{A}_p^{\mp}(y;\ell)\,\underline{\hat{\rho}}(y;\ell)$$
$$\text{where } p = 1,2$$
$$\ell = 0,\ldots,n \tag{5.29}$$
$$x \le y \le z$$
$$\text{and } \underline{A}_p^{\pm}(y;\ell) = [A_p^{\pm}(y;1;\ell),\ldots,A_p^{\pm}(y;m;\ell)]$$

These equations are the *local interaction equations* for the radiance amplitudes. Henceforth, whenever (5.29) is referred to, it will be assumed that all vectors and matrices involved are m-dimensional. There is only one exception to this convention; it occurs in §10; and the reason for the exception is discussed there.

b. Symmetry Implications for the Spectral Form of the Surface Boundary Reflectance and Transmittance Functions

The discrete geometric boundary conditions at the water surface are given by (3.17) and (3.18). These equations involve four quad-averaged reflectance and transmittance functions which have the symmetries expressed by (3.24).

For fixed non-polar indexes r and u, i.e. where $r \neq m$ and $u \neq m$, these reflectance and transmittance arrays can be viewed as discrete functions of the azimuthal angles ϕ_s and ϕ_v. As such they can be represented by an expansion of the form of (4.13). Thus for example,

$$\begin{aligned} t(a,x;r,s|u,v) = &\sum_{k=0}^{n}\sum_{\ell=0}^{n} \hat{t}_{11}(a,x;r,k|u,\ell)\cos(k\phi_s)\cos(\ell\phi_v) \\ &+ \sum_{k=0}^{n}\sum_{\ell=0}^{n} \hat{t}_{12}(a,x;r,k|u,\ell)\cos(k\phi_s)\sin(\ell\phi_v) \\ &+ \sum_{k=0}^{n}\sum_{\ell=0}^{n} \hat{t}_{21}(a,x;r,k|u,\ell)\sin(k\phi_s)\cos(\ell\phi_v) \\ &+ \sum_{k=0}^{n}\sum_{\ell=0}^{n} \hat{t}_{22}(a,x;r,k|u,\ell)\sin(k\phi_s)\sin(\ell\phi_v) , \end{aligned} \tag{5.30}$$

where the $\hat{t}_{ij}(a,x;r,k|u,\ell)$ are given by equations of the form of (4.14).

The symmetries expressed by (3.24) lead to a considerable simplification of (5.30). Consider for example the $\hat{t}_{12}$ term patterned after the $\hat{h}_{12}$ term of (4.14):

$$\hat{t}_{12}(a,x;r,k|u,\ell) \equiv \frac{1}{\varepsilon_k \gamma_\ell} \sum_{s=1}^{2n}\sum_{v=1}^{2n} t(a,x;r,s|u,v)\cos(k\phi_s)\sin(\ell\phi_v) .$$

By (3.24a) we have

$$\hat{t}_{12}(a,x;r,k|u,\ell) = \frac{1}{\varepsilon_k \gamma_\ell} \sum_{s=1}^{2n}\sum_{v=1}^{2n} t(a,x;r,2n+2-s|u,2n+2-v)\cos(\ell\phi_s)\sin(\ell\phi_v) .$$

Changing summation indices to $s' \equiv 2n+2-s$ and $v' \equiv 2n+2-v$ gives

$$\hat{t}_{12}(a,x;r,k|u,\ell) = \frac{1}{\varepsilon_k \gamma_\ell} \sum_{s'=2n+1}^{2}\sum_{v'=2n+1}^{2} t(a,x;r,s'|u,v')\cos(k\phi_{2n+2-s'})\sin(\ell\phi_{2n+2-v'})$$

Since $\phi_{2n+2-w} = 2\pi - \phi_w$, and by the evenness of the cosine and the oddness of the sine we get

$$\hat{t}_{12}(a,x;r,k|u,\ell) = \frac{1}{\epsilon_k \gamma_\ell} \sum_{s'=2n+1}^{2} \sum_{v'=2n+1}^{2} t(a,x;r,s'|u,v') \cos(k\phi_{s'})[-\sin(\ell\phi_{v'})] .$$

Noting that quad $s = 2n+1$ is the same quad as $s = 1$ (cf., Fig. 5b) and reordering sums we find

$$\hat{t}_{12}(a,x;r,k|u,\ell) = -\frac{1}{\epsilon_k \gamma_\ell} \sum_{s'=1}^{2n} \sum_{v'=1}^{2n} t(a,x;r,s'|u,v') \cos(k\phi_{s'}) \sin(\ell\phi_{v'})$$

$$= -\hat{t}_{12}(a,x;r,k|u,\ell) .$$

Therefore it follows that

$$\hat{t}_{12}(a,x;r,k|u,\ell) \equiv 0 , \tag{5.30a}$$

for $r,u = 1,\ldots,m$ and $k,\ell = 0,\ldots,n$.

An identical analysis shows that $\hat{t}_{21}(a,x;r,k|u,\ell) \equiv 0$, over the full r,k, u,ℓ ranges, and the same results are found for the other three reflectance and transmittance functions. Thus the bilateral symmetry of the surface about the wind direction eliminates two of the four terms in (5.30).

Another important simplification is obtained from (3.24b). Consider the evaluation of the $\hat{t}_{11}$ term in (5.30) using the pattern of the $\hat{h}_{11}$ term in (4.14):

$$\hat{t}_{11}(a,x;r,k|u,\ell) = \frac{1}{\varepsilon_k \varepsilon_\ell} \sum_{s=1}^{2n} \sum_{v=1}^{2n} t(a,x;r,s|u,v) \cos(k\phi_s) \cos(\ell\phi_v)$$

$$= \frac{1}{\varepsilon_k \varepsilon_\ell} \sum_{s=1}^{2n} \sum_{v=1}^{2n} t(a,x;r,n+2-s|u,n+2-v) \cos(k\phi_s) \cos(\ell\phi_v) ,$$

where the last equation results from the application of (3.24b). Changing summation indices to $s' \equiv n+2-s$ and $v' = n+2-v$ gives

$$\hat{t}_{11}(a,x;r,k|u,\ell) = \frac{1}{\varepsilon_k \varepsilon_\ell} \sum_{s'=n+1}^{2-n} \sum_{v'=n+1}^{2-n} t(a,x;r,s'|u,v') \cos(k\phi_{n+2-s'}) \cos(\ell\phi_{n+2-s'}) ,$$

wherein a nonpositive value of s' references quad $s'+2n$, as is illustrated in Fig. 5b. Since $\phi_{n+2-s'} = \pi-\phi_{s'}$ we have

$$\cos(k\phi_{n+2-s'}) = \cos k(\pi-\phi_{s'}) = (-1)^k \cos(k\phi_{s'})$$

and our last equation for $\hat{t}_{11}$ becomes

$$\hat{t}_{11}(a,x;r,k|u,\ell) = \frac{1}{\varepsilon_k \varepsilon_\ell} \sum_{s'=n+1}^{2-n} \sum_{v'=n+1}^{2-n} t(a,x;r,s'|u,v')(-1)^k \cos(k\phi_{s'})(-1)^\ell \cos(\ell\phi_{v'}) ,$$

which upon reordering the summations becomes

$$\hat{t}_{11}(a,x;r,k|u,\ell) = (-1)^{k+\ell} \frac{1}{\varepsilon_k \varepsilon_\ell} \sum_{s'=1}^{2n} \sum_{v'=1}^{2n} t(a,x;r,s'|u,v') \cos(k\phi_{s'}) \cos(\ell\phi_{v'})$$

$$= (-1)^{k+\ell} \hat{t}_{11}(a,x;r,k|u,\ell) .$$

Therefore it follows that

$$\hat{t}_{11}(a,x;r,k|u,\ell) \equiv 0 \qquad \text{if } k+\ell \text{ is odd,} \tag{5.30b}$$

and $r,u = 1,\ldots,m$ and $k,\ell = 0,\ldots,n$.

The symmetry expressed by (3.24b) thus eliminates the need to explicitly compute one half of the $\hat{t}_{11}(a,x;r,k|u,\ell)$ matrix elements. Corresponding results are obtained for $\hat{t}_{22}(a,x;r,k|u,\ell)$ and for the other three reflectance and transmittance functions.

The elliptical symmetry of the wind-blown water surface clearly results in a major computational savings in the treatment of the surface boundary. We can also simplify the notation to one subscript for $\hat{r}$ and $\hat{t}$ functions, e.g. $\hat{t}_1(a,x;r,k|u,\ell) \equiv \hat{t}_{11}(a,x;r,k|u,\ell)$ in (5.23), since the cross product terms are zero. Equation (5.30) then can be replaced by

$$t(a,x;r,s|u,v) = \sum_{k=0}^{n} \sum_{\ell=0}^{n} \hat{t}_1(a,x;r,k|u,\ell) \cos(k\phi_s) \cos(\ell\phi_v) + \sum_{k=0}^{n} \sum_{\ell=0}^{n} \hat{t}_2(a,x;r,k|u,\ell) \sin(k\phi_s) \sin(\ell\phi_v) \tag{5.31a}$$

where

$$\hat{t}_1(a,x;r,k|u,\ell) \equiv \frac{1}{\varepsilon_k \varepsilon_\ell} \sum_{s=1}^{2n} \sum_{v=1}^{2n} t(a,x;r,s|u,v) \cos(k\phi_s) \cos(\ell\phi_v)$$

$$\text{for } k,\ell = 0,\ldots,n$$

and where

$$\hat{t}_2(a,x;r,k|u,\ell) \equiv \begin{cases} \dfrac{1}{\gamma_k \gamma_\ell} \displaystyle\sum_{s=1}^{2n} \sum_{v=1}^{2n} t(a,x;r,s|u,v) \sin(k\phi_s) \sin(\ell\phi_v) \\ \quad \text{if } k,\ell = 1,\ldots,n-1 \\ 0 \text{ if } k = 0, \quad \ell = 0,\ldots,n \\ 0 \text{ if } \ell = 0, \quad k = 0,\ldots,n \end{cases} \tag{5.31b}$$

These equations are patterned after (4.14) and hold for all u,r = 1,...,m; and moreover, $\hat{t}_1$ and $\hat{t}_2$ are zero when k+ℓ is odd, as noted above.

It will be convenient for future reference to explicitly consider the four main cases of (5.31b) for the r and u variables. These cases are the four possibilities of whether the initial and final indexes are associated with quads or with polar caps. Thus we have the

1) *Quad-to-Quad Case* (u,r = 1,...,m-1). Then (5.31b) is unchanged:

$$\hat{t}_1(a,x;r,k|u,\ell) \equiv \frac{1}{\epsilon_k \epsilon_\ell} \sum_{s=1}^{2n} \sum_{v=1}^{2n} t(a,x;r,s|u,v) \cos(k\phi_s) \cos(\ell\phi_v)$$

$$\text{for } k,\ell = 0,\ldots,n \tag{5.31c}$$

$$\hat{t}_2(a,x;r,k|u,\ell) \equiv \begin{cases} \dfrac{1}{\gamma_k \gamma_\ell} \displaystyle\sum_{s=1}^{2n} \sum_{v=1}^{2n} t(a,x;r,s|u,v) \sin(k\phi_s) \sin(\ell\phi_v) \\ \quad \text{if } k,\ell = 1,\ldots,n-1 \\ 0 \text{ if } k = 0, \quad \ell = 0,\ldots,n \\ 0 \text{ if } \ell = 0, \quad k = 0,\ldots,n \end{cases}$$

2) *Cap-to-Quad Case* (r = m; u = 1,...,m-1). Then (5.31b) reduces to

$$\left.\begin{aligned} \hat{t}_1(a,x;\, m,0|u,\ell) &\equiv \frac{1}{\epsilon_\ell} \sum_{v=1}^{2n} t(a,x;m,\cdot|u,v) \cos(\ell\phi_v) \\ &\qquad \ell = 0,\ldots,n \\ \hat{t}_1(a,x;m,k|u,\ell) &\equiv 0 \begin{cases} k = 1,\ldots,n \\ \ell = 0,\ldots,n \end{cases} \\ \hat{t}_2(a,x;m,k|u,\ell) &\equiv 0 \quad k,\ell = 0,\ldots,n \end{aligned}\right\} \tag{5.32}$$

The amplitudes in (5.32) give rise to the representation

$$t(a,x;m,\cdot|u,v) = \sum_{\ell=0}^{n} \hat{t}_1(a,x;m,0|u,\ell)\cos(\ell\phi_v) \tag{5.33}$$

3) *Quad-to-Cap Case* ($r = 1,\ldots,m-1$; $u = m$). Then (5.31b) reduces to

$$\left.\begin{aligned} \hat{t}_1(a,x;r,k|m,0) &\equiv \frac{1}{\varepsilon_k}\sum_{s=1}^{2n} t(a,x;r,s|m,\cdot)\cos(k\phi_s) \\ & \qquad k = 0,\ldots,n \\ \hat{t}_1(a,x;r,k|m,\ell) &\equiv 0 \quad \begin{cases} k = 0,\ldots,n \\ \ell = 1,\ldots,n \end{cases} \\ \hat{t}_2(a,x;r,k|m,\ell) &\equiv 0 \quad k,\ell = 0,\ldots,n \end{aligned}\right\} \tag{5.34}$$

The amplitudes in (5.34) give rise to the representation

$$t(a,x;r,s|m,\cdot) = \sum_{k=0}^{n} \hat{t}_1(a,x;r,k|m,0)\cos(k\phi_s) \tag{5.35}$$

4) *Cap-to-Cap Case* ($r = m$; $u = m$). Then (5.31b) reduces to

$$\left.\begin{aligned} \hat{t}_1(a,x;m,0|m,0) &\equiv t(a,x;m,\cdot|m,\cdot) \\ \hat{t}_1(a,x;m,k|m,\ell) &\equiv 0 \;;\; k,\ell = 1,\ldots,n \\ \hat{t}_2(a,x;m,k|m,\ell) &\equiv 0 \;;\; k,\ell = 0,\ldots,n \end{aligned}\right\} \tag{5.36}$$

The formulas (5.31c)-(5.36) for $\hat{t}_p(a,x;r,k|u,\ell)$ form the requisite pattern for the remaining three transfer functions of the air water surface: $\hat{t}_p(x,a;r,k|u,\ell)$, $\hat{r}_p(a,x;r,k|u,\ell)$, and $\hat{r}_p(x,a;r,k|u,\ell)$, p = 1,2. Except for the switches of position of "a" and "x" and going from "$\hat{t}$" to "$\hat{r}$", the patterns set by (5.31)-(5.36) are identical to the patterns found for the remaining three cases.

c. Transformation of the Surface Boundary Conditions to Spectral Form

We are now in a position to transform the discrete geometric boundary conditions (3.17), (3.18) and (3.25) into a discrete spectral form. The same general procedure as was used on the radiative transfer equation in §5a is applicable. We shall illustrate the process with eq. (3.17), which can be written as

$$N^-(x;u,v) = \sum_{r=1}^{m-1}\sum_{s=1}^{2n} N^-(a;r,s)\, t(a,x;r,s|u,v) + N^-(a;m,\cdot)\, t(a,x;m,\cdot|u,v) \tag{5.37}$$
$$+ \sum_{r=1}^{m-1}\sum_{s=1}^{2n} N^+(x;r,s)\, r(x,a;r,s|u,v) + N^+(x;m,\cdot)\, r(x,a;m,\cdot|u,v) .$$

Once again we must treat the polar cap terms explicitly. The radiances can be represented as in (5.3), and the r and t functions can be represented as in (5.31a). Then for u = 1,...,m-1 (5.37) becomes

$$\sum_{\ell=0}^{n} \left[A_1^-(x;u;\ell) \cos(\ell\phi_v) + A_2^-(x;u;\ell) \sin(\ell\phi_v) \right]$$

$$= \sum_{r=1}^{m-1} \sum_{s=1}^{2n} \sum_{k=0}^{n} \left\{ \left[A_1^-(a;r;k) \cos(k\phi_s) + A_2^-(a;r;k) \sin(k\phi_s) \right] \right\}$$

$$\times \left\{ \sum_{k'=0}^{n} \sum_{\ell=0}^{n} \hat{t}_1(a,x;r,k'|u,\ell) \cos(k'\phi_s) \cos(\ell\phi_v) + \right.$$

$$\left. + \sum_{k'=0}^{n} \sum_{\ell=0}^{n} \hat{t}_2(a,x;r,k'|u,\ell) \sin(k'\phi_s) \sin(\ell\phi_v) \right\} \qquad (5.38)$$

$$+ A_1^-(a;m;0) \sum_{\ell=0}^{n} \hat{t}_1(a,x;m,0|u,\ell) \cos(\ell\phi_v)$$

$$+ \text{a similar set of terms in } A^+ \text{ and } \hat{r}(x,a).$$

Note that the polar cap terms have been represented by the appropriate Eqs. (5.4) and (5.33). The first term in the right side of this equation can be regrouped as

$$\sum_{r=1}^{m-1} \sum_{k} \sum_{k'} \sum_{\ell} \left\{ A_1^-(a;r;k) \hat{t}_1(a,x;r,k'|u,\ell) \left[\sum_{s=1}^{2n} \cos(k\phi_s) \cos(k'\phi_s) \right] \cos(\ell\phi_v) \right.$$

$$+ A_2^-(a;r;k) \hat{t}_1(a,x;r,k'|u,\ell) \left[\sum_{s=1}^{2n} \sin(k\phi_s) \cos(k'\phi_s) \right] \cos(\ell\phi_v)$$

$$+ A_1^-(a;r;k) \hat{t}_2(a,x;r,k'|u,\ell) \left[\sum_{s=1}^{2n} \cos(k\phi_s) \sin(k'\phi_s) \right] \sin(\ell\phi_v)$$

$$\left. + A_2^-(a;r;k) \hat{t}_2(a,x;r,k'|u,\ell) \left[\sum_{s=1}^{2n} \sin(k\phi_s) \sin(k'\phi_s) \right] \sin(\ell\phi_v) \right\} .$$

Using the orthogonality conditions (4.1)-(4.3) on the sums over s reduces this expression to

$$\sum_{r=1}^{m-1} \sum_{k} \sum_{k'} \sum_{\ell} \Big\{ A_1^-(a;r;k)\ \hat{t}_1(a,x;r,k'|u,\ell)\ n(\delta_{k+k'} + \delta_{k-k'} + \delta_{k+k'-2n})\ \cos(\ell\phi_v)$$

$$+ A_2^-(a;r;k)\ \hat{t}_2(a,x;r,k'|u,\ell)\ n(\delta_{k-k'} - \delta_{k+k'} - \delta_{k+k'-2n})\ \sin(\ell\phi_v) \Big\}.$$

The Kronecker δ-functions force k' = k, leaving ε_k and γ_k factors, so that (5.38) becomes

$$\sum_{\ell} A_1^-(x;u;\ell)\ \cos(\ell\phi_v) + \sum_{\ell} A_2^-(x;u;\ell)\ \sin(\ell\phi_v) \tag{5.39}$$

$$= \sum_{\ell} \left[\sum_{r=1}^{m-1} \sum_{k} A_1^-(a;r;k)\ \hat{t}_1(a,x;r,k|u,\ell)\ \varepsilon_k + A_1^-(a;m;k)\ \hat{t}_1(a,x;m,k|u,\ell)\ \delta_k \right] \cos(\ell\phi_v)$$

$$+ \sum_{\ell} \left[\sum_{r=1}^{m-1} \sum_{k} A_2^-(a;r;k)\ \hat{t}_2(a,x;r,k|u,\ell)\ \gamma_k \right] \sin(\ell\phi_v)$$

+ a similar set of terms in A^+ and $\hat{r}(x,a)$.

We now once again call upon the linear independence of the cosine and sine functions. In particular we can in (5.39) equate the coefficients of $\cos(\ell\phi_v)$ to get, after reordering the r and k sums,

$$A_1^-(x;u;\ell) =$$

$$\sum_{k} \left\{ \sum_{r=1}^{m-1} A_1^-(a;r;k)\ \hat{t}_1(a,x;r,k|u,\ell)\ \varepsilon_k + A_1^-(a;m;k)\ \hat{t}_1(a,x;m,k|u,\ell)\delta_k \right\} \tag{5.40a}$$

$$+ \sum_{k} \left\{ \sum_{r=1}^{m-1} A_1^+(x;r;k)\ \hat{r}_1(x,a;r,k|u,\ell)\ \varepsilon_k + A_1^+(x;m;k)\ \hat{r}_1(x,a;m,k|u,\ell)\ \delta_k \right\}.$$

This expression holds for u = 1,...,m-1; ℓ = 0,...,n.

We return now to (5.37) to take care of the polar cap case, i.e., the case of $u = m$. Setting $u = m$ in (5.37) and recalling what happens in this case (cf. (5.4), (5.35), (5.36)), we have the present version of (5.38):

$$A_1^-(x;m;0) = \sum_{r=1}^{m-1} \sum_{s=1}^{2n} \left\{ \sum_{k=0}^{n} [A_1^-(a;r;k) \cos(k\phi_s) + A_2^-(a;r;k) \sin(k\phi_s)] \right\}$$

$$\times \left\{ \sum_{k'=0}^{n} \hat{t}_1(a,x;r,k'|m,0) \cos(k'\phi_s) \right\}$$

$$+ A_1^-(a;m;0)\, \hat{t}_1(a,x;m,0|m,0)$$

$$+ \text{a similar set of terms in } A^+ \text{ and } r(x,a)$$

Rearranging this to use the orthogonality properties of the trigonometric functions, we find

$$A_1^-(x;m;0) = \sum_{r=1}^{m-1} \sum_{k} \sum_{k'} \left\{ A_1^-(a;r;k)\, \hat{t}_1(a,x;r,k'|m,0) \left[\sum_{s=1}^{2n} \cos(k\phi_s) \cos(k'\phi_s) \right] \right.$$

$$\left. + A_2^-(a;r;k)\, \hat{t}_1(a,x;r,k'(m,0) \left[\sum_{s=1}^{2n} \sin(k\phi_s) \sin(k'\phi_s) \right] \right\}$$

$$+ A_1^-(a;m;0)\, \hat{t}_1(a,x;m,0|m,0)$$

$$+ \text{a similar set of terms in } A^+ \text{ and } r(x,a)$$

This reduces to

$$A_l^-(x;m;0) =$$

$$\sum_{k=0}^{n}\left\{\sum_{r=1}^{m-1} A_l^-(a;r;k)\ \varepsilon_k \hat{t}_l(a,x;r,k|m,0) + A_l^-(a;m;0)\ \delta_k \hat{t}_l(a,x;m,k|m,0)\right\}$$

$$+ \sum_{k=0}^{n}\left\{\sum_{r=1}^{m-1} A_l^+(x;r;k)\ \varepsilon_k \hat{r}_l(x,a;r,k|m,0) + A_l^+(x;m;0)\ \delta_k \hat{r}_l(x,a;m,k|m,0)\right\} \tag{5.40b}$$

Now define the (r,u) elements of an m×m matrix $\underline{\hat{t}}_l(a,x;k|\ell)$ via

$$[\underline{\hat{t}}_l(a,x;k|\ell)]_{ru} \equiv \begin{cases} \varepsilon_k \hat{t}_l(a,x;r,k|u,\ell) & \text{for} \quad r = 1,\ldots,m-1 \\ \delta_k \hat{t}_l(a,x;r,k|u,\ell) & \text{for} \quad r = m, \end{cases} \tag{5.41}$$

and for $u = 1,\ldots,m$; $k,\ell = 0,\ldots,n$

with corresponding definitions for the other three $\hat{r}_l$ and $\hat{t}_l$ matrices. Note that (5.32), (5.34) and (5.36) imply that many of the matrix elements of (5.41) are zero for $\ell = 1,\ldots,n$.

The amplitude equations (5.40a,b) then can be written

$$A_l^-(x;u;\ell) = \sum_k\left\{\sum_{r=1}^{m} A_l^-(a;r;k)\left[\underline{\hat{t}}_l(a,x;k|\ell)\right]_{ru}\right\}$$

$$+ \sum_k\left\{\sum_{r=1}^{m} A_l^+(x;r;k)\left[\underline{\hat{r}}_l(x,a;k|\ell)\right]_{ru}\right\},$$

which hold for $u = 1,\ldots,m$ and $\ell = 0,1,\ldots,n$. Using the full 1×m vectors of amplitudes defined as in (5.29), these equations and hence the spectral version of (5.37) for the cosine amplitudes can be placed in the matrix form

$$\underline{A}_l^-(x;\ell) = \sum_{\substack{k=0 \\ (k+\ell \text{ even})}}^{n} \underline{A}_l^+(x;k)\ \underline{\hat{r}}_l(x,a;k|\ell) + \sum_{\substack{k=0 \\ (k+\ell \text{ even})}}^{n} \underline{A}_l^-(a;k)\ \underline{\hat{t}}_l(a,x;k|\ell)\ . \tag{5.42}$$

The notation "k+ℓ even" on the sums reminds us that, as was seen in the preceding section, those $\hat{t}$ and $\hat{r}$ terms for which k+ℓ is odd are identically zero and need not be included in the sums.

Table 1 displays the pattern of zero and non-zero elements in the matrices defined by (5.41) and used in (5.42).

Equating the coefficients of $\sin(\ell\phi_v)$ in (5.39) gives an equation for $\underline{A}_2^-(x;\ell)$ which has the same form as (5.42). Moreover, recall (cf. (5.4)) that $A_2^-(x;m;\ell) = 0$ for $\ell = 0,\ldots,n$. We can then define the m×m matrix $\underline{\hat{t}}_2(a,x;k|\ell)$ via

$$[\underline{\hat{t}}_2(a,x;k|\ell)]_{ru} \equiv \begin{cases} \gamma_k \hat{t}_2(a,x;r,k|u,\ell) & \text{for } r = 1,\ldots,m-1 \text{ and } \ell = 1,\ldots,n-1 \\ 0 & \text{for } r = m \text{ and } \ell = 0 \text{ or } \ell = n \end{cases} \tag{5.43}$$

and for $u = 1,\ldots,m$; $k = 0,\ldots,n$

with corresponding definitions of the same form for the other $\hat{r}_2$ and $\hat{t}_2$ functions. Table 2 displays the pattern of zero and non-zero elements in the matrices defined by (5.43).

Thus (5.37) and hence (3.17) reduce to the following pair of matrix statements:

$$\underline{A}_p^-(x;\ell) = \sum_{\substack{k=0 \\ (k+\ell \text{ even})}}^{n} \underline{A}_p^+(x;k)\, \underline{\hat{r}}_p(x,a;k|\ell) + \sum_{\substack{k=0 \\ (k+\ell \text{ even})}}^{n} \underline{A}_p^-(a;k)\, \underline{\hat{t}}_p(a,x;k|\ell) \tag{5.44}$$

where p = 1 or 2 and $\ell = 0,\ldots,n$.

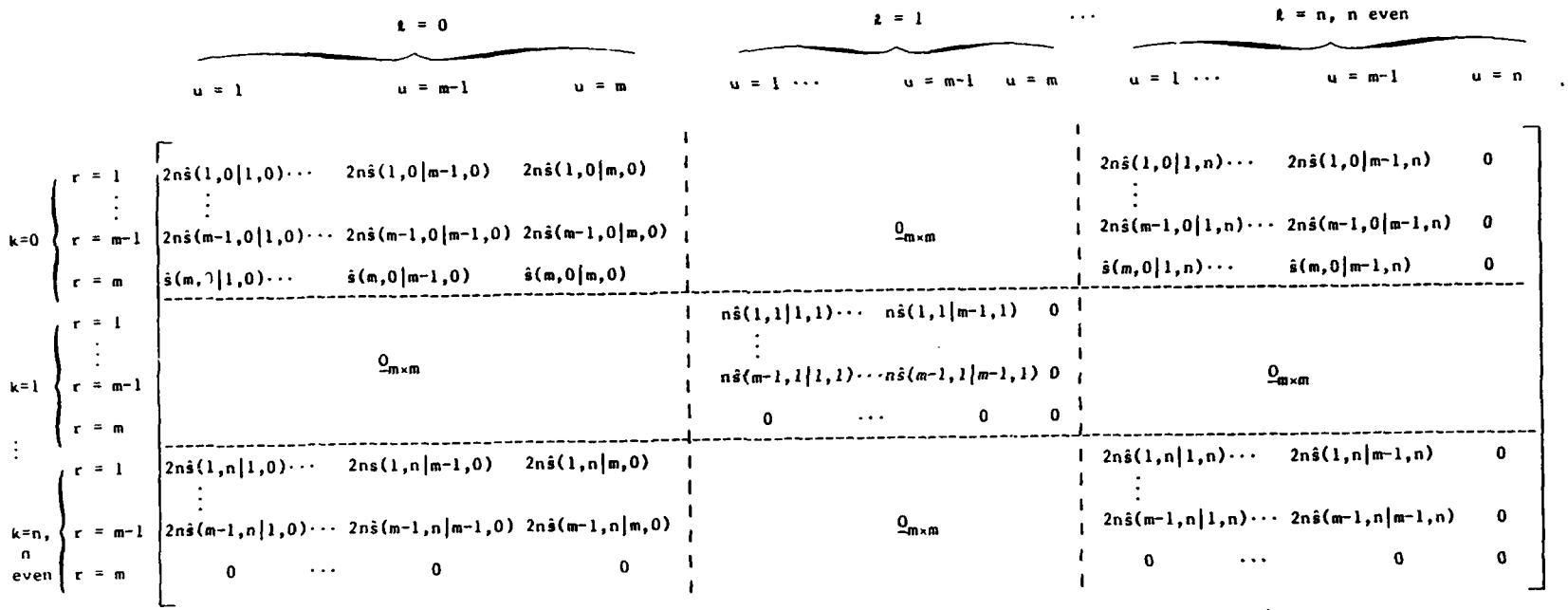

Table 1.--Illustration of the structure of the cosine spectral arrays defined by Eq. (5.41). $\hat{s}(r,k|u,\ell)$ represents any of the four cosine amplitudes, $\hat{t}_1(a,x;r,k|u,\ell)$, $\hat{t}_1(x,a;r,k|u,\ell)$, $\hat{r}_1(a,x;r,k|u,\ell)$, or $\hat{r}_1(x,a;r,k|u,\ell)$. The factors of 2n, n, 0 or 1 multiplying these elements are special values of ε_k and δ_k. The requirement that n be even goes back to Fig. 5b. Observe that half of the block matrices are zero (cf. (5.30b)), and that every block matrix has zeros in its m^{th} row and m^{th} column, except for the k = 0, ℓ = 0 block matrices (cf. (5.32)-(5.36)).

AD-A197 287 A NUMERICAL MODEL FOR THE COMPUTATION OF RADIANCE DISTRIBUTIONS IN NATURA..(U) WASHINGTON UNIV SEATTLE JOINT INST FOR STUDY OF ATMOSPHERE AN.. 2/3

UNCLASSIFIED C D MOBLEY ET AL. JAN 88 CONTRIB-40 F/G 8/8 NL

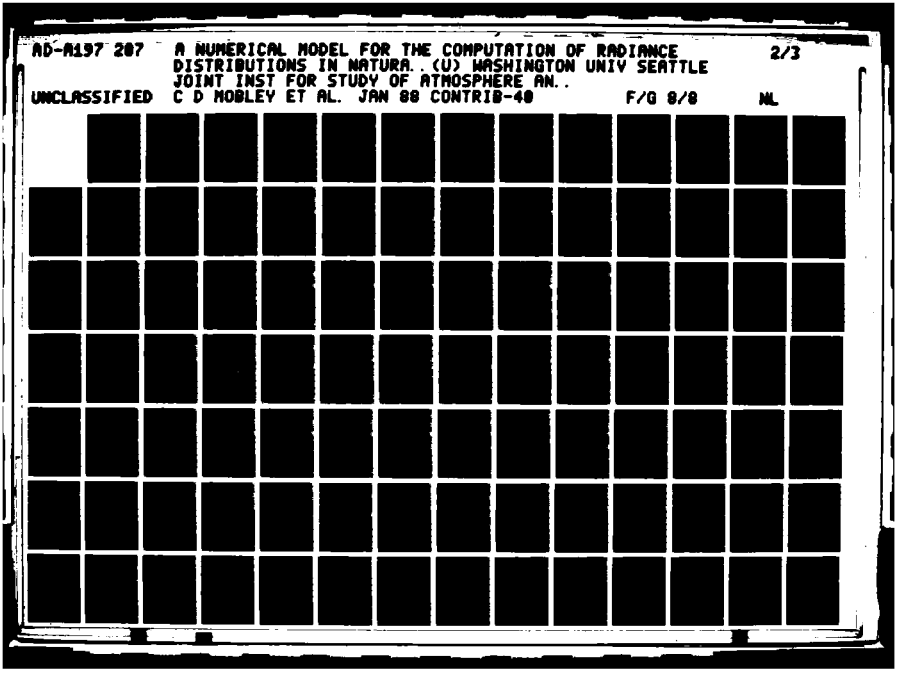

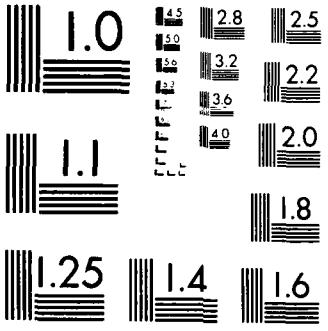

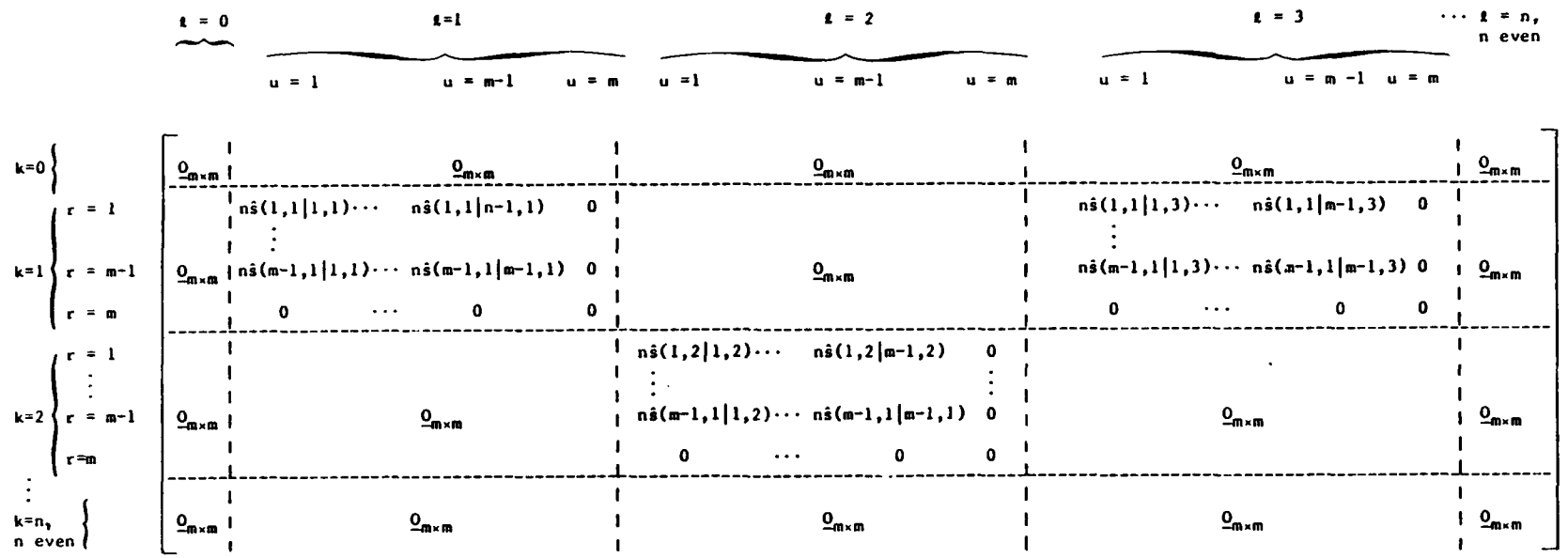

Table 2.--Illustration of the structure of the sine spectral arrays defined by Eq. (5.43). $\hat{s}(r,k|u,\ell)$ represents any of the four sine amplitudes, $\hat{t}_2(a,x;r,k|u,\ell)$, $\hat{t}_2(x,a;r,k|u,\ell)$, $\hat{r}_2(a,x;r,k|u,\ell)$, or $\hat{r}_2(x,a;r,k|u,\ell)$. The factors of n multiplying these elements are explicit values of γ_k. Note that all blocks with k=0 or n, or ℓ=0 or n, are zero. Blocks with $0<k<n$ and $0<\ell<n$ have the same form as the cosine case of Table 1.

With a corresponding development, the surface boundary condition (3.18) in spectral matrix form becomes

$$\underline{A}_p^+(a;\ell) = \sum_{\substack{k=0 \\ (k+\ell \text{ even})}}^{n} \underline{A}_p^+(x;k)\, \underline{\hat{t}}_p(x,a;k|\ell) + \sum_{\substack{k=0 \\ (k+\ell \text{ even})}}^{n} \underline{A}_p^-(a;k)\, \underline{\hat{r}}_p(a,x;k|\ell) \qquad (5.45)$$

where $p = 1$ or 2 and $\ell = 0,\ldots,n$.

Equations (5.44) and (5.45) are the desired spectral forms of the surface boundary conditions and are at a notational level equivalent to the radiative transfer equation (5.29).

It should not be overlooked that when the upper boundary is involved, the amplitude for one ℓ-mode is directly coupled to the amplitudes for all other ℓ-modes. Thus in (5.44), $\underline{A}_p^-(x;\ell)$ is determined by sums over k involving $\underline{A}_p^-(a;k)$ and $\underline{A}_p^+(x;k)$ with $k \neq \ell$. This coupling of ℓ-modes is a consequence of the anisotropy of the upper boundary. In contrast, we recall from the local interaction equations (5.29) that, within the isotropic water medium (i.e., over the depth range $x \leq y \leq z$), the amplitude for a given ℓ-mode is independent of the amplitudes for other k-modes, $k \neq \ell$. If the upper boundary were isotropic, symmetry would cause the sums over k in (5.44) and (5.45) to collapse to single terms for the ℓ^{th} modes, i.e., the ℓ-modes would decouple. This is the case at the bottom boundary.

d. Transformation of the Bottom Boundary Conditions to Spectral Form

The isotropy of the bottom boundary means that the quad-averaged reflectance $r(z,b;r,s|u,v)$ depends azimuthally on $|s-v|$, not upon s and v independently, for non-polar quads Q_{rs} and Q_{uv}. In particular, the azimuthal dependence is on $\cos(\phi_s-\phi_v)$, as was the case for the isotropic phase

function. Just as for the phase function (recall (5.5)) we can represent $r(z,b;r,s|u,v)$ by the form (4.11):

$$r(z,b;r,s|u,v) = \sum_{\ell=0}^{n} \hat{r}(z,b;r,u|\ell)\cos\ell(\phi_s-\phi_v) \tag{5.46}$$

which holds for all Q_{rs} in Ξ_- and Q_{uv} in Ξ_+ and where from (4.12)

$$\hat{r}(z,b;r,u|\ell) \equiv \frac{1}{\varepsilon_\ell \cos(\ell\phi_s)} \sum_{v=1}^{2n} r(z,b;r,s|u,v)\cos(\ell\phi_v) \ . \tag{5.47}$$

We now evaluate (5.47) by going through the four main cases, as in (5.6a,b,c,d):

Quad-to-Quad Case ($r = 1,\ldots,m-1$; $u = 1,\ldots,m-1$). Then with $s = 1$, (5.47) becomes

$$\hat{r}(z,b;r,u|\ell) = \frac{1}{\varepsilon_\ell} \sum_{v=1}^{2n} r(z,b;r,1|u,v)\cos(\ell\phi_v) \tag{5.47a}$$
$$\ell = 0,\ldots,n$$

Quad-to-Cap Case ($r = 1,\ldots,m-1$; $u = m$). Then (5.47) becomes

$$\hat{r}(z,b;r,m|0) = r(z,b;r,1|m,\cdot)$$
$$\hat{r}(z,b;r,m|\ell) = 0 \qquad \ell = 1,\ldots,n \tag{5.47b}$$

Cap-to-Quad Case (r = m; u = 1,...,m-1). Then (5.47) becomes

$$\hat{r}(z,b;\, m,u|0) = r(z,b;\, m,\cdot|u,1)$$

$$\hat{r}(z,b;m,u|\ell) = 0 \qquad \ell = 1,\ldots,n \tag{5.47c}$$

Cap-to-Cap Case (r = m; u = m). Then (5.47) becomes

$$\hat{r}(z,b;m,m|0) = r(z,b;\, m,\cdot|m,\cdot)$$

$$\hat{r}(z,b;m,m|\ell) = 0 \qquad \ell = 1,\ldots,n \tag{5.47d}$$

When the bottom boundary condition (3.25), viz.

$$N^{+}(z;u,v) = \sum_{r}\sum_{s} N^{-}(z;r,s)\; r(z,b;r,s|u,v)\;, \tag{5.48}$$

is rewritten for u = 1,...,m-1 using (5.3), (5.4), (5.47) and the specific cases of (5.47), we have

$$\sum_{\ell=0}^{n} \left[A_1^+(z;u;\ell) \cos(\ell\phi_v) + A_2^+(z;u;\ell) \sin\ell\phi_v) \right]$$

$$= \sum_{r=1}^{m-1} \sum_{s=1}^{2n} \left[\sum_{k=0}^{n} A_1^-(z;r;k) \cos(k\phi_s) + A_2^-(z;r;k) \sin(k\phi_s) \right] \left[\sum_{\ell=0}^{n} \hat{r}(z,b;r,u|\ell) \cos\ell(\phi_s-\phi_v) \right]$$

$$+ A_1^-(z;m;0)\, \hat{r}(z,b;m,u|0) \qquad (5.48a)$$

$$= \sum_{r=1}^{m-1} \sum_{k} A_1^-(z;r;k) \sum_{\ell} \hat{r}(z,b;r,u|\ell) \left[\sum_{s=1}^{2n} \cos(k\phi_s) \cos\ell(\phi_v-\phi_s) \right]$$

$$+ \sum_{r=1}^{m-1} \sum_{k} A_2^-(z;r;k) \sum_{\ell} \hat{r}(z;b;r,u|\ell) \left[\sum_{s=1}^{2n} \sin(k\phi_s) \cos\ell(\phi_v-\phi_s) \right]$$

$$+ A_1^-(z;m;0)\, \hat{r}(z,b;m,u|0) \,.$$

The sums over s can be reduced by (4.4) and (4.5) so that the right side becomes

$$\sum_{r=1}^{m-1} \sum_{k} A_1^-(z;r;k) \sum_{\ell} \hat{r}(z,b;r,u|\ell)\, n(\delta_{k+\ell} + \delta_{k-\ell} + \delta_{k+\ell-2n}) \cos(\ell\phi_v)$$

$$+ \sum_{r=1}^{m-1} \sum_{k} A_2^-(z;r;k) \sum_{\ell} \hat{r}(z,b;r,u|\ell)\, n(\delta_{k-\ell} - \delta_{k+\ell} - \delta_{k+\ell-2n}) \sin(\ell\phi_v)$$

$$+ A_1^-(z;m;0)\, \hat{r}(z,b;m,u|0) \,.$$

The Kronecker deltas leave only terms with $k = \ell$, with ε_ℓ and γ_ℓ multipliers, so that we have left just the following for $u = 1,\ldots,m-1$:

$$\sum_{\ell=0}^{n} \left[A_1^+(z;u;\ell) \cos(\ell\phi_v) + A_2^+(z;u;\ell) \sin(\ell\phi_v) \right]$$

$$= \sum_{\ell=0}^{n} \sum_{r=1}^{m-1} \left[A_1^-(z;r;\ell)\, \hat{r}(z,b;r,u|\ell)\, \varepsilon_\ell \cos(\ell\phi_v) + A_1^-(z;m;\ell)\, \hat{r}(z,b;m,u|\ell)\, \delta_\ell \right] \tag{5.49}$$

$$+ \sum_{\ell=0}^{n} \sum_{r=1}^{m-1} A_2^-(z;r;\ell)\, \hat{r}(z,b;r,u|\ell)\, \gamma_\ell \sin(\ell\phi_v) \, .$$

For the case u = m, we return to (5.48a), set u = m, recall (5.4) and (5.47a-d), and find

$$A_1^+(z;m;0) = \sum_{r=1}^{m-1} \sum_{k=0}^{n} \left\{ A_1^-(z;r;k) \left[\sum_{s=1}^{2n} \cos(k\phi_s) \right] + A_2^-(z;r;k) \left[\sum_{s=1}^{2n} \sin(k\phi_s) \right] \right\}$$

$$\times \hat{r}(z,b;r,m|0) + A_1^-(z;m;0)\, \hat{r}(z,b;m,m|0)$$

$$= \sum_{r=1}^{m-1} A_1^-(z;r;0)\, \varepsilon_0\, \hat{r}(z,b;r,m|0) +$$

$$+ A_1^-(z;m;0)\, \hat{r}(z,b;m,m|0)$$

We can now define the m×m matrices $\underline{\hat{r}}_p(z,b;\ell)$ for p = 1,2 via

$$[\underline{\hat{r}}_1(z,b;\ell)]_{ru} \equiv \begin{cases} \varepsilon_\ell \hat{r}(z,b;r,u|\ell) & \text{for} \quad r = 1,\ldots,m-1 \\ \delta_\ell \hat{r}(z,b;m,u|\ell) & \text{for} \quad r = m \end{cases} \tag{5.50}$$

and for u = 1,...,m ; ℓ = 0,...,n

$$[\underline{\hat{r}}_2(z,b;\ell)]_{ru} = \begin{cases} \gamma_\ell \hat{r}(z,b;r,u|\ell) & \text{for } r = 1,\ldots,m-1 \text{ and } \ell = 1,\ldots,n-1 \\ 0 & \text{for } r = m \text{ and } \ell = 0 \text{ or } \ell = n \end{cases} \tag{5.51}$$

and for u = 1,...,m.

These definitions hold for u = 1,...,m, keeping in mind (5.47b,c,d) for the four main cases. By means of these definitions, Eq. (5.49) then can be written for u = 1,...,m-1, and also for the case u = m, as

$$\sum_{\ell=0}^{n} \left\{ A_1^+(z;u;\ell)\cos(\ell\phi_v) + A_2^+(z;u;\ell)\sin(\ell\phi_v) \right\}$$

$$= \sum_{\ell=0}^{n} \left\{ \sum_{r=1}^{m} A_1^-(z;r;\ell) \left[\underline{\hat{r}}_1(z,b;\ell) \right]_{ru} \right\} \cos(\ell\phi_v)$$

$$+ \sum_{\ell=0}^{n} \left\{ \sum_{r=1}^{m} A_2^-(z;r;\ell) \left[\underline{\hat{r}}_2(z,b;\ell) \right]_{ru} \right\} \sin(\ell\phi_v) \ .$$

Using the 1×m amplitude vectors of (5.29) we find

$$\sum_{\ell=0}^{n} \left[\underline{A}_1^+(z;\ell)\cos(\ell\phi_v) + \underline{A}_2^+(z;\ell)\sin(\ell\phi_v) \right]$$

$$= \sum_{\ell=0}^{n} \underline{A}_1^-(z;\ell)\ \underline{\hat{r}}_1(z,b;\ell)\cos(\ell\phi_v) + \sum_{\ell=0}^{n} \underline{A}_2^-(z;\ell)\ \underline{\hat{r}}_2(z,b;\ell)\sin(\ell\phi_v) \ .$$

Invoking the linear independence of $\cos(\ell\phi_v)$ and $\sin(\ell\phi_v)$, we obtain a matrix equation for the spectral form of the bottom boundary condition:

$$\underline{A}_p^+(z;\ell) = \underline{A}_p^-(z;\ell)\ \underline{\hat{r}}_p(z,b;\ell) \qquad (5.52)$$

where p = 1 or 2 and ℓ = 0,1,...,n.

Equation (5.52) is the general spectral form of the lower boundary condition (3.25). Under assumption (3) in §1a, the lower boundary is azimuthally isotropic. Hence, unlike the surface boundary conditions (5.44) and (5.45), the bottom boundary condition exhibits decoupling of the

ℓ-modes. There are two cases we consider; a matte surface and a plane surface above an infinitely deep homogeneous hydrosol.

We recall from (3.26) that for the special case of a matte bottom, $r(z,b;r,s|u,v) = -\frac{r_-}{\pi}\mu_r\Omega_r$. This function in (5.47) leaves just

$$\hat{r}(z,b;r,u|\ell) = \frac{1}{\varepsilon_\ell \cos(\ell\phi_s)}\left(-\frac{r_-}{\pi}\mu_r\Omega_r\right)\sum_{v=1}^{2n}\cos(\ell\phi_v), \quad \begin{cases} r,u=1,\ldots,m \\ \ell = 0,\ldots,n \end{cases},$$

whence

$$\hat{r}(z,b;r,u|0) = -\frac{r_-}{\pi}\mu_r\Omega_r \quad \left(\equiv r(z,b;r,1|u,v) \text{ for } \begin{cases} r,u = 1,\ldots,m \\ v = 1,\ldots,2n \end{cases}\right), \quad (5.53a)$$

and

$$\hat{r}(z,b;r,u|\ell) = 0 \text{ for } \begin{cases} r,u = 1,\ldots,m \\ \ell = 1,\ldots,n \end{cases} \quad (5.53b)$$

Hence only the case $\ell = 0$ is non-trivial. That is, by (5.50) and (5.53) we have $[\hat{r}_1(z,b;\ell)]_{ru} = 0$ for $\ell = 1,\ldots,n$ and $u,r = 1,\ldots,m$. Further, $[\hat{r}_2(z,b;\ell)]_{ru} = 0$ for all $\ell = 0,\ldots,n$ and $u,r = 1,\ldots,m$. Hence (5.53) is consistent with the cases in (5.47a,b,c,d) for a reflectance $r(z,b;r,1|u,v)$ that is independent of u and v and that depends only on r. Then the lower boundary condition (5.52) for a matte bottom reduces to just

$$\underline{A}_1^+(z;0) = \underline{A}_1^-(z;0)\,\underline{\hat{r}}_1(z,b;0)\,, \quad (5.54)$$

with $\underline{A}_1^+(z;\ell) \equiv \underline{0}$ for $\ell = 1,\ldots,n$, and $\underline{A}_2^+(z;\ell) \equiv \underline{0}$ for $\ell = 0,\ldots,n$.

The case of the reflectance of an infinitely deep hydrosol is discussed in §10.

We have now obtained a discrete, spectral form of the Natural Hydrosol Model in the form of equations (5.29), (5.44), (5.45) and (5.52). However, we are not yet ready to proceed with the numerical solution of the local interaction equations (5.29). In order to integrate (5.29) down into the

water column, i.e., over all depths y such that $x \leq y \leq z$, we need the initial values for the amplitudes namely $\underline{A}_p^{\pm}(x;\ell)$. The upper surface boundary conditions (5.44) and (5.45) relate the needed $\underline{A}_p^{\pm}(x;\ell)$ to each other and to known or measurable quantities such as $\underline{A}_p^{\pm}(a;\ell)$ and the $\hat{\underline{r}}$ and $\hat{\underline{t}}$ matrices of the air-water surface, but the boundary conditions by themselves cannot be solved to obtain the needed initial conditions (there are four unknown vectors $\underline{A}_p^{\pm}$ and only two equations). A reformulation of the spectral model is clearly needed, and this is done in the next section.

We do note in passing, however, that the present spectral model could be solved approximately as a series of upward and downward integration sweeps of the local interaction equations (5.29). This is a rather quixotic approach, but it is worth a momentary consideration in order to make a general point. To see how this might be done, consider the following. Radiance passes through the upper boundary (e.g., from the sun) and into the water column (using the transmittance part of (5.44)), where the light field varies with depth according to the local interaction equations. Some light is scattered back toward the surface at each depth y, and some light eventually reaches the lower boundary where it is partially reflected (using (5.52)). This upwardly scattered and reflected radiance is itself partly scattered again into downward directions at each y level, and some radiance reaches the water surface, where it is partly transmitted into the air and partly reflected back into the water column. And so it goes, ad infinitum. *The radiance field which we desire is the total of the contributions of an infinite number of*

*scatterings and interreflections like those just described.** The solution field can be approximately obtained by a finite sequence of integrations of (5.29) back and forth between the boundaries; termination of the integration sequence is made when the contribution of another sweep to the accumulating sum of sweep contributions is acceptably small. *However, an exact summation of the infinite number of interreflections can be made in closed form by the powerful algebraic techniques of invariant imbedding theory when the media are of the one-parameter type.* The resulting equations are solved by just one pair of integration sweeps and give the desired total radiance field. This algebraic reformulation of the spectral model is the subject of the next section.

e. The Case of the Vanishing Polar Caps

We pause to examine what happens to the basic equation systems (5.11) and (5.12) when we let the radii of the polar caps go to zero. First, recall from (5.6b) that $\hat{p}^{\pm}(y;m,u;0) = p^{\pm}(y;m,\cdot|u,1)$. Next observe from (3.11) that generally $p(y;r,s|u,v) \to 0$ as $\Omega_{rs} \to 0$. In the case that $Q_{rs} = Q_m$, a polar cap, it follows that $\hat{p}^{\pm}(y;m,u;0) \to 0$ as a polar cap's radius approaches 0. Since $A_1(y;m;\ell)$ goes to a finite limit (namely the radiance $N(y;m,\cdot)$ for

* What is being described here is a fundamental and powerful heuristic approach to scattering problems known as the "natural solution" procedure. See, for example, Preisendorfer (1965, p. 73) and H.O., Vol. II, p. 203 for the case of photons; and Preisendorfer (1973, pp. 47-48) for the case of water waves, which explicitly realizes the above multiple scattering procedure. These references also contain some historical notes on the natural solution procedure. This procedure is so powerful that it can operate on all levels of radiative transfer theory, from obtaining simple estimates of radiance fields by single or double scattering order calculations, to establishing the existence of solutions of the equation of transfer for radiance in arbitrary geometrical settings. Ultimately, as computer power continues to evolve, the natural solution may be the way to go in general, irregular geometries and for polarized fields in such geometries.

$\ell = 0$, and vanishes otherwise ($\ell = 1,\ldots,n$) we conclude that the two cap terms in (5.11) vanish along with the caps. The set (5.12) is unaffected as the caps go to zero. These effects also can be seen in (5.15) and (5.16). *The result is that (5.15) and (5.16), for the case of zero-radius caps, are autonomous equations (e.g., m-1 equations in m-1 unknowns) as are also (5.17) and (5.18). Similar observations can be made for the boundary conditions. The present theory can therefore be applied to natural hydrosols with capless direction spaces.*

It is interesting to see that (5.19) and (5.20) reduce under these conditions to useless appendixes: one can integrate (5.19) and (5.20) down into the hydrosol provided $A_I^{\pm}(y;m;0) = N^{\pm}(y;m,\cdot)$ are known at some depth $y \geq x$. However, such information is not accessible within the context of the Natural Hydrosol Model: the continuous-direction information $N^{-}(a;\underline{\xi})$ is the given input to the NHM. Upon undergoing quad averaging, this purely directional information at level a is smeared out. The model solution then determines the quad-averaged radiances $N^{\pm}(x;u,v)$ at level x below the surface. There is no unique road back, however, to $N^{\pm}(x;\underline{\xi})$ at level x. Hence we get the interesting "mule" equations (5.19) and (5.20). That is, these equations, born of quad averaging $p^{\pm}(y;\underline{\xi}';\underline{\xi})$ only over the $\underline{\xi}'$, cannot have any progeny (solutions) in the NHM context.

This mule equation phenomenon can be witnessed quite generally by allowing Ω_{uv} (but not Ω_{rs}) in (3.12) shrink to zero. The result is the hybrid equation

$$-\mu \frac{d}{dy} N(y;\underline{\xi}) = -N(y;\underline{\xi}) + \omega(y) \sum_r \sum_s N(y;r,s)\, p(y;r,s;\underline{\xi}) \qquad (5.55)$$

where

$$p(y;r,s;\underline{\xi}) \equiv \int_{Q_{rs}} \int p(y;\underline{\xi}';\underline{\xi})\, d\Omega(\underline{\xi}') \ .$$

Suppose then we have used the NHM to compute the quad-averaged radiances $N(y;r,s)$ for all Q_{rs} in Ξ. Can we make use of (5.55) to compute $N(y;\underline{\xi})$ at some y for any $\underline{\xi}$ in Ξ? It would at first seem that this is possible. The equation set could obviously be integrated at once over all y, $x \leq y \leq z$, knowing $N(y;\underline{\xi})$ for a single depth, say x, and for some fixed direction $\underline{\xi}_0$. But how is one to come by knowledge of $N(x;\underline{\xi}_0)$? This, as we saw above, is inaccessible knowledge at level x in the context of the NHM.

In sum, then, equations (5.15)-(5.18) hold if the polar cap terms are removed from (5.15) and (5.16). The quads around the polar cap are replaced by triangles sharing a common vertex at the poles of the unit sphere of directions (cf. Fig. 3; and let the polar cap shrink to a point). If we index the quads, starting at the equator, from 1 to m-1, where the polar triangles are indexed by m-1, then (5.15)-(5.18) apply at once with the polar terms removed from (5.15) and (5.16). The resultant four equations for $A_1^{\pm}$ and $A_2^{\pm}$ then have identical forms. Of course (5.15) and (5.16) apply, as before, to ℓ in the range $0,\ldots,$; while (5.17) and (5.18) still apply to ℓ in the range $1,\ldots,n-1$. Equations (5.19) and (5.20) become infertile, in the sense described above, and are disregarded.

What then is to be gained by deriving the local interaction equations (5.29) with polar caps included as part of the decomposition of the unit sphere Ξ? The answer is in the economy of description of radiance around the polar region: one small cap will do just as well in resolving zenith or nadir radiances as 2n triangles. However, it should be clear to the reader, who has closely followed the derivation of (5.29) to its very end, that a much simpler and cleaner derivation results by eliminating the polar caps. So take your pick as to which derivation you prefer; and remember: the present polar cap

derivation includes the non-polar cap alternate as a special case, but not conversely.

6. TRANSPORT FORM OF THE SPECTRAL EQUATIONS

a. Fundamental Solutions: Motivation

In this section we review some results from the elementary theory of differential equations, and then go on to introduce the notion of the global interaction principles. These will be the global versions of the local interaction equations (5.29). We then can establish the imbed and union rules for optical media, and also the Riccati differential equations for the global reflectance and transmittance operators. These topics constitute the modern transport approach to solving radiative transfer problems in lakes and seas.

To fix ideas, we consider a coupled system of two equations; the generalization to a system of many equations (in particular, to the local interaction equations (5.29)) will then be obvious.

Consider the pair of equations*

$$
\begin{aligned}
-\frac{d\eta(y)}{dy} &= \eta(y)\,\tau(y) + \zeta(y)\,\rho(y) \\
\frac{d\zeta(y)}{dy} &= \zeta(y)\,\tau(y) + \eta(y)\,\rho(y)
\end{aligned}
\tag{6.1}
$$

where $\rho(y)$ and $\tau(y)$ are continuous functions on $x \le y \le z$. This system can be placed in matrix form by defining the two-element row vector

$$
\underline{H}(y) \equiv [\eta(y),\ \zeta(y)] \qquad (1 \times 2)
$$

and the *system matrix*

---

* For a reader familiar with the two-flow irradiance model (cf., Preisendorfer and Mobley, 1984), the following introductory exercise is directly applicable to that model. Set $\eta(y) \equiv H(y,+)$, and $\zeta(y) \equiv H(y,-)$, and generalize $\rho(y)$, $\tau(y)$ to $\rho(y,\pm)$, $\tau(y,\pm)$.

$$\underline{K}(y) \equiv \begin{bmatrix} -\tau(y) & \rho(y) \\ -\rho(y) & \tau(y) \end{bmatrix} \qquad (2 \times 2)$$

to get

$$\frac{d}{dy}\,\underline{H}(y) = \underline{H}(y)\,\underline{K}(y)\ . \qquad (6.2)$$

The system (6.1) can be integrated from x to any point y, using as initial conditions $\eta(x) = 1$ and $\zeta(x) = 0$. Let the solutions at y be $\eta_1(y)$ and $\zeta_0(y)$. Likewise, (6.1) can be integrated with the initial conditions $\eta(x) = 0$ and $\zeta(x) = 1$. Let these solutions be $\eta_0(y)$ and $\zeta_1(y)$. Each pair of solution vectors $[\eta_1(y), \zeta_0(y)]$ and $[\eta_0(y), \zeta_1(x)]$ is a *fundamental solution* of (6.1). Note that at $y = x$ the fundamental solution vectors are [1,0] and [0,1], and are clearly linearly independent. It is easily shown (see, for example, Coddington and Levinson, 1955, pp. 28, 69) that the fundamental solutions associated with (6.1) for continuous $\rho(y)$ and $\tau(y)$ remain linearly independent for all y values in $x \le y \le z$. Therefore the general solution of (6.1) over the range $x \le y \le z$ can be written as a linear combination of the fundamental solution vectors. Now use the fundamental solution vectors to define the *fundamental matrix*

$$\underline{M}(x,y) \equiv \begin{bmatrix} \eta_1(y) & \zeta_0(y) \\ \eta_0(y) & \zeta_1(y) \end{bmatrix}\ . \qquad (2 \times 2) \qquad (6.3)$$

The linear independence of the fundamental solutions guarantees the nonsingularity of $\underline{M}(x,y)$. Note that

$$\underline{M}(x,x) = \begin{bmatrix} 1 & 0 \\ 0 & 1 \end{bmatrix} \equiv \underline{I}\ . \qquad (6.4)$$

Since the fundamental solutions each satisfy (6.1), it follows that

$$\eta(y) \equiv \eta(x)\ \eta_1(y) + \zeta(x)\ \eta_0(y)$$
$$\zeta(y) \equiv \eta(x)\ \zeta_0(y) + \zeta(x)\ \zeta_1(y)$$

gives the general solution of (6.1) for arbitrary initial conditions $[\eta(x), \zeta(x)]$. In matrix form this equation is

$$\boxed{\underline{H}(y) = \underline{H}(x)\ \underline{M}(x,y)\ ,} \tag{6.5}$$

which is known as the *mapping property* of $\underline{M}(x,y)$, since $\underline{M}(x,y)$ maps the initial vector $\underline{H}(x)$ into the solution vector $\underline{H}(y)$.

Two important properties of $\underline{M}(x,y)$ can be obtained from (6.5). Differentiating (6.5), applying (6.2), and letting the initial conditions $\underline{H}(x)$ be arbitrary leads to the conclusion

$$\frac{d}{dy}\ \underline{M}(x,y) = \underline{M}(x,y)\ \underline{K}(y)\ . \tag{6.6}$$

This equation merely states that the fundamental solutions satisfy (6.1). A second property is found from the observation that the solution at z, $\underline{H}(z)$, can be expressed two ways using the mapping property:

$$\underline{H}(z) = \underline{H}(x)\ \underline{M}(x,z)$$

or

$$\underline{H}(z) = \underline{H}(y)\ \underline{M}(y,z)\ ,$$

where $\underline{M}(y,z)$ is constructed as a set of fundamental solutions whose initial values are taken at y rather than at x (thus $\underline{M}(y,y) = \underline{I}$). Substituting (6.5) into the second of these two equations and using the arbitrary initial condition $\underline{H}(x)$ yields the *group property* for $\underline{M}$:

$$\boxed{\underline{M}(x,z) = \underline{M}(x,y)\,\underline{M}(y,z)\ .} \tag{6.7}$$

It follows from (6.7) (upon setting x = z) that

$$\underline{M}^{-1}(x,y) = \underline{M}(y,x)\ .$$

It is clear that the general solution of (6.1) or (6.2) is closely tied to the linear algebra of the system matrix $\underline{K}(y)$ and the fundamental matrix $\underline{M}(x,y)$.

b. Fundamental Solutions: Application

We next apply the concepts introduced in the previous section to the local interaction equations, (5.29). Now the 1×m vector of upward amplitudes, $\underline{A}_p^+(y;\ell)$, takes the place of $\eta(y)$; and the 1×m vector of downward amplitudes $\underline{A}_p^-(y;\ell)$ takes the place of $\zeta(y)$. Likewise the m×m matrices $\hat{\underline{\rho}}(y;\ell)$ and $\hat{\underline{\tau}}(y;\ell)$ replace $\rho(y)$ and $\tau(y)$, respectively, in (6.1). Then (5.29) can be written as

$$\frac{d}{dy}\,[\underline{A}_p^+(y;\ell),\ \underline{A}_p^-(y;\ell)] = [\underline{A}_p^+(y;\ell),\ \underline{A}_p^-(y;\ell)] \begin{bmatrix} -\hat{\underline{\tau}}(y;\ell) & \hat{\underline{\rho}}(y;\ell) \\ -\hat{\underline{\rho}}(y;\ell) & \hat{\underline{\tau}}(y;\ell) \end{bmatrix}\ .$$

Defining

$$\underline{A}_p(y;\ell) \equiv [\underline{A}_p^+(y;\ell),\ \underline{A}_p^-(y;\ell)]\ , \qquad (1 \times 2m)$$

and

$$\underline{K}(y;\ell) \equiv \begin{bmatrix} -\hat{\underline{\tau}}(y;\ell) & \hat{\underline{\rho}}(y;\ell) \\ -\hat{\underline{\rho}}(y;\ell) & \hat{\underline{\tau}}(y;\ell) \end{bmatrix} , \qquad (2m \times 2m) \tag{6.8}$$

the local interaction equations can be written as

$$\frac{d}{dy} \underline{A}_p(y;\ell) = \underline{A}_p(y;\ell)\, \underline{K}(y;\ell) \tag{6.9}$$

where $p = 1$ or 2 and $\ell = 0,\ldots,n$. Observe that the system matrix is independent of $p = 1,2$.

In analogy to the pair (6.2) and (6.6), we have the present pair (6.9) and

$$\frac{d}{dy} \underline{M}(x,y;\ell) = \underline{M}(x,y;\ell)\, \underline{K}(y;\ell) \tag{6.10}$$

for $\ell = 0,\ldots,n$ and for $x \le y \le z$. The fundamental matrix $\underline{M}$ depends on the ℓ-mode, but is the same for $p = 1$ or $p = 2$. $\underline{M}$ is now $(2m) \times (2m)$ in size, and the initial conditions for (6.10) are

$$\underline{M}(x,x;\ell) \equiv \underline{I} , \tag{6.11}$$

where $\underline{I}$ is the $(2m)\times(2m)$ identity matrix.

The group property (6.7) is now, for each $\ell = 0,\ldots,n$, and $x \le y \le z$,

$$\underline{M}(x,z;\ell) = \underline{M}(x,y;\ell)\, \underline{M}(y,z;\ell), \tag{6.12}$$

and we can write the mapping property (6.5) as

$$\underline{A}_p(y;\ell) = \underline{A}_p(x;\ell)\ \underline{M}(x,y;\ell), \tag{6.13}$$

for $p = 1,2$ and $\ell = 0,\ldots,n$, with $x \le y \le z$.

The results just presented apply to a downward integration of (6.9) along the water column from x to y. We can also consider an upward integration from z to y, for which a corresponding set of fundamental solutions exists. For an upward sweep we have the corresponding development:

$$\frac{d}{dy}\ \underline{M}(z,y;\ell) = \underline{M}(z,y;\ell)\ \underline{K}(y;\ell) \tag{6.14}$$

$$\underline{M}(z,z;\ell) = \underline{I}$$

$$\underline{M}(z,x;\ell) = \underline{M}(z,y;\ell)\ \underline{M}(y,x;\ell)$$

and

$$\underline{A}_p(y;\ell) = \underline{A}_p(z;\ell)\ \underline{M}(z,y;\ell)$$

where $p = 1,2$; $\ell = 0,\ldots,n$; and $x \le y \le z$.

It should be noted that the integration sweeps of (6.10) or (6.14) proceed routinely as long as $\underline{K}(y;\ell)$ is continuous. If $\underline{K}(y;\ell)$ is discontinuous, as at the air-water boundary, we can cross the discontinuity not by integration but by an extended form of the group property (6.12). Thus, for example, given the incident amplitude vector $\underline{A}_p(a;\ell)$ just above the air-water surface, and given the fundamental matrix $\underline{M}(a,x;\ell)$ which we assume for the moment to be associated with the air-water surface in some way, we can integrate (6.10) from x to y (since $\underline{K}(y;\ell)$ is continuous in the water column) to find $\underline{M}(x,y;\ell)$. We would then use the extended form of (6.12) to obtain

$\underline{M}(a,y;\ell)$, and thus the solution $\underline{A}_p(y;\ell)$ via (6.13). However, we will not proceed this way, since the fundamental solution, while a beautiful analytic tool, is not readily amenable to the preceding kind of hybrid integration-algebraic task. This is the case since the fundamental matrix $M(a,x;\ell)$ for the air-water surface must first be derived by certain algebraic procedures from the basic reflectance and transmittance matrices $\hat{\underline{r}}$ and $\hat{\underline{t}}$ of the air-water surface. Perhaps more importantly, the fundamental solution procedure is numerically inherently unstable,* so that great care must be exercised in the integration of (6.10) and (6.14) over ranges of y on the order of 10 or more optical depths. For all these reasons, therefore, we turn to a more versatile and physically more meaningful mode of solution of (6.10).

c. Global Interaction Equations

Let us expand the general solution (6.13) so that the upward and downward amplitudes are visible:

$$[\underline{A}_p^+(y;\ell),\ \underline{A}_p^-(y;\ell)] = [\underline{A}_p^+(x;\ell),\ \underline{A}_p^-(x;\ell)]\ \underline{M}(x,y;\ell) \tag{6.15}$$

For the slab X[x,y] of the plane-parallel medium (cf. Fig. 1) we think of $\underline{A}_p^-(x;\ell)$ as being *incident* on X[x,y] from above at level x, and $\underline{A}_p^+(y;\ell)$ as being *incident on* X[x,y] *from* below at level y. These incident amplitudes are thought of as initiating the light field in X[x,y]. Hence, we may think of $\underline{A}_p^+(x;\ell)$ as being the associated *response* of the slab X[x,y] at x, and $\underline{A}_p^-(y;\ell)$ as being the *response* of the slab X[x,y] at y. The term "incident" is motivated by the idea of light shining downward into the slab at

* An examination of the numerical instability of the fundamental solution procedure was made in the water-wave context of invariant imbedding theory; see Preisendorfer (1977, p. 40).

x and upward into the slab at y. "Response" calls to mind the light leaving the slab at x and y after the slab has responded at all internal levels to the light incident on its boundaries. We now see that (6.15) gives the incident and response amplitudes at level y as a function of the incident and response amplitudes at level x, and thus is not in a useful form even if $\underline{M}(x,y;\ell)$ is known. What is needed is an equation relating the response amplitudes at x and y to the incident amplitudes at x and y. Such an equation can be obtained by rewriting (6.15), as follows.

Recall first that here $\underline{I}$ and $\underline{M}$ are each (2m)×(2m). Then write (6.15) as

$$[\underline{A}_p^+(y;\ell),\ \underline{A}_p^-(y;\ell),\ \underline{A}_p^+(x;\ell),\ \underline{A}_p^-(x;\ell)] \begin{bmatrix} \underline{I} \\ -\underline{M}(x,y;\ell) \end{bmatrix} = \underline{0}\ . \qquad (6.16a)$$

We wish to reorder the extended horizontal vector into the form

$$[\underline{A}_p^+(x;\ell),\ \underline{A}_p^-(y;\ell),\ \underline{A}_p^+(y;\ell),\ \underline{A}_p^-(x;\ell)]\ ,$$

in which the first two vectors are the response vectors and the second two are the incident vectors. This can be accomplished by the following matrix mapping of the two kinds of vectors, above:

$$[\underline{A}_p^+(y;\ell),\ \underline{A}_p^-(y;\ell),\ \underline{A}_p^+(x,\ell),\ \underline{A}_p^-(x,\ell)] \begin{bmatrix} \underline{0} & 0 & \underline{I} & \underline{0} \\ 0 & I & 0 & 0 \\ I & 0 & 0 & 0 \\ \underline{0} & 0 & 0 & \underline{I} \end{bmatrix} = [\underline{A}_p^+(x;\ell),\ \underline{A}_p^-(y;\ell),\ \underline{A}_p^+(y;\ell),\ \underline{A}_p^-(x;\ell)]\ .$$

The 0 and I elements of the matrix operator are each m×m matrices. We can partition this matrix operator as

$$\underline{P} \equiv \left[\begin{array}{cc:cc} \underline{0} & 0 & \underline{I} & \underline{0} \\ 0 & \underline{I} & 0 & 0 \\ \hdashline \underline{I} & 0 & 0 & 0 \\ \underline{0} & 0 & 0 & \underline{I} \end{array}\right] \equiv \left[\begin{array}{c:c} \underline{P}_2 & \underline{P}_1 \\ \hdashline \underline{P}_1 & \underline{P}_2 \end{array}\right]\ ,$$

where $\underline{P}_1$ and $\underline{P}_2$ are each $(2m)\times(2m)$. Now observe that

$$\underline{P}^2 = \begin{bmatrix} \underline{P}_2 & \underline{P}_1 \\ \underline{P}_1 & \underline{P}_2 \end{bmatrix}^2 = \underline{I}$$

so that $\underline{P}^2$ can be inserted into (6.16a):

$$[\underline{A}_p^+(y;\ell),\ \underline{A}_p^-(y;\ell),\ \underline{A}_p^+(x;\ell),\ \underline{A}_p^-(x,\ell)] \begin{bmatrix} \underline{P}_2 & \underline{P}_1 \\ \underline{P}_1 & \underline{P}_2 \end{bmatrix}^2 \begin{bmatrix} \underline{I} \\ -\underline{M}(x,y;\ell) \end{bmatrix} = \underline{0} \ .$$

Performing the indicated multiplications of $\underline{P}$ acting to the left and to the right yields

$$[\underline{A}_p^+(x;\ell),\ \underline{A}_p^-(y;\ell),\ \underline{A}_p^+(y;\ell),\ \underline{A}_p^-(x;\ell)] \begin{bmatrix} \underline{P}_2 - \underline{P}_1\underline{M}(x,y;\ell) \\ \underline{P}_1 - \underline{P}_2\underline{M}(x,y;\ell) \end{bmatrix} = \underline{0} \ .$$

Expanding this equation gives

$$[\underline{A}_p^+(x;\ell),\ \underline{A}_p^-(y;\ell)][\underline{P}_2-\underline{P}_1\ \underline{M}(x,y;\ell)] + [\underline{A}_p^+(y;\ell),\ \underline{A}_p^-(x;\ell)][\underline{P}_1-\underline{P}_2\ \underline{M}(x,y;\ell)] = \underline{0}$$

or

$$[\underline{A}_p^+(x;\ell),\ \underline{A}_p^-(y;\ell)] = [\underline{A}_p^+(y;\ell),\ \underline{A}_p^-(x;\ell)][\underline{P}_2\ \underline{M}(x,y;\ell) - \underline{P}_1][\underline{P}_2-\underline{P}_1\ \underline{M}(x,y;\ell)]^{-1} \ , \tag{6.16b}$$

which gives the desired reordering of the amplitude vectors.

We define

$$\underline{M}(x,y;\ell) \equiv [\underline{P}_2\ \underline{M}(x,y;\ell) - \underline{P}_1][\underline{P}_2-\underline{P}_1\ \underline{M}(x,y;\ell)]^{-1} \qquad (2m)\times(2m) \tag{6.17}$$

and note that $\underline{M}(x,x;\ell) = \underline{I}$. The continuity of $\underline{K}(y;\ell)$ guarantees the existence of the inverse in the definition of $\underline{M}(x,y;\ell)$. We can partition $\underline{M}(x,y;\ell)$ as

$$\underline{M}(x,y;\ell) \equiv \left[\begin{array}{c|c} \underline{T}(y,x;\ell) & \underline{R}(y,x;\ell) \\ \hline \underline{R}(x,y;\ell) & \underline{T}(x,y;\ell) \end{array}\right],$$

where the $\underline{R}$ and $\underline{T}$ matrices are defined in context and are each m×m. They are termed, respectively, the *standard reflectance* and *standard transmittance* matrices. These matrices may be defined explicitly by performing the indicated operations in (6.17). First, we define four m×m submatrices of $\underline{M}(x,y;\ell)$ in context by writing

$$\underline{M}(x,y;\ell) \equiv \begin{bmatrix} \underline{M}_{++}(x,y;\ell) & \underline{M}_{+-}(x,y;\ell) \\ \underline{M}_{-+}(x,y;\ell) & \underline{M}_{--}(x,y,\ell) \end{bmatrix} \tag{6.18}$$

Then we find from (6.17) that (cf. H.O., Vol. IV, p. 43)

$$\underline{R}(y,x;\ell) = \underline{M}_{++}^{-1}(x,y;\ell)\, \underline{M}_{+-}(x,y;\ell) \tag{6.17a}$$

$$\underline{T}(x,y;\ell) = \underline{M}_{--}(x,y;\ell) - \underline{M}_{-+}(x,y;\ell)\, \underline{M}_{++}^{-1}(x,y;\ell)\, \underline{M}_{+-}(x,y;\ell) \tag{6.17b}$$

$$\underline{T}(y,x;\ell) = \underline{M}_{++}^{-1}(x,y;\ell) \tag{6.17c}$$

$$\underline{R}(x,y;\ell) = -\underline{M}_{-+}(x,y;\ell)\, \underline{M}_{++}^{-1}(x,y;\ell) \tag{6.17d}$$

From (6.11) it is clear that, for $\ell = 0,\ldots,n$,

$$\underline{M}_{++}(x,x;\ell) = \underline{M}_{--}(x,x,;\ell) = \underline{I} \qquad (m\times m) \tag{6.17e}$$

$$\underline{M}_{+-}(x,x;\ell) = \underline{M}_{-+}(x,x;\ell) = \underline{0} \qquad (m\times m) \tag{6.17f}$$

By what we have just observed about $M(x,y;\ell)$, at $y = x$ we have

$$\underline{T}(x,x;\ell) = \underline{I}$$

$$\underline{R}(x,x;\ell) = \underline{0} \ .$$

which express the intuitively clear idea that a water slab of zero thickness has unit transmittance and zero reflectance. Observe that the $\underline{R}$ and $\underline{T}$ matrices are independent of p = 1 or 2. Therefore, (6.16b) can be written

$$[\underline{A}_p^+(x;\ell),\ \underline{A}_p^-(y;\ell)] = [\underline{A}_p^+(y;\ell),\ \underline{A}_p^-(x;\ell)] \begin{bmatrix} \underline{T}(y,x;\ell) & \underline{R}(y,x;\ell) \\ \underline{R}(x,y;\ell) & \underline{T}(x,y;\ell) \end{bmatrix} .$$

Expanding this equation gives the *global interaction equations* for the slab X[x,y] and azimuthal spectral indexes $\ell = 0,\ldots,n$:

$$\underline{A}_p^+(x;\ell) = \underline{A}_p^+(y;\ell)\ \underline{T}(y,x;\ell) + \underline{A}_p^-(x;\ell)\ \underline{R}(x,y;\ell) \tag{6.19}$$

$$\underline{A}_p^-(y;\ell) = \underline{A}_p^+(y;\ell)\ \underline{R}(y,x;\ell) + \underline{A}_p^-(x;\ell)\ \underline{T}(x,y;\ell) \ . \tag{6.20}$$

for the cases p = 1 or 2.

An analogous development can be made for slab X[y,x] with $\underline{A}_p(y;\ell) = \underline{A}_p(z;\ell)\ \underline{M}(z,y;\ell)$ as the starting point. Moreover, representations analogous to (6.17a-d) can be made. We then obtain the global interaction equations for the slab X[y,z]:

$$\underline{A}_p^+(y;\ell) = \underline{A}_p^+(z;\ell)\ \underline{T}(z,y;\ell) + \underline{A}_p^-(y;\ell)\ \underline{R}(y,z;\ell) \tag{6.21}$$

$$\underline{A}_p^-(z;\ell) = \underline{A}_p^+(z;\ell)\ \underline{R}(z,y;\ell) + \underline{A}_p^-(y;\ell)\ \underline{T}(y,z;\ell) \tag{6.22}$$

where $\underline{T}(z,z;\ell) = \underline{I}$ and $\underline{R}(z,z;\ell) = \underline{0}$.

The $\underline{R}$ and $\underline{T}$ matrices for X[x,y] or X[y,z] therefore can be evaluated at once using (6.17) or its analogs for X[y,x], knowing the fundamental operators $\underline{M}(x,y;\ell)$ or $\underline{M}(y,z;\ell)$, respectively. However, except for (6.17c), we will use a numerically more expedient procedure, to be outlined in paragraph f, below. The exception, wherein we use (6.17c), will occur in §10.

For future reference, these analogs for the slab X[y,z], are

$$\underline{R}(y,z;\ell) = \underline{M}_{--}^{-1}(z,y;\ell)\ \underline{M}_{-+}(z,y;\ell) \tag{6.21a}$$

$$\underline{T}(z,y;\ell) = \underline{M}_{++}(z,y;\ell) - \underline{M}_{+-}(z,y;\ell)\ \underline{M}_{--}^{-1}(z,y;\ell)\ \underline{M}_{-+}(z,y;\ell) \tag{6.21b}$$

$$\underline{T}(y,z;\ell) = \underline{M}_{--}^{-1}(z,y;\ell) \tag{6.21c}$$

$$\underline{R}(z,y;\ell) = -\underline{M}_{+-}(z,y;\ell)\ \underline{M}_{--}^{-1}(z,y;\ell) \tag{6.21d}$$

The standard transmittance and reflectance operators, in (6.19) and (6.20) describe the transmittance and reflectance of the entire slab X[x,y], and thus carry two depth arguments to show the slab in question. The order of the depth arguments, e.g. T(y,x;ℓ) vs. T(x,y;ℓ), is related to the direction in which the photons are traveling. Thus in (6.19) we see that the upward (response) amplitude $\underline{A}_p^+(x;\ell)$ at the top of slab X[x,y] is equal to the upward (incident) amplitude $A_p^+(y;\ell)$ at the bottom of the slab, as transmitted through the slab from y to x, plus the downward (incident) amplitude $A_p^-(x;\ell)$ at the top of the slab, as reflected by the entire slab between x and y. Analogous interpretations hold for (6.21) and (6.22). This notation is designed to be intuitively clear and allows us to write down by inspection the global interaction equations for arbitrary slabs.

We also note that equations such as (6.19)-(6.22), which hold for each azimuthal spectral ℓ value independently, are easily written in a form which incorporates all ℓ-modes together. To do this, we concatenate the 1×m vectors $\underline{A}_p^+(x;\ell)$, ℓ=0,1,.. ,n, into a 1×m(n+1) vector $\underline{A}_p^+(x)$ via

$$\underline{A}_p^+(x) \equiv [\underline{A}_p^+(x;0),\ \underline{A}_p^+(x;1),\cdots,\underline{A}_p^+(x;n)] \ , \tag{6.23}$$

with corresponding definitions for the other amplitude vectors. Likewise we define an $m(n+1) \times m(n+1)$ block-diagonal matrix

$$\underline{T}(y,x) \equiv \begin{bmatrix} \underline{T}(y,x;0) & \underline{0} & \underline{0} & \cdots & \underline{0} \\ \underline{0} & \underline{T}(y,x;1) & \underline{0} & \cdots & \underline{0} \\ \vdots & & \ddots & & \vdots \\ \underline{0} & \cdots & & & \underline{T}(y,x;n) \end{bmatrix} , \tag{6.24}$$

with corresponding definitions for the other $\underline{R}$ and $\underline{T}$ arrays. Then (6.19) can be written

$$\underline{A}_p^+(x) = \underline{A}_p^+(y)\ \underline{T}(y,x) + \underline{A}_p^-(x)\ \underline{R}(x,y) \qquad 1 \times m(n+1) \ . \tag{6.25}$$
$$x \le y \le z$$

If the water itself were an anisotropic scattering medium, then the full form (6.25) would be required for the interior slab $X[x,y]$, since the ℓ-modes would not decouple and thus $\underline{T}(y,x)$ and the other related matrices would not be block-diagonal. We shall retain where possible the explicit ℓ-mode notation, as in (6.19), in order to emphasize the simplifications obtained from the scattering isotropy of the water body. When developing global interaction equations for the surface boundary slab $X[a,x]$, we will find that the full matrix form, as in (6.25), is required due to the scattering anisotropy of the upper boundary. Our notation thus highlights the effects of the model assumptions about an isotropic medium with an anisotropic boundary.

d. Invariant Imbedding Equations - Imbed Rules

Useful rules for finding the radiance amplitudes within a slab, knowing the incident amplitudes, can be derived from the global interaction equations. Consider a general slab X[x,z] composed of slabs X[x,y] and X[y,z]. These subslabs may be surfaces or bodies of water. The results below will show how to find the radiance distribution at level y knowing the distributions at x and z. The global interaction equations for X[x,y] are given by (6.19) and (6.20), and the corresponding equations for X(y,z) are given by (6.21) and (6.22). We now solve these equations for $\underline{A}_p^+(y;\ell)$ and $\underline{A}_p^-(y;\ell)$, the amplitudes at the level y between the two slabs X[x,y] and X[y,z], using, say, (6.20) to replace $\underline{A}_p^-(y;\ell)$ in (6.21):

$$\underline{A}_p^+(y;\ell) = \underline{A}_p^+(z;\ell)\ \underline{T}(z,y;\ell) + [\underline{A}_p^+(y;\ell)\ \underline{R}(y,x;\ell) + \underline{A}_p^-(x,\ell)\ \underline{T}(x,y;\ell)]\ \underline{R}(y,z;\ell)\ .$$

This equation yields

$$\underline{A}_p^+(y;\ell) = \underline{A}_p^+(z;\ell)\ \underline{T}(z,y;\ell)[\underline{I} - \underline{R}(y,x;\ell)\ \underline{R}(y,z;\ell)]^{-1}$$

$$+ \underline{A}_p^-(x;\ell)\ \underline{T}(x,y;\ell)\ \underline{R}(y,z;\ell)[\underline{I} - \underline{R}(y,x;\ell)\ \underline{R}(y,z;\ell)]^{-1}$$

or

$$\boxed{\begin{array}{l}\underline{A}_p^+(y;\ell) = \underline{A}_p^+(z;\ell)\ \underline{T}(z,y,x;\ell) + \underline{A}_p^-(x;\ell)\ \underline{R}(x,y,z;\ell)\ , \\ a \le x \le y \le z \le b\end{array}} \qquad (6.28)$$

for $\ell = 0,\ldots,n$ and $p = 1$ or 2, where the *complete transmittance* and *complete reflectance* functions are defined by

$$\underline{T}(z,y,x;\ell) \equiv \underline{T}(z,y;\ell)[\underline{I} - \underline{R}(y,x;\ell)\ \underline{R}(y,z;\ell)]^{-1} \tag{6.29}$$

and

$$\begin{aligned}\underline{R}(x,y,z;\ell) &\equiv \underline{T}(x,y;\ell)\ \underline{R}(y,z;\ell)[\underline{I} - \underline{R}(y,x;\ell)\ \underline{R}(y,z;\ell)]^{-1} \\ &= \underline{T}(x,y;\ell)[\underline{I} - \underline{R}(y,z;\ell)\ \underline{R}(y,x;\ell)]^{-1}\ \underline{R}(y,z;\ell)\ .\end{aligned} \tag{6.30}$$

The last equation results from use of the matrix identity $\underline{W}(\underline{I} - \underline{V}\ \underline{W})^{-1} = (\underline{I} - \underline{W}\ \underline{V})^{-1}\ \underline{W}$. Substituting $\underline{A}_p^+(y;\ell)$ from (6.21) into (6.20) and solving for $\underline{A}_p^-(y;\ell)$ yields, for $\ell = 0,\ldots,n$, and $p = 1$, or 2:

$$\boxed{\begin{aligned}&\underline{A}_p^-(y;\ell) = \underline{A}_p^+(z;\ell)\ \underline{R}(z,y,x;\ell) + \underline{A}_p^-(x;\ell)\ \underline{T}(x,y,z;\ell)\ , \\ &a \le x \le y \le z \le b\end{aligned}} \tag{6.31}$$

for $\ell = 0,\ldots,n$ and $p = 1$ or 2, where

$$\begin{aligned}\underline{R}(z,y,x;\ell) &\equiv \underline{T}(z,y;\ell)\ \underline{R}(y,x;\ell)[\underline{I} - \underline{R}(y,z;\ell)\ \underline{R}(y,x;\ell)]^{-1} \\ &= \underline{T}(z,y;\ell)[\underline{I} - \underline{R}(y,x;\ell)\ \underline{R}(y,z;\ell)]^{-1}\ \underline{R}(y,x;\ell)\end{aligned} \tag{6.32}$$

and

$$\underline{T}(x,y,z;\ell) \equiv \underline{T}(x,y;\ell)[\underline{I} - \underline{R}(y,z;\ell)\ \underline{R}(y,x;\ell)]^{-1}\ . \tag{6.33}$$

Equations (6.28) and (6.31) are the *invariant imbedding equations*, or *imbed rules*, which relate the response amplitudes at any level y within a slab to the incident amplitudes at the boundaries x and z of the slab (cf.

Preisendorfer, 1958, 1961. For a recent application, see Preisendorfer and Mobley, 1984). Note that the complete $\underline{R}$ and $\underline{T}$ functions require three depth arguments in order to specify the slab boundaries x and z, and the intermediate level, y. The orders of these arguments, (x,y,z) or (z,y,x), once again serve to keep in mind the various directions of photon travel ultimately making up a reflection or transmission.

The ℓ-mode invariant imbedding equations can be written so as to incorporate all ℓ-modes together, just as was done for (6.19) via (6.23) and (6.24) to get (6.25). Then (6.28) and (6.31) read, for p = 1 or 2:

$$\underline{A}_p^+(y) = \underline{A}_p^+(z)\,\underline{T}(z,y,x) + \underline{A}_p^-(x)\,\underline{R}(x,y,z) \tag{6.34}$$

and

$$\underline{A}_p^-(y) = \underline{A}_p^+(z)\,\underline{R}(z,y,x) + \underline{A}_p^-(x)\,\underline{T}(x,y,z)\ , \tag{6.35}$$

$$a \le x \le y \le z \le b$$

where the amplitude vectors are now $1 \times m(n+1)$ and the complete reflectance and transmittances matrices are $m(n+1) \times m(n+1)$ block diagonal matrices.

The invariant imbedding equations will find their application in §7 below, where we a[illegible]ble the final solution from its constituent parts.

e. Partition Relations - Union Rules

The partition relations we derive here serve to give the standard reflectance and transmittance matrix operators for the union of two contiguous slabs in the natural hydrosol, knowing these operators for each part of the union (cf. Fig. 1).

Thus suppose we have the four matrix operators each for X[x,y] and for X[y,z], $a \le x \le y \le z \le b$. We wish to find the four operators for

$X[x,z] = X[x,y] \cup X[y,z]$. We seek $\underline{R}(x,z;\ell)$, $\underline{T}(z,x;\ell)$, and $\underline{R}(z,x;\ell)$, $T(x,z;\ell)$ such that

$$\underline{A}_p^+(x;\ell) = \underline{A}_p^+(z;\ell)\ \underline{T}(z,x;\ell) + \underline{A}_p^-(x;\ell)\ \underline{R}(x,z;\ell) \tag{6.36}$$

and

$$\underline{A}_p^-(z;\ell) = \underline{A}_p^+(z;\ell)\ \underline{R}(z,x;\ell) + \underline{A}_p^-(x;\ell)\ \underline{T}(x,z;\ell) \tag{6.37}$$

Now, starting with global interaction equation (6.19) we replace $\underline{A}_p^+(y;\ell)$ there by means of the representation of $\underline{A}_p^+(y;\ell)$ given by the imbed rule (6.28):

$$\begin{aligned}\underline{A}_p^+(x;\ell) = {} & [\underline{A}_p^+(z;\ell)\ \underline{T}(z,y,x;\ell) + \underline{A}_p^-(x;\ell)\ \underline{R}(x,y,z;\ell)]\underline{T}(y,x;\ell) \\ & + \underline{A}_p^-(x;\ell)\ \underline{R}(x,y;\ell)\end{aligned}$$

which, on collecting coefficients of the incident amplitudes on $X[x,z]$, becomes

$$\begin{aligned}\underline{A}_p^+(x;\ell) = {} & \underline{A}_p^+(z;\ell)[\underline{T}(z,y,x;\ell)\ \underline{T}(y,x;\ell)] \\ & + \underline{A}_p^-(x;\ell)[\underline{R}(x,y;\ell) + \underline{R}(x,y,z;\ell)\ \underline{T}(y,x;\ell)]\end{aligned} \tag{6.38}$$

Since both (6.36) and (6.38) are general descriptions of the response amplitude $\underline{A}_p^+(x;\ell)$ of the slab $X[x,z]$ subject to arbitrary incident amplitudes $\underline{A}_p^-(x;\ell)$, $\underline{A}_p^+(z;\ell)$, we conclude that for $\ell = 0,\ldots,n$,

$$\underline{T}(z,x;\ell) = \underline{T}(z,y,x;\ell)\ \underline{T}(y,x;\ell) \tag{6.39}$$

$$\underline{R}(x,z;\ell) = \underline{R}(x,y;\ell) + \underline{R}(x,y,z;\ell)\ \underline{T}(y,x;\ell) \tag{6.40}$$

$$a \le x \le y \le z \le b$$

In like manner, now starting with global interaction equation (6.22) and replacing $\underline{A}_p^-(y;\ell)$ there by means of imbed rule (6.31) and comparing the result with (6.37), we find for $\ell = 0,\ldots,n$:

$$\underline{T}(x,z;\ell) = \underline{T}(x,y,z;\ell)\ \underline{T}(y,z;\ell) \tag{6.41}$$

$$\underline{R}(z,x;\ell) = \underline{R}(z,y;\ell) + \underline{R}(z,y,x;\ell)\ \underline{T}(y,z;\ell) \tag{6.42}$$

$$a \le x \le y \le z \le b$$

Equations (6.39)-(6.42) are the *union rules* for finding the $\underline{R},\underline{T}$ quartet associated with X[x,z] knowing each of the quartets for X[x,y] and X[y,z].

f. Riccati Equations for the Standard Operators

The global interaction equations and the invariant imbedding equations all involve the various standard reflectance and transmittance operators. We now derive a set of differential equations governing the $\underline{R}$ and $\underline{T}$ operators within the water column X[x,z], and show how these equations can be integrated to obtain the needed $\underline{R}$ and $\underline{T}$ operators.

Consider the slab X[x,y], and the associated global interaction equation (6.20):

$$\underline{A}_p^-(y;\ell) = \underline{A}_p^+(y;\ell)\ \underline{R}(y,x;\ell) + \underline{A}_p^-(x;\ell)\ \underline{T}(x,y;\ell)\ .$$

Differentiating this equation with respect to y gives

$$\frac{d\underline{A}_p^-(y;\ell)}{dy} = \frac{d\underline{A}_p^+(y;\ell)}{dy}\ \underline{R}(y,x;\ell) + \underline{A}_p^+(y;\ell)\ \frac{d\underline{R}(y,x;\ell)}{dy} + A_p^-(x;\ell)\ \frac{d\underline{T}(x,y;\ell)}{dy}\ .$$

The local interaction equation (5.29) can be used to replace the derivatives of the amplitudes:

$$\underline{A}_p^-(y;\ell)\ \underline{\hat{\tau}}(y;\ell) + \underline{A}_p^+(y;\ell)\ \underline{\hat{\rho}}(y;\ell) = [-\underline{A}_p^+(y;\ell)\ \underline{\hat{\tau}}(y;\ell) - \underline{A}_p^-(y;\ell)\ \underline{\hat{\rho}}(y;\ell)]\ \underline{R}(y,x;\ell) +$$

$$\underline{A}_p^+(y;\ell)\ \frac{d\underline{R}(y,x;\ell)}{dy} + \underline{A}_p^-(x;\ell)\ \frac{d\underline{T}(x,y;\ell)}{dy}\ .$$

The two occurrences of $\underline{A}_p^-(y;\ell)$ in the last equation can be replaced via the global interaction equation (6.20). On rearranging the result, we find

$$\underline{0} = \underline{A}_p^+(y;\ell)\left[\frac{d\underline{R}(y,x;\ell)}{dy} - \underline{\hat{\rho}}(y;\ell) - \underline{\hat{\tau}}(y;\ell)\ \underline{R}(y,x;\ell) - \underline{R}(y,x;\ell)\ \underline{\hat{\tau}}(y;\ell) - \right.$$

$$\left. \underline{R}(y,x;\ell)\ \underline{\hat{\rho}}(y;\ell)\ \underline{R}(y,x;\ell)\right] +$$

$$\underline{A}_p^-(x;\ell)\left[\frac{d\underline{T}(x,y;\ell)}{dy} - \underline{T}(x,y;\ell)\ \underline{\hat{\tau}}(y;\ell) - \underline{T}(x,y;\ell)\ \underline{\hat{\rho}}(y;\ell)\ \underline{R}(y,x;\ell)\right]\ .$$

This equation must hold for arbitrary incident amplitudes $\underline{A}_p^-(x;\ell)$ and $\underline{A}_p^+(y;\ell)$ on the slab X[x,y]. Therefore the coefficients of the incident amplitudes must be individually zero, from which we obtain (6.43) and (6.44), below. Repeating this procedure beginning with (6.19) yields (6.45) and (6.46), below, for $\ell = 0,\ldots,n$; and $x \le y \le z$:

$$\frac{d}{dy}\,\underline{R}(y,x;\ell) = [\underline{\hat{\rho}}(y;\ell) + \underline{\hat{t}}(y;\ell)\,\underline{R}(y,x;\ell)] + \underline{R}(y,x;\ell)\left[\underline{\hat{t}}(y;\ell) + \underline{\hat{\rho}}(y;\ell)\,\underline{R}(y,x;\ell)\right] \tag{6.43}$$

$$\frac{d}{dy}\,\underline{T}(x,y;\ell) = \underline{T}(x,y;\ell)\left[\underline{\hat{t}}(y;\ell) + \underline{\hat{\rho}}(y;\ell)\,\underline{R}(y,x;\ell)\right] . \tag{6.44}$$

$$\frac{d}{dy}\,\underline{T}(y,x;\ell) = [\underline{\hat{t}}(y;\ell) + \underline{R}(y,x;\ell)\,\underline{\hat{\rho}}(y;\ell)]\,\underline{T}(y,x;\ell) \tag{6.45}$$

$$\frac{d}{dy}\,\underline{R}(x,y;\ell) = \underline{T}(x,y;\ell)\,\underline{\hat{\rho}}(y;\ell)\,\underline{T}(y,x;\ell) \tag{6.46}$$

We recall from the defining equation for the standard operators that

$$\underline{R}(x,x;\ell) = \underline{0} \text{ and } \underline{T}(x,x;\ell) = \underline{I} \text{ , for } \ell = 0,\ldots,n. \tag{6.47}$$

The *Riccati equations* (6.43)-(6.46) are called the *downward Riccati quartet*, since they can be simultaneously integrated with a downward sweep from x to any depth y, $x \le y \le z$, beginning with the initial conditions (6.47). Note that the $\underline{\hat{\rho}}(y,\ell)$ and $\underline{\hat{t}}(y;\ell)$ matrices (defined in (5.21) and (5.24)) are in general different for different azimuthal spectral ℓ values, so that $\underline{R}(y,x;\ell)$, $\underline{T}(x,y;\ell)$, etc., also depend on ℓ, even though the initial conditions are independent of ℓ.

Now consider the slab X[y,z]. We can differentiate the global interaction equations (6.21) and (6.22) with respect to y and, following the procedure leading to (6.43)-(6.46), eventually arrive at the *upward Riccati quartet* for each $\ell = 0,\ldots,n$; and $x \le y \le z$:

$$-\frac{d}{dy}\underline{R}(y,z;\ell) = [\hat{\underline{\rho}}(y;\ell) + \hat{\underline{\tau}}(y;\ell)\,\underline{R}(y,z;\ell)] + \underline{R}(y,z;\ell)\left[\hat{\underline{\tau}}(y;\ell) + \hat{\underline{\rho}}(y;\ell)\,\underline{R}(y,z;\ell)\right] \tag{6.48}$$

$$-\frac{d}{dy}\underline{T}(z,y;\ell) = \underline{T}(z,y;\ell)\left[\hat{\underline{\tau}}(y;\ell) + \hat{\underline{\rho}}(y;\ell)\,\underline{R}(y,z;\ell)\right] \tag{6.49}$$

$$-\frac{d}{dy}\underline{T}(y,z;\ell) = [\hat{\underline{\tau}}(y;\ell) + \underline{R}(y,z;\ell)\,\hat{\underline{\rho}}(y;\ell)]\,\underline{T}(y,z;\ell) \tag{6.50}$$

$$-\frac{d}{dy}\underline{R}(z,y;\ell) = \underline{T}(z,y;\ell)\,\hat{\underline{\rho}}(y;\ell)\,\underline{T}(y,z;\ell) \tag{6.51}$$

with the initial conditions

$$\underline{R}(z,z;\ell) = 0 \text{ and } \underline{T}(z,z;\ell) = \underline{I}\ , \text{ for } \ell = 0,\ldots,n. \tag{6.52}$$

Equations (6.48)-(6.51) can be integrated in an upward sweep from z to x, with initial conditions given by (6.52).

The Riccati equation quartets (6.43)-(6.46) and (6.48)-(6.51) are the heart of the Natural Hydrosol Model's solution procedure. In particular the two pairs (6.43), (6.44) and (6.48), (6.49) are the main workhorses in this study. These two pairs of equations are integrated by n+1 independent downward and upward sweeps: one sweep in each direction for each ℓ value, $\ell = 0,1,\ldots,n$. The equations are numerically well behaved in the sense that there is no possibility of a solution growing exponentially with depth (physical reflectances and transmittances are bounded by 0 and 1, so their spectral equivalents are also bounded). By using a sufficiently small step increment Δy and a high-order integration scheme (e.g., a sixth order Runge-Kutta algorithm), the standard reflectances and transmittances can be obtained with any desired degree of accuracy. The $\underline{R}$ and $\underline{T}$ arrays need be saved only for a prechosen set of y values, $x = y_1 \le y_2 \le \cdots \le y_q \equiv z$, where final output of the radiance field is desired.

The power of the Riccati equations in the present hydrosol model is revealed by noting that they allow us to solve the radiative transfer problem within the water body itself, without any consideration whatsoever of the surface and bottom boundary conditions to be imposed on the water body.* In particular we are able to avoid coupling with the anisotropic surface until the last minute. We thus first solve the radiative transfer equation for a "bare slab" X[x,z]. It then remains to couple this interior solution for slab X[x,z] with the boundary conditions for slabs X[a,x] and X[z,b] in order to obtain a complete solution for the entire water body.

g. Global Interaction Equations for the Surface Boundary

Recall eq. (5.44) which gives one of the surface boundary conditions on the amplitudes:

$$\underline{A}_p^-(x;\ell) = \sum_{\substack{k=0 \\ (k+\ell \text{ even})}}^{n} \underline{A}_p^+(x;k)\, \hat{\underline{r}}_p(x,a;k|\ell) + \sum_{\substack{k=0 \\ (k+\ell \text{ even})}}^{n} \underline{A}_p^-(a;k)\, \hat{\underline{t}}_p(a,x;k|\ell) \qquad (6.53)$$

where p = 1 or 2 and $\ell = 0,1,\ldots,n$. The amplitude vectors in (6.53) are 1×m (recall (5.22) and (5.25)) and the $\hat{\underline{t}}$ and $\hat{\underline{r}}$ matrices are m×m (recall (5.41) and (5.43)). Now define 1 × m(n+1) amplitude vectors as in (6.23), i.e.

$$\underline{A}_p^-(x) \equiv [\underline{A}_p^-(x;0),\ \underline{A}_p^-(x;1),\ \cdots,\ \underline{A}_p^-(x;n)]\ ,$$

with corresponding definitions for $\underline{A}_p^-(a)$ and $\underline{A}_p^+(x)$. Also define an m(n+1) × m(n+1) transmittance matrix using blocks of the form $\hat{\underline{t}}_p(a,x;k|\ell)$:

* For an application of the Riccatian quartets to linear hydrodynamics, see Preisendorfer, 1975, pp. 62-63. Once again the power of the transport solution procedure applied to systems of linear differential equations is evident.

$$\underline{\hat{t}}_p(a,x) \equiv \tag{6.54}$$

$$\begin{bmatrix}
\underline{\hat{t}}_p(a,x;0|0) & \underline{0} & \underline{\hat{t}}_p(a,x;0|2) & \underline{0} & \cdots & \underline{\hat{t}}_p(a,x;0|n) \\
\underline{0} & \underline{\hat{t}}_p(a,x;1|1) & \underline{0} & \hat{t}_p(a,x;1|3) & \cdots & \underline{0} \\
\hat{t}_p(a,x;2|0) & \underline{0} & \underline{\hat{t}}_p(a,x;2|2) & \underline{0} & \cdots & \hat{t}_p(a,x;2,n) \\
\vdots & \vdots & \vdots & \vdots & \vdots & \vdots \\
\underline{\hat{t}}_p(a,x;n|0) & \underline{0} & \hat{t}_p(a,x;|n,2) & \underline{0} & \cdots & \underline{\hat{t}}_p(a,x;n|n)
\end{bmatrix} .$$

The matrix $\underline{\hat{t}}_p(a,x)$ is a block matrix with a checkerboard pattern of m×m zero and non-zero blocks, the details of which were seen in Tables 1 and 2. With a similar definition for $\underline{\hat{r}}_p(x,a)$, (6.53) becomes, for boundary X[a,x]

$$\underline{A}_p^-(x) = \underline{A}_p^+(x)\, \underline{\hat{r}}_p(x,a) + \underline{A}_p^-(a)\, \underline{\hat{t}}_p(a,x) . \tag{6.55}$$

Likewise, boundary condition (5.45) for boundary X[a,x] can be written

$$\underline{A}_p^+(a) = \underline{A}_p^+(x)\, \underline{\hat{t}}_p(x,a) + \underline{A}_p^-(a)\, \underline{\hat{r}}_p(a,x) . \tag{6.56}$$

Comparison of (6.56) with (6.25) shows that the matrix version of this upper boundary condition is formally just like the global interaction equation for a water slab X[x,y]. But unlike (6.25), which decomposes into the individual mode equations (6.19) and thus holds for each ℓ value separately, (6.56) incorporates all ℓ-modes into the same equation and cannot be further decomposed since $\underline{\hat{t}}_p(x,a)$ and $\underline{\hat{r}}_p(a,x)$ are not block-diagonal. Corresponding comments apply to (6.55). The computer code handling of (6.55) and (6.56) is discussed in §12b, below.

We see that the upper surface transmittance and reflectance arrays $\underline{\hat{t}}_p$ and $\underline{\hat{r}}_p$ are acting like standard $\underline{T}$ and $\underline{R}$ operators but now for the infinitesimally thin slab X[a,x] which constitutes the upper boundary. The operators $\underline{\hat{t}}_p$ and $\underline{\hat{r}}_p$ for the surface boundary are now order m(n+1) square matrices, due to the coupling of the ℓ-modes; and, moreover, they depend on p.

h. Global Interaction Equation for the Bottom Boundary

The bottom boundary condition (5.52), i.e.,

$$\underline{A}_p^+(z;\ell) = \underline{A}_p^-(z;\ell)\ \underline{\hat{r}}_p(z,b|\ell)\ ,\ \ell = 0,\ldots,n \tag{6.57}$$

is much simpler than the corresponding upper boundary equations (5.44) and (5.45) for the air-water surface. From (6.57) with the help of (5.54) (for the case of a matte bottom) or the results of §10 (for the case $b = \infty$), we immediately identify the required standard reflectance operator for the lower boundary slab X[z,b]:

$$\underline{R}_p(z,b;\ell) \equiv \underline{\hat{r}}_p(z,b;\ell)\ ,\ \ell = 0,\ldots,n. \tag{6.58}$$

Since X[z,b] is defined to be opaque in all cases we consider here, it follows that the remaining three $\underline{R}$ and $\underline{T}$ operators need not be defined for the present hydrosol model.

In the solution procedure of the present model (in §7b.4) it will be required to find the reflectance $\underline{R}_p(y,b;\ell)$ of the composite slab $X[y,b] = X[y,z] \cup X[z,b]$ as seen from the water side for all y, $x \le y \le z$. We can find an explicit formula for $\underline{R}_p(y,b;\ell)$, for $x \le y \le z$, using the union rule (6.40) along with (6.30) applied to this case by replacing the arguments (x,y,z) with (y,z,b), respectively. The desired result is

$$\underline{R}_p(y,b;\ell) = \underline{R}(y,z;\ell) + \underline{T}(y,z;\ell)[\underline{I} - \hat{\underline{r}}_p(z,b;\ell)\ \underline{R}(z,y;\ell)]^{-1}\ \hat{\underline{r}}_p(z,b;\ell)\ \underline{T}(z,y;\ell) \tag{6.59}$$

for any y in the range $x \le y \le z$. We will now show how to simplify the task of finding $\underline{R}_p(y,b;\ell)$. Two facts about this formula are of interest here:

(i) $\underline{R}_p(y,b;\ell) \to \hat{\underline{r}}_p(z,b;\ell)$ as $y \to z$

(ii) $\underline{R}_p(y,b;\ell)$, as a function of y, obeys (6.48) for each fixed p, b, and ℓ.

Property (i) follows by inspection of (6.59), using the continuity of the $\underline{R}$ and $\underline{T}$ matrices with respect to y, and initial conditions (6.52) for the upward Riccati quartet (6.48)-(6.51). Property (ii) is either immediately obvious on physical grounds (think of the photons sensing the change of $\underline{R}_p(y,b;\ell)$ through the incremental growth of X[y,b] at level y) or it is not. In the latter case, one verifies the assertion by differentiating (6.59) with respect to y, and then reducing the derivatives of the $\underline{R}$ and $\underline{T}$ matrices using all four members of the upward Riccati quartet (6.48)-(6.51).

As a consequence of these observations, we may generate $\underline{R}_p(y,b;\ell)$ by simply sweeping (6.48) upward with the initial condition (6.58).

7. SOLUTION PROCEDURES FOR THE NATURAL HYDROSOL MODEL

We are finally in a position to numerically solve the present Natural Hydrosol Model for the radiance distribution throughout the water column, given (1) an input radiance distribution from the sky, (2) the various reflectance and transmittance operators which describe the upper and lower boundaries, and (3) the scattering and absorption functions which describe the water itself.

a. Initial Calculations

When faced with a physical setting in a lake or sea, for which we would like to compute the radiance distribution, we must first choose the quad resolution. As discussed in §3a, we must pick m and n, so that the unit sphere Ξ is partitioned into 2m latitude bands and 2n longitude bands, as in Figs. 3 and 4. Of course, the larger m and n are, the better is the angular resolution of the solution radiance $N^{\pm}(y;u,v)$, but the more expensive are the computations. Storage and computation requirements generally depend on m^2n^2, so doubling the angular or quad resolution in both the μ and ϕ directions results in a factor of 16 increase in computer requirements. Once m and n are chosen, we must pick a particular algorithm for determining the quad size $\Delta\mu_u$, $u = 1,2,\ldots,m$, as discussed in §3a. Thus the first task of the program is

(1) Given: Values of m and n and the desired type of quad partitioning.

Compute: The layout of the quads Q_{uv} on the unit sphere Ξ.

After the directional resolution of the Natural Hydrosol Model has been fixed in the manner just described, the next order of business is the determination of the upper surface transmittance and reflectance arrays:

(2) Given: The wind speed over the water surface.

Compute: The four quad-averaged transmittance and reflectance functions $t(a,x;r,s|u,v)$, etc., using the ray-tracing technique of §9, below, and equations (9.1) and (9.7) therein.

Compute: The spectral forms $\underline{\hat{t}}_p(a,x;k|\ell)$, etc., using (5.31b), (5.32), (5.34) and (5.36).

The computations of initial step (2) form a major part of the work in the Natural Hydrosol Model. The determination of the reflectance at the bottom boundary is much easier:

(3) Given: The desired type of bottom boundary--either matte or infinitely deep and homogeneous.

Compute: The spectral reflectance matrix for the bottom boundary, $\underline{\hat{r}}_p(z,b;\ell)$.

(a) If the bottom is a matte surface, use (5.50), (5.51) and (5.53).

(b) If the bottom boundary $X[z,b]$ represents an infinitely deep, homogeneous water column, use (10.8) and (10.9).

We next prepare the input radiances:

(4) Given: A sky radiance distribution incident on the water surface, $N(a;\underline{\xi}) = N(a;\mu,\phi)$, $-1 \le \mu < 0$, $0 \le \phi < 2\pi$

Compute: The quad-averaged radiances $N^-(a;u,v)$, using (3.3).

Compute: The incident radiance amplitudes $\underline{A}_p^-(a;\ell)$, using (4.8), (4.9) and (5.22), (5.25), (5.27).

The final initialization task is the processing of the volume scattering and volume attenuation functions which describe the water column itself:

(5) Given: The volume scattering function $\sigma(y;\xi';\xi) = s(y)p(y;\mu',\phi';\mu,\phi)$ and the volume attenuation function $\alpha(y)$ for the water column, $x \le y \le z$.

Compute: The scattering-attenuation ratio $\omega(y) = s(y)/\alpha(y)$ and the quad-averaged phase function $p(y;r,s|u,v)$, using (3.11) as evaluated in (11.3).

Compute: The spectral phase functions $\hat{p}^{\pm}(y;r,u|\ell)$ using (5.5b) as specialized in (5.6a)-(5.6d).

The volume scattering function σ and volume attenuation function α may in some cases be given as functions of the *optical* depth y. This is likely to be the case if σ and α are analytic functions, based perhaps on theoretical work. On the other hand, an experimenter measures optical properties as a function of the *geometric* depth ζ. Thus a set of optical properties measured at geometric depths must be converted into optical depth form before being used as input to the Natural Hydrosol Model. This conversion is easily made by integrating the equation which defines the optical depth y:

$$\frac{dy}{d\zeta} \equiv \alpha(\zeta) \ , \tag{7.1}$$

where $\alpha(\zeta)$ is the (measured or given) volume attenuation function at geometric depth ζ.

Let $\alpha(\zeta)$ be given at a set of geometric depths $\zeta_1,\zeta_2, \cdots ,\zeta_{ZGEO}$. Then the simplest approach to integrating (7.1) is to assume that $\alpha(\zeta)$ varies linearly with ζ between each (ζ_i,ζ_{i+1}) pair of points, that $\alpha(\zeta) = \alpha(\zeta_1)$ if $\zeta \le \zeta_1$, and that $\alpha(\zeta) = \alpha(\zeta_{ZGEO})$ if $\zeta \ge \zeta_{ZGEO}$. One could also use a more sophisticated approach, such as spline fitting, to define a continuous $\alpha(\zeta)$ from the measured set of $\alpha(\zeta_i)$ values. With the linear assumption, $\alpha(\zeta)$ has the form $\alpha(\zeta) = a_i + b_i\zeta$ for $\zeta_i \le \zeta < \zeta_{i+1}$, i = 0,1,...,ZGEO, where $\zeta_0 \equiv x$ and $\zeta_{ZGEO+1} \equiv Z$. Integrating (7.1) with the linear form of $\alpha(\zeta)$ gives

$$y(\zeta) = a_i\zeta + \tfrac{1}{2}b_i\zeta^2 + [y(\zeta_i) - a_i\zeta_i - \tfrac{1}{2}b_i\zeta_i^2] \ , \qquad (7.2)$$

where $\zeta_i \le \zeta \le \zeta_{i+1}$, and where

$$a_i = \alpha(\zeta_i) - \zeta_i\left[\frac{\alpha(\zeta_{i+1}) - \alpha(\zeta_i)}{\zeta_{i+1} - \zeta_i}\right] \ , \ b_i = \frac{\alpha(\zeta_{i+1}) - \alpha(\zeta_i)}{\zeta_{i+1} - \zeta_i} \ .$$

Equation (7.2) can be used to find the optical depths at which the measured scattering and attenuation functions are given.

We thus consider $\omega(y)$ and $\hat{p}^{\pm}(y;r,s|\ell)$, as computed above, to be known at a discrete set of optical depths y_i, $i = 1,2,\ldots,YOP$, where in the notation of Fig. 1, $x \le y_1 < y_2 < \cdots < y_{YOP} \le z$.

We note that steps (2)-(5) above are independent. Therefore we can perform these initial computations and save the results for several selected wind speeds, bottom boundary types, incident radiance distributions, and water types. Then a great many radiance solutions can be obtained from the various combinations of the above inputs, without having to repeat the initial computations. In practice, the computation of the surface boundary spectral arrays in step (2) is especially expensive, and step (5) may or may not be expensive, depending on the nature of the scattering function. Steps (3) and (4) are trivial in cost, so that it is generally more convenient to repeat these calculations with each model run than it is to save their results.

In summary, we now have available the following quantities:

$\underline{A}^{-}(a;\ell)$, a $1\times m$ incident radiance matrix for each ℓ-mode ($\ell=0,1,\ldots,n$).

$\underline{\hat{t}}_p(a,x;k|\ell)$, an $m\times m$ surface transmittance matrix for each p value, $p = 1,2$; and for those k and ℓ values for which $(k+\ell)$ is even (k and $\ell = 0,\ldots,n$), and likewise we have the remaining air-water surface transfer matrices $\underline{\hat{t}}_p(x,a;k|\ell)$, $\underline{\hat{r}}_p(a,x;k|\ell)$ and $\underline{\hat{r}}_p(x,a;k|\ell)$.

$\underline{\hat{r}}_p(z,b;\ell)$, an m×m bottom reflectance matrix for each p and ℓ value, $p = 1,2$; $\ell = 0,\ldots,n$.

$\alpha(y_i)$, the volume attenuation function on a set of optical depths y_i, $i = 1,2,\ldots,YOP$.

$\hat{p}^{\pm}(y_i;r,u|\ell)$, the phase function amplitudes on the set of optical depths y_i, and for $r,u = 1,2,\ldots,m$, and $\ell = 0,\ldots,n$.

b. Assembling the Solution

We are now prepared to enter the main solution algorithm. At this point we must select a set of depths y_j, $j = 1,2,\ldots,YOUT$, where we wish to save the model output for later displays and finding of derived quantities. We fix the endpoints at x and z, i.e., $x = y_1 < y_2 < \cdots < y_{YOUT-1} < y_{YOUT} = z$, but otherwise the internal depths y_j are arbitrary. Note that the set of depths y_j where model output is desired is independent of the depths y_i where the inherent optical properties of the water are specified. Figure 6 compares the various depths which have been referenced in the preceding paragraphs.

We now proceed to integrate the Riccati equations for each ℓ-mode. We enter a loop over all ℓ values, $\ell = 0,1,\ldots,n$, where for each ℓ value the following computations are performed.

(1) Compute $\underline{\hat{\rho}}(y_i;\ell)$ and $\underline{\hat{\tau}}(y_i;\ell)$ using (5.20b-e). The arrays are computed at each y_i level where the optical properties $\alpha(y_i)$ and $p^{\pm}(y_i;r,u|\ell)$ are known, $i = 1,\ldots,YOP$.

(2) Obtain $\underline{\hat{r}}_1(z,b;\ell)$ for the desired bottom boundary. This array may have been previously computed in step 7a.3, or it may be computed at this time.

(3) Integrate the Riccati equations (6.43) and (6.44) with initial conditions (6.47), in a downward sweep from x to z. The integration

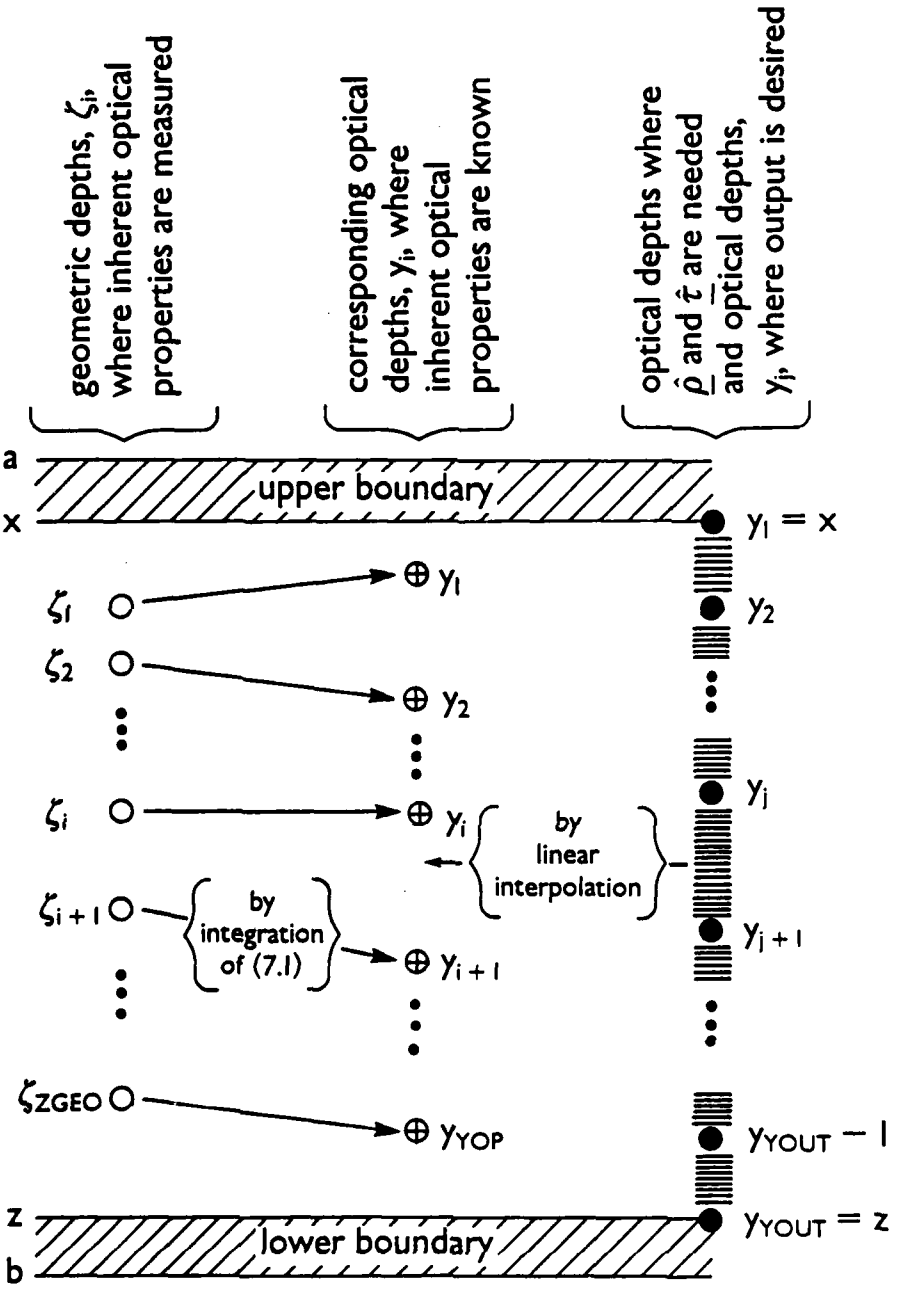

Figure 6.--Comparison of the three sets of depths referred to in the NHM. To the left the "o" symbol shows the geometric depths where attenuation and scattering functions are measured, and in the center "⊕" shows the corresponding optical depths. To the right, the "—" symbol shows the optical depths where the Riccati equation solution routine requires values of the local reflectance and transmittance matrices $\hat{\rho}$ and $\hat{\tau}$ and "●" shows the optical depths where the final radiance solution is to be obtained.

requires that $\underline{\hat{\rho}}(y;\ell)$ and $\underline{\hat{\tau}}(y;\ell)$ be continuous functions of y. Such continuous functions are defined as needed by linear interpolation of the known $\underline{\hat{\rho}}(y_i;\ell)$ and $\underline{\hat{\tau}}(y_i;\ell)$, which were computed in step (1) above for the discrete set of y values, y_i, i = 1,2,...,YOP. The interpolation is done element by element; thus for example

$$\hat{\rho}(y;r,u;\ell) = \hat{\rho}(y_i;r,u;\ell) + [\hat{\rho}(y_{i+1};r,u;\ell) - \hat{\rho}(y_i;r,u;\ell)]\left[\frac{y - y_i}{y_{i+1} - y_i}\right],$$

where $y_i \le y \le y_{i+1}$. The results of the integration, $\underline{R}(y_j,x;\ell)$ and $\underline{T}(x,y_j;\ell)$, are saved at each optical depth y_j, j = 1,2,...,YOUT, where the solution field is desired.

(4) Integrate the Riccati equation (6.48) with initial condition $R_p(z,b;\ell) = \hat{r}_p(z,b;\ell)$ (cf. eq. (6.58)) in an upward sweep from z to x for p = 1,2. The results $R_p(y_j,b;\ell)$ are saved for ℓ = 0,...,n and p = 1 and 2, at each y_j level where the final output is desired. There are two types of bottom boundary that may be considered. (i) The matte bottom at a finite depth z below x. In this case, as seen in (5.54), only the ℓ = 0 case for $\hat{r}_1(z,b;0)$ is nontrivial. The Riccati equation (6.48) need be integrated only with $\hat{r}_1(z,b;0)$ as initial condition. Thus we need find only $\underline{R}_1(y_j,b;0)$ at various levels y_j, (since $\underline{R}_1(y_j,b;\ell) = \underline{0}$, ℓ = 1,...,n) and we see also that $\underline{R}_2(y_j,b;\ell) \equiv \underline{0}$, ℓ = 0,...,n; in the case of a matte lower boundary. (ii) The medium $X[z,\infty]$ constitutes the homogeneous region below the boundary plane at level z. The initial matrices $\underline{\hat{r}}_p(z,\infty;\ell)$ needed here are described in (10.8) and (10.9), and in the discussion below (10.9).

As we cycle through steps (1)-(4) of this ℓ-mode loop, we save the matrices $\underline{R}(y_j,x;\ell)$, $\underline{T}(x,y_j;\ell)$, $\underline{R}_1(y_j,b;\ell)$ and $\underline{R}_2(y_j,b;\ell)$ for each y_j and ℓ value. At this point we now know the standard reflectance and transmittance operators for each y_j level, from x to z, where output is desired.

The invariant imbedding rule (6.35) written for the three levels (a,x,b), and which incorporates all modes at once, is

$$\underline{A}_p^-(x) = \underline{A}_p^+(b)\ \underline{R}_p(b,x,a) + \underline{A}_p^-(a)\ \underline{T}_p(a,x,b) \ .$$

Note that since the boundary surfaces X[a,x] and X[z,b] are involved, $\underline{R}$ and $\underline{T}$ are in general different for the p = 1 (cosine) and p = 2 (sine) cases. However, there is no light incident from below on the bottom boundary, that is, $\underline{A}_p^+(b) = \underline{0}$; and we are left with just

$$\underline{A}_p^-(x) = \underline{A}_p^-(a)\ \underline{T}_p(a,x,b) \ ,$$

or

$$\underline{A}_p^-(x) = \underline{A}_p^-(a)\ \underline{T}_p(a,x)\ [\underline{I} - \underline{R}_p(x,b)\ \underline{R}_p(x,a)]^{-1} \ ,$$

Here we have used (6.33) to write the complete transmittance in terms of the standard transmittance and reflectance operators. Since $\underline{T}_p(a,x)$ and $\underline{R}_p(x,a)$ refer to the upper surface boundary, we can write the last equation as

$$\boxed{\underline{A}_p^-(x) = \underline{A}_p^-(a)\ \hat{\underline{t}}_p(a,x)\ [\underline{I} - \underline{R}_p(x,b)\ \hat{\underline{r}}_p(x,a)]^{-1} \ .} \qquad (7.3)$$

Since (7.3) is written for levels (a,x,b) and involves the anisotropic surface X[a,x], this equation of necessity involves all ℓ-modes and does not decouple as does the corresponding equation (6.35), when interpreted as written for

levels (x,y,z) in the water column. $\underline{R}_p(x,b)$ is an m(n+1) × m(n+1) block-diagonal matrix composed of the m×m matrices $\underline{R}_p(x,b;\ell)$, as in (6.24). Since the dimensions of the matrices in (7.3) are quite large, finding the indicated inverse could be numerically troublesome. However, the matrices are sparse and their elements are bounded, so we can expect that the approximation

$$[\underline{I} - \underline{R}_p(x,b)\ \hat{\underline{r}}_p(x,a)]^{-1} \approx \underline{I} + \sum_{j=1}^{J} [\underline{R}_p(x,b)\ \hat{\underline{r}}_p(x,a)]^j \qquad (7.4)$$

should give an acceptably accurate inverse with only a few terms in the sum. In practice, J = 3 or 4 gives quite good results. The computer code handling of (7.3) and (7.4) is discussed in §12b, below.

A brief comment on (6.55) and (7.3) is perhaps justified; both equations give $\underline{A}_p^-(x)$, but in apparently different forms. Equation (6.55) is a boundary condition relating the final solution amplitudes $\underline{A}_p^-(x)$ to $\underline{A}_p^-(a)$ and $\underline{A}_p^+(x)$, whereas (7.3) relates $\underline{A}_p^-(x)$ to $\underline{A}_p^-(a)$ only. At this step of the solution procedure, $\underline{A}_p^+(x)$ is not yet known, so (7.3) is the only available means of obtaining $\underline{A}_p^-(x)$. The two forms of $\underline{A}_p^-(x)$ are however equivalent, as is easily shown by substituting the form of $A_p^+(x)$ from step 5 below into (6.55) in order to obtain (7.3). The powers of j in the expansion (7.4) can in fact be interpreted physically as the higher order scattering contributions to the total solution. The zero order term of (7.3), $\underline{A}_p^-(a)\ \hat{\underline{t}}_p(a,x)$, is just the direct beam, or unscattered, contribution of $\underline{A}_p^-(a)$ to $\underline{A}_p^-(x)$. Values of J = 3 or 4 used in (7.4) represent 6^{th} and 8^{th} order scattering, respectively.

(5) Compute $\underline{A}_p^-(x)$ for p = 1,2 from (7.3) and (7.4).

The invariant imbedding equation (6.34) now written for (a,x,b) is

$$\underline{A}_p^+(x) = \underline{A}_p^+(b)\ \underline{T}_p(b,x,a) + \underline{A}_p^-(a)\ \underline{R}_p(a,x,b)\ ,$$

which, since $\underline{A}_p^+(b) = \underline{0}$, reduces to

$$\underline{A}_p^+(x) = \underline{A}_p^-(a)\ \hat{\underline{t}}_p(a,x)[\underline{I} - \underline{R}_p(x,b)\ \hat{\underline{r}}_p(x,a)]^{-1}\ \underline{R}_p(x,b)\ ,$$

where $\underline{R}_p(a,x,b)$ has been written out using its definition (6.30), and $\underline{T}_p(a,x)$ and $\underline{R}_p(x,a)$ have been written in their specific boundary value forms. But from (7.3), we see that this last equation is just

$$\underline{A}_p^+(x) = \underline{A}_p^-(x)\ \underline{R}_p(x,b)\ , \tag{7.5a}$$

and since $\underline{R}_p(x,b)$ is block diagonal, this equation decouples to

$$\underline{A}_p^+(x;\ell) = \underline{A}_p^-(x;\ell)\ \underline{R}_p(x,b;\ell)\ ,\ \ell = 0,\ldots,n. \tag{7.5b}$$

The next step of the solution is then

(6) Compute $\underline{A}_p^+(x;\ell)$ for p = 1,2 and for each ℓ-mode, using (7.5b).

At this stage of the solution we have the upward and downward amplitudes just below the water surface, at y = x, and the effects of the anisotropic surface have been fully accounted for. We can now find the amplitudes within the water column, $x < y \leq z$, using the invariant imbedding relations written for levels (x,y,b). From (6.31) we have

$$\underline{A}_p^-(y;\ell) = \underline{A}_p^+(b;\ell)\ \underline{R}_p(b,y,x;\ell) + \underline{A}_p^-(x;\ell)\ \underline{T}_p(x,y,b;\ell)$$

which, since $\underline{A}_p^+(b;\ell) = 0$, reduces to (cf. 6.33)

$$\underline{A}_p^-(y;\ell) = \underline{A}_p^-(x;\ell)\ \underline{T}(x,y;\ell)[\underline{I} - \underline{R}_p(y,b;\ell)\ \underline{R}_p(y,x,;\ell)]^{-1} \qquad (7.6)$$

for $\ell = 0,\ldots,n$.

Since levels (x,y,b) involve only the isotropic water and the isotropic lower boundary, the ℓ-modes decouple and this form of the imbed rule can be evaluated separately for each ℓ-mode. The $\underline{T}$ and $\underline{R}$ matrices in (7.6) are known from the Riccati equation integrations. Thus we are ready to

(7) Compute $\underline{A}_p^-(y_j;\ell)$ for p = 1,2, using (7.6), for each interior y level, $y_2,y_3,\cdots,y_{YOUT} = z$, where final output is desired, and for each ℓ-mode.

The invariant imbedding rule (6.28) now written for levels (x,y,b) is

$$\underline{A}_p^+(y;\ell) = \underline{A}_p^+(b;\ell)\ \underline{T}_p(b,y,x;\ell) + \underline{A}_p^-(x;\ell)\ \underline{R}_p(x,y,b;\ell)\ ,$$

which, since $\underline{A}_p^+(b;\ell) = \underline{0}$, reduces to (cf. 6.30)

$$\underline{A}_p^+(y;\ell) = \underline{A}_p^-(x;\ell)\ \underline{T}(x,y;\ell)[\underline{I} - \underline{R}_p(y,b;\ell)\ \underline{R}_p(y,x;\ell)]^{-1}\ \underline{R}_p(y,b;\ell)$$

or, by (7.6), to

$$\underline{A}_p^+(y;\ell) = \underline{A}_p^-(y;\ell)\ \underline{R}_p(y,b;\ell)\ , \qquad (7.7)$$

for $\ell = 0,\ldots,n$.

The next step is then

(8) Compute $\underline{A}_p^+(y_j;\ell)$ for p = 1,2 using (7.7), for each interior y level, $y_2,y_3,\ldots,y_{YOUT} = z$, where final output is desired, and for each ℓ-mode.

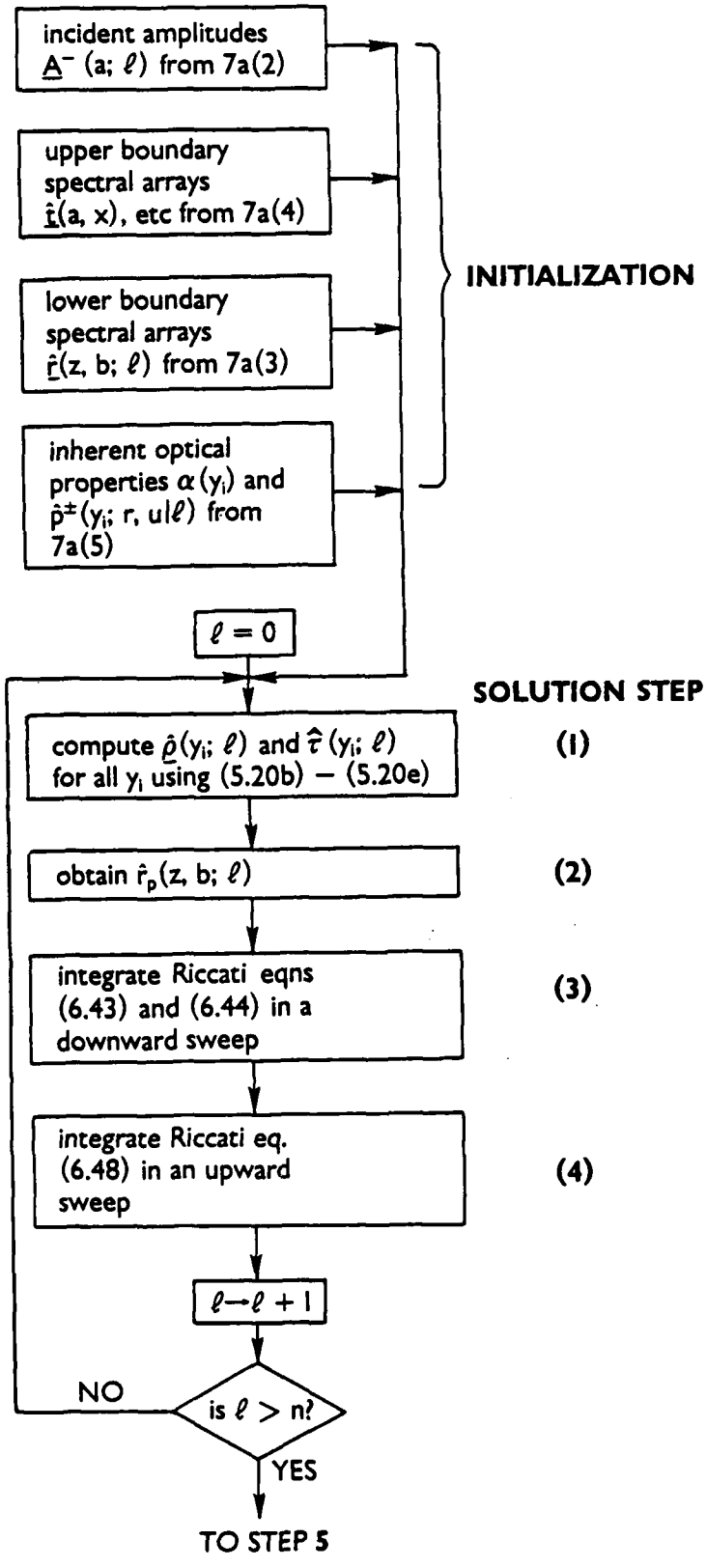
incident amplitudes $\underline{A}^-(a; \ell)$ from 7a(2)
upper boundary spectral arrays $\underline{\hat{t}}(a, x)$, etc from 7a(4)
lower boundary spectral arrays $\underline{\hat{r}}(z, b; \ell)$ from 7a(3)
inherent optical properties $\alpha(y_i)$ and $\hat{p}^{\pm}(y_i; r, u|\ell)$ from 7a(5)
INITIALIZATION
$\ell = 0$
SOLUTION STEP
compute $\underline{\hat{\rho}}(y_i; \ell)$ and $\underline{\hat{\tau}}(y_i; \ell)$ for all y_i using (5.20b) – (5.20e)
(1)
obtain $\hat{r}_p(z, b; \ell)$
(2)
integrate Riccati eqns (6.43) and (6.44) in a downward sweep
(3)
integrate Riccati eq. (6.48) in an upward sweep
(4)
$\ell \rightarrow \ell + 1$
NO
is $\ell > n$?
YES
TO STEP 5

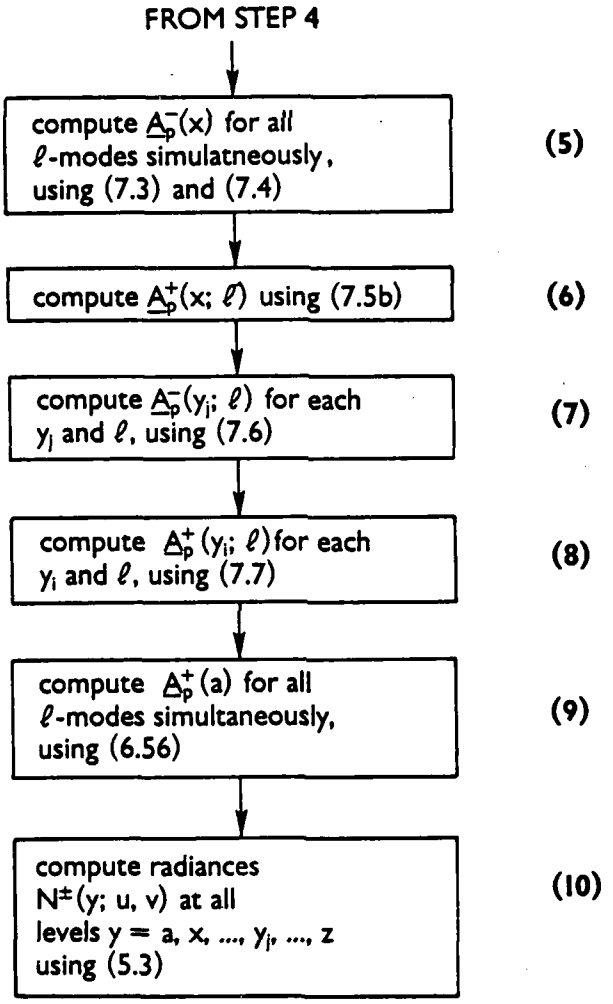

Figure 7.--Flow chart for the ten-step solution procedure described in §7b. The incident radiance amplitudes, air-water surface spectral arrays, bottom boundary spectral arrays, and inherent optical properties of the water column are computed as in §7a and are assumed known.

We now have the upward and downward amplitudes at all desired levels in the water column, $x \equiv y_1, y_2, \cdots, y_j, \cdots, y_{YOUT} \equiv z$. The only remaining step is to compute the upward amplitudes at the water surface. This is done using the appropriate upper surface boundary condition:

(9) Compute $\underline{A}_p^+(a)$ for p = 1,2 using (6.56):

$$\underline{A}_p^+(a) = \underline{A}_p^+(x)\ \hat{t}_p(x,a) + \underline{A}_p^-(a)\ \hat{r}_p(a,x).$$

The amplitudes $\underline{A}_p^{\pm}(y)$, i.e., $A_p^{\pm}(y;u;\ell)$, for u = 1,...,m; and ℓ = 0,...,n are now known for all desired depths a, $x = y_1, y_2, \cdots, y_j, \cdots, y_{YOUT} = z$. The only remaining step is to reconstitute the radiance field from these amplitudes:

(10) Compute $N^{\pm}(y;u,v)$, for (u,v) over the respective hemispheres, from (5.3), at all required depths $y = a$, $x = y_1, y_2, \ldots, y_j, \ldots, y_{YOUT} = z$.

The solution is now complete. The above steps are graphically summarized in Fig. 7.

8. DERIVED QUANTITIES

There are a number of interesting quantities which can be computed from the quad-averaged radiances of the present Natural Hydrosol Model. Among these are the various irradiances, irradiance reflectances, distribution functions, K-functions, backward and forward scattering functions, and eccentricities. Also, various checks on the present numerical radiance model itself can be made. In particular we can make certain that our solution radiances satisfy the radiative transfer equation. Moreover, graphical output of the radiance distribution can be displayed as functions of depth y, polar angle θ, and azimuthal angle ϕ, for various choices of wavelength of photons. In this section we list a number of derived quantities, show how they can be computed from the model output, and explain their significance to hydrologic optics applications.

a. Balancing the Radiative Transfer Equation

A complex numerical model and the associated computer code are subject to many types of error. Simply removing all typographical errors from thousands of lines of code is a major task. As shown in §12, various tricks are used to store sparse or symmetric arrays, thus creating possibilities for errors in array indexing. Moreover, the various numerical algorithms may introduce subtle errors. For example, algorithms for integrating the Riccati differential equations may introduce errors due to taking too large a step Δy when performing the upward and downward integration sweeps. Matrix inversions, or their approximations like (7.4), are another source of purely numerical error. Therefore, once the solution radiances have been obtained, the first order of business should be to see that they actually do satisfy the radiative transfer equation.

The quad-averaged radiative transfer equation split into separate equations for the upward and downward components as in (5.2), and rearranged for a null check, becomes

$$\mu_u \frac{dN^+(y;u,v)}{dy} - N^+(y;u,v) + \omega(y) \sum_r \sum_s N^+(y;r,s)\, p^+(y;r,s|u,v) + \omega(y) \sum_r \sum_s N^-(y;r,s)\, p^-(y;r,s|u,v) = 0 \ , \tag{8.1}$$

for Q_{uv} in Ξ_+, and

$$-\mu_u \frac{dN^-(y;u,v)}{dy} - N^-(y;u,v) + \omega(y) \sum_r \sum_s N^+(y;r,s)\, p^-(y;r,s|u,v) + \omega(y) \sum_r \sum_s N^-(y;r,s)\, p^+(y;r,s|u,v) = 0 \ , \tag{8.2}$$

for Q_{uv} in Ξ_-. Recall from (5.2) that by convention $\mu_u > 0$ in both (8.1) and (8.2). The y-derivatives in (8.1) and (8.2) at level y_j can be approximated by centered differences:

$$\frac{dN^\pm(y_j;u,v)}{dy} \approx \frac{N^\pm(y_{j+1};u,v) - N^\pm(y_{j-1};u,v)}{y_{j+1} - y_{j-1}} \ . \tag{8.3}$$

For an accurate approximation, the three depths (y_{j-1}, y_j, y_{j+1}) should be *closely spaced* optical depths. If the y-levels are too widely spaced, the approximation (8.3) can give an inaccurate result for the derivative, and thus a poor balance for the radiative transfer equation, even though the radiances themselves are quite accurate. When the left hand sides of (8.1) and (8.2) are evaluated using the solution radiances, the terms will not sum to zero as indicated, owing to computer roundoff error, if for no other reason. However,

we expect the net value of the left sides of (8.1) and (8.2) to be small relative to the individual terms on those sides. We would be in possession of a good balance if the net values of the left sides of (8.1) and (8.2) are two to three orders of magnitude smaller than the individual terms comprising those sides.

Unfortunately, a good balance of the radiative transfer equation does not guarantee the correctness of the solution radiances. For example, the radiances can be in error by a constant factor without affecting the radiative transfer equation. But more subtly, it must be remembered that the solution radiances are solutions consistent with the computed quad-averaged phase functions and boundary reflectance and transmittance arrays. If these quantities are inaccurately evaluated, then the radiances will not be a good approximation to the true radiances in nature. Evaluation of the quad-averaged phase function from a given continuous phase function via the numerical integration of (3.11) is particularly touchy because of the highly peaked angular dependence of phase functions. This integration is discussed further in §11.

b. Irradiances

We have by definition the hemispherical *scalar irradiances*

$$h_{\pm}(y) \equiv \iint_{\Xi_{\pm}} N^{\pm}(y;\mu,\phi)d\Omega \ , \ a \le x \le y \le z \le b.$$

These are usually measured by spherical radiant flux collecting surfaces exposed to the appropriate upper or lower hemisphere of directions of photon flow. This equation is easily discretized by using (3.4) to replace the continuous radiance function by its step function form, as was often done in §3. The result is

$$h_{\pm}(y) = \sum_{u=1}^{m-1} \sum_{v=1}^{2n} N^{\pm}(y;u,v)\ \Omega_{uv} + N^{\pm}(y;m,\cdot)\ \Omega_{m} \ . \tag{8.4}$$

An even simpler form is obtained in terms of the radiance amplitudes on using the representation (5.3). Since the quad solid angles Ω_{uv} are independent of v, (8.4) can be reduced to

$$h_{\pm}(y) = 2\pi \sum_{u=1}^{m} A_1^{\pm}(y;u;0)\ \Delta\mu_u \ . \tag{8.5}$$

Note that only the $\ell = 0$ mode cosine amplitudes contribute to the scalar irradiance. The *total scalar irradiance* is defined as

$$h(y) \equiv h_{+}(y) + h_{-}(y) \ . \tag{8.6}$$

By inserting a cosine directionality factor $|\mu|$ into the equation defining the scalar irradiances, we obtain the *irradiances*

$$H_{\pm}(y) \equiv \int_{\Xi_{\pm}} N^{\pm}(y;\mu,\phi)\ |\mu|\ d\Omega \ , \ a \le x \le y \le z \le b$$

These are usually measured by flat plate radiant flux collectors exposed to the appropriate upper or lower hemisphere. Simple derivations lead to the quad-averaged forms

$$H_{\pm}(y) = \sum_{u=1}^{m-1} \sum_{v=1}^{2n} N^{\pm}(y;u,v) \, |\mu_u| \, \Omega_{uv} + N^{\pm}(y;m,\cdot) \, |\mu_m| \, \Omega_m \tag{8.7}$$

which reduces to

$$H_{\pm}(y) = 2\pi \sum_{u=1}^{m} A_1^{\pm}(y;u;0) \, |\mu_u| \, \Delta\mu_u \tag{8.8}$$

Note once again that only the $\ell = 0$ mode contributes to the irradiance. Hence both scalar irradiances $h_{\pm}(y)$ and horizontal irradiances $H_{\pm}(y)$ can be determined by using only the transport theory for zero mode amplitudes (cf. (5.23), and all statements in §6 for the special case $\ell = 0$).

A check on the four computed irradiances is given by the divergence relation for the light field (cf. H.O., Vol. I, p. 62):

$$\frac{d}{dy} [H_+(y) - H_-(y)] = [1 - \omega(y)][h_+(y) + h_-(y)] \, . \tag{8.9}$$

Recall that we are working with optical depth y; hence the volume absorption function takes the form $1-\omega(y)$. Equation (8.9) can be computed as

$$\frac{[H_+(y_{j+1}) - H_-(y_{j+1})] - [H_+(y_{j-1}) - H_-(y_{j-1})]}{y_{j+1} - y_{j-1}} = [1 - \omega(y_j)][h_+(y_j) + h_-(y_j)] \, , \tag{8.10}$$

where (y_{j-1}, y_j, y_{j+1}) are three closely spaced optical depths, with the same caveat on derivative evaluation as was made for (8.3).

The divergence relation is useful in estimating the local heating rate of the near-surface water layers in a lake or sea. In this sense it has potentially important applications to climate prediction, by incorporating these estimates in coupled global circulation models for the atmosphere and oceans of the world.

c. Apparent Optical Properties

Once the irradiances $H_{\pm}(y)$ and the scalar irradiances $h_{\pm}(y)$ have been obtained, we can easily compute various *apparent optical properties* arising in the two-flow irradiance model of light in natural waters. Some of them are (cf. H.O., Vol. V, pp. 115-126):*

(1) The distribution functions,

$$D_{\pm}(y) \equiv \frac{h_{\pm}(y)}{H_{\pm}(y)} . \tag{8.11}$$

(2) The K-functions for irradiance,

$$K_{\pm}(y) \equiv \frac{-1}{H_{\pm}(y)} \frac{dH_{\pm}(y)}{dy} . \tag{8.12}$$

(3) The k-functions for hemispherical scalar irradiance,

$$k_{\pm}(y) \equiv \frac{-1}{h_{\pm}(y)} \frac{dh_{\pm}(y)}{dy} . \tag{8.13}$$

(4) The reflectance functions for irradiance,

$$R_{\pm}(y) \equiv \frac{H_{\mp}(y)}{H_{\pm}(y)} , \text{ so that } R_{+}(y) = R_{-}^{-1}(y) \tag{8.14}$$

The NHM can be used to determine the conditions on sun and skylight geometry, and size of $\omega(y)$ that tend to make $D_{\pm}(y)$, $K_{\pm}(y)$, and $R_{\pm}(y)$ essentially

* The notation continues to be formed by computer programming needs (see footnote to (5.3)). Ordinarily we would write "D(y,±), h(y,±), H(y,±)", etc. In the last analysis, however, it is the concept that matters, not how it is clothed.

independent of depth. This will have consequences for the validity of the two-flow model for irradiance fields in natural hydrosols. For example, the constancy of $D_{\pm}(y)$ with depth y is an important assumption of the two-flow irradiance model.

d. Backward and Forward Scattering Functions

The *backward scattering*, or *backscatter*, function for the two-flow irradiance model is defined by (cf. H.O., Vol. V, pp. 10-11)

$$b_{\pm}(y) \equiv \frac{1}{H_{\pm}(y)} \int_{\Xi_{\mp}} d\Omega(\underline{\xi}) \int_{\Xi_{\pm}} d\Omega(\underline{\xi}') \; N^{\pm}(y;\underline{\xi}') \; \sigma(y;\underline{\xi}';\underline{\xi}) \; ,$$

which can be discretized in the usual manner to become

$$b_{\pm}(y) = \frac{s(y)}{H_{\pm}(y)} \sum_u \sum_v \Omega_{uv} \sum_r \sum_s N^{\pm}(y;r,s) \; p^{-}(r,s|u,v) \; . \tag{8.15}$$

$$\equiv D_{\pm}(y) \; s(y) \; \varepsilon_b(y;\pm)$$

where we define

$$\varepsilon_b(y;\pm) \equiv \frac{1}{h_{\pm}(y)} \sum_u \sum_v \Omega_{uv} \sum_r \sum_s N^{\pm}(y;r,s) \; p^{-}(r,s|u,v) \; . \tag{8.15a}$$

Here s(y) is the volume total scattering function of (2.6). $\varepsilon_b(y;\pm)$ is the *eccentricity function* for the backscatter function and generally lies between 0 and 1. Note that only the p^- phase function appears in (8.15), since $\underline{\xi}'$ and $\underline{\xi}$ are always in opposite hemispheres. As always, sums over quads are evaluated as in (3.2). In the same fashion, the *forward scattering* function for the two-flow irradiance model is defined by

$$f_{\pm}(y) \equiv \frac{1}{H_{\pm}(y)} \int_{\Xi_{\pm}} d\Omega(\underline{\xi}) \int_{\Xi_{\pm}} d\Omega(\underline{\xi}') \; N^{\pm}(y;\underline{\xi}') \; \sigma(y;\underline{\xi}';\underline{\xi}),$$

which becomes

$$f_{\pm}(y) = \frac{s(y)}{H_{\pm}(y)} \sum_u \sum_v \Omega_{uv} \sum_r \sum_s N^{\pm}(y;r,s) \; p^{+}(r,s|u,v). \tag{8.16}$$

$$\equiv D_{\pm}(y) \; s(y) \; \varepsilon_f(y;\pm)$$

where we define

$$\varepsilon_f(y;\pm) \equiv \frac{1}{h_{\pm}(y)} \sum_u \sum_v \Omega_{uv} \sum_r \sum_s N^{\pm}(y;r,s) \; p^{+}(r,s|u,v) \; . \tag{8.16b}$$

$\varepsilon_f(y;\pm)$ is the *eccentricity function* for forward scattering and generally lies between 0 and 1. Here only p^{+} appears, since $\underline{\xi}'$ and $\underline{\xi}$ are always in the same hemisphere. A check on these calculations is provided by

$$\varepsilon_f(y;\pm) + \varepsilon_b(y;\pm) = 1 \tag{8.17}$$

and

$$s(y) \; D_{\pm}(y) \equiv s_{\pm}(y) = f_{\pm}(y) + b_{\pm}(y) \; . \tag{8.17a}$$

which follow from the quad-averaged form (11.5) of the normalization property (2.7) of $p(y;\mu',\phi';\mu,\phi)$.

There is a close relative of $b_{\pm}(y)$ that is of particular interest to the two-flow model for irradiance (cf. Preisendorfer and Mobley, 1984, Eq. (12)) and that is the *mean backscatter coefficient* defined by writing

$$\bar{b}_{\pm}(y) \equiv b_{\pm}(y)/D_{\pm}(y) \qquad (= s(y)\ \varepsilon_b(y;\pm)) \tag{8.18}$$

It may be the case that, in some media under natural lighting conditions, $\bar{b}_+(y)$ is nearly equal to $\bar{b}_-(y)$. This will be the case if $\varepsilon_b(y;+) \approx \varepsilon_b(y;-)$. When this is so one writes "$\bar{b}(y)$" for this common value of $\bar{b}_{\pm}(y)$. The present NHM can explore the likelihood of this possibility. Whenever the NHM verifies that, to good working order, $\bar{b}_+(y) \approx \bar{b}_-(y)$, then the procedures of Preisendorfer and Mobley (1984) can be used to find the volume absorption function $a(y)$ and the mean backscatter function $\bar{b}(y)$ and hence $b_{\pm}(y)$ of a natural hydrosol from measurements of the irradiance quartet $[h_{\pm}(y), H_{\pm}(y)]$.

When it is the case that $\bar{b}_+(y) \neq \bar{b}_-(y)$ and when the ratio $\bar{b}_+(y)/\bar{b}_-(y)$ is unacceptably far from 1, then it may be possible to establish an empirical link between $\bar{b}_+(y)$ and $\bar{b}_-(y)$ using the NHM.

e. Horizontal Radiances; Horizontal Equilibrium Radiance

The partitioning of the unit sphere Ξ into quads does not have a band of quads centered at $\mu = 0$, i.e., on the horizon where $\theta = 90°$. However, it is often of interest to have the horizontal radiance $N(y;0,\phi)$ in tabulated displays. The radiative transfer equation (2.8) with $\mu = 0$ gives the desired radiance. Thus, for $\underline{\xi}$ such that $\mu = \underline{\xi}\cdot\underline{k} = 0$ (cf. Fig. 1), we have

$$\begin{aligned} N(y;\underline{\xi}) &= \omega(y) \int_{\Xi} N(y;\underline{\xi}')\ p(y;\underline{\xi}';\underline{\xi})\ d\Omega(\underline{\xi}') \\ &= \alpha^{-1}(y) \int_{\Xi} N(y;\underline{\xi}')\ \sigma(y;\underline{\xi}';\underline{\xi})\ d\Omega(\underline{\xi}') \\ &\equiv N_q(y;0,\phi)\ . \end{aligned} \tag{8.19}$$

$N_q(y;0,\phi)$ is known as the *horizontal equilibrium radiance*, since as one advances underwater in a horizontal direction $\underline{\xi} = (0,\phi)$, $N_q(y;0,\phi)$ does not change in a plane-parallel setting. In the atmosphere, one would call $N_q(y;0,\phi)$ the "horizon brightness".

The quad-averaged form of $N_q(y;0,\phi)$ does not exist for the reason mentioned above. However, the general quad-averaged form of (8.19) does exist:

$$N_q^{\pm}(y;u,v) \equiv \omega(y) \sum_r \sum_s N(r,s)\ p(y;r,s|u,v) \tag{8.20}$$

for Q_{uv} in $\Xi_{\pm}$, respectively. The *quad-averaged approximation to* $N_q(y;0,\phi)$ *is* therefore

$$N_q(y;0,v) \equiv \tfrac{1}{2}[N^+(y;1,v) + N^-(y;1,v)] \tag{8.21}$$

for $v = 1,\ldots,2n$ and $x \le y \le z$.

f. Diffuse Radiances

The radiance $N^{\pm}(y;u,v)$ is the *total radiance*, which is the observable sum of the *directly transmitted*, or unscattered, radiance $N_0^{\pm}(y;u,v)$ and the *diffuse*,* or scattered, radiance $N_*^{\pm}(y;u,v)$. Since near the surface of the hydrosol the direct beams from sun and sky are usually many orders of magnitude stronger than the diffuse light, it is often desirable to separate the direct and diffuse radiances, especially for simple analytical models or for descriptive graphical output.

---

* When we drop the $\pm$ superscripts, then $N_*^{\pm}(y;u,v)$ is traditionally written as "$N^*(y;u,v)$", and $N_0^{\pm}(y;u,v)$ as "$N^0(y;u,v)$".

The radiance from the sun incident on the water surface is by convention entirely composed of a direct beam, $N^-(a;r,s) = N_0^-(a;r,s)$, since we consider atmospheric scattering as bringing to us radiant flux whose scattering order index can be set to zero.* Thus, we can have direct beams $N_0^-(a;r,s)$ from any number of quads Q_{rs}. After light enters the water, upward and downward diffuse radiances are generated as described by the scattering term in the radiative transfer equation and by reflection of the downward direct beam back from the bottom boundary. The upward radiance in the present model is composed entirely of scattered light, i.e., $N^+(y;u,v) = N_*^+(y;u,v)$, since there are no incident light sources at the lower boundary. The incident direct beam, $N_0^-(a;r,s)$, is transmitted through the upper surface via (3.17) in the form

$$N_0^-(x;u,v) = \sum_r \sum_s N_0^-(a;r,s)\ t(a,x;r,s|u,v)$$

(since there is no upward direct beam $N_0^+(x;u,v)$). The direct beam is then transmitted to optical depth y by a simple exponential law of decrease,

$$N_0^-(y;u,v) = N_0^-(x;u,v)\ \exp[-(y-x)/|\mu_u|]\ , \tag{8.22}$$

which is also obeyed by the associated amplitudes $A_{0_p}^-(y;u;\ell)$. The argument of the exponential, $(y-x)/|\mu_u|$, is the optical path length measured along the path of the direct beam descending from level x to level y. Using the total radiances from the solution of the numerical model, and the direct beam radiances from (8.22), we can find by definition the downward diffuse radiance

* This is based on the *principle of relative scattering order*. See Preisendorfer (1965, p. 78).

$$N_*^-(y;u,v) \equiv N^-(y;u,v) - N_0^-(y;u,v)$$

and the upward diffuse radiance (8.23)

$$N_*^+(y;u,v) \equiv N^+(y;u,v) \ .$$

g. Path Function, Equilibrium Radiance

In the discussion of (2.2) we noted the importance of the scattered radiance term. It is of interest to use the solution of the NHM to plot this term as a function of direction $\underline{\xi}$ and depth y. Specifically, we are interested in the *path function* (in standard, radiometric, non-Fortran notation):

$$N_*(y;\underline{\xi}) = \int_{\Xi} N(y;\underline{\xi}')\ \sigma(y;\underline{\xi}';\underline{\xi})\ d\Omega(\underline{\xi}') \tag{8.24}$$

or in the quad-averaged approximation:

$$N_*(y;u,v) = s(y) \sum_r \sum_s N(y;r,s)\ p(y;r,s|u,v) \equiv \alpha(y)\ N_q(y;u,v) \tag{8.25}$$
$$Q_{uv} \text{ in } \Xi$$

where we implicitly define the *equilibrium radiance* $N_q(y;u,v)$ for general quad direction (u,v) (cf. (8.19)).

An important simple model of the light field can be built from $N_*(y;\xi)$ or, equivalently, the equilibrium radiance $N_q(y;u,v)$ if the latter decreases nearly exponentially with depth y (cf. H.O., Vol. I, p. 81).

h. K-Function for Radiance, Canonical Equation of Transfer

Another quantity of interest in the study of light fields in natural hydrosols is the K-function for radiance (cf. H.O., Vol. V, pp. 125-126):

$$K(y;\underline{\xi}) = \frac{-1}{N(y;\underline{\xi})} \frac{dN(y;\underline{\xi})}{dy} , \qquad (8.26a)$$

$$\xi \in \Xi, \; x \leq y \leq z$$

or in quad-averaged form,

$$K(y;u,v) = \frac{-1}{N(y;u,v)} \frac{dN(y;u,v)}{dy} \qquad (8.26b)$$

$$Q_{uv} \text{ in } \Xi, \; x \leq y \leq z$$

An important phenomenon in infinitely deep homogeneous hydrosols is referred to by the *asymptotic radiance hypothesis*, in which the radiance distribution below a certain depth is held to decrease exponentially in size without change of shape. Thus for $y > y_0$, in the hypothesis it is assumed that

$$N(y;\underline{\xi}) = N(y_0;\underline{\xi}) \exp[-k_\infty(y-y_0)] \qquad (8.27)$$

At such depths y below y_0, it follows from (8.26a) that $K(y;\underline{\xi})$ is very nearly some constant

$$K(y;\underline{\xi}) \equiv k_\infty/\alpha \qquad (8.28)$$

for all $\underline{\xi}$ in Ξ. (Recall that y is dimensionless optical depth; hence k_∞ has units m^{-1}.) The NHM can be used to explore this phenomenon. In particular, given conditions on surface winds, sky and sun geometry, and values of scattering-attenuation ratio $\omega(y)$, y_0 can be determined in (8.27) and k_∞ evaluated. Such knowledge is of importance to the practical aspects of hydrologic optics (cf. H.O., Vol. V, §10.7 and §10.8).

We note in passing that K(y;u,v) in (8.26b) allows us to reformulate the quad-averaged equation of transfer (3.12) into the form

$$N(y;u,v) = \frac{N_q(y;u,v)}{1 + \mu_u K(y;u,v)} , \tag{8.29}$$

which is very useful in exploring asymptotic radiance distributions (cf. H.O., Vol. V, p. 243, Eq. (16)). Eq. (8.29) is the *canonical* form of the equation of transfer.

i. The Radiance-Irradiance Reflectance

The ratio $r_N(y)$ defined at any depth y, $a \le x \le y \le z \le b$, by

$$r_N(y) \equiv N^+(y;m,\cdot)/H_-(y) \tag{8.30}$$

is sometimes of use in the remote sensing of seas and lakes (Austin, 1980). In such exercises, it is of interest to estimate the upward radiance $N^+(y;m,\cdot)$ of the photons within the medium (so that $x < y$) or at the surface of the hydrosol, (so that $y = a$) knowing only the downward irradiance $H_-(y)$ there. If some idea of the size of the ratio $r_N(y)$ also exists, then $N^+(y;m,\cdot) = r_N(y)\, H_-(y)$ is estimable. The present Natural Hydrosol Model can yield estimates of $r_N(y)$ over all depths y under a wide variety of lighting and wind conditions on the hydrosol surface.

j. The Upward Irradiance-Radiance Ratio

Another ratio of current use in the remote sensing of lakes and seas is the Upward Irradiance-Radiance Ratio Q(y) defined by

$$Q(y) \equiv \frac{H_+(y)}{N^+(y;m,\cdot)} \tag{8.31}$$

This ratio is also of interest to *in situ* measurements of the light field. With current technology it is simpler to measure $N^+(y;m,\cdot)$ than $H_+(y)$. Hence knowledge of Q(y) enables an estimate of $H_+(y) = Q(y)\ N^+(y;m,\cdot)$ to be made if $N^+(y;m,\cdot)$ is known. The Natural Hydrosol Model can provide representative values of Q(y) for various lighting conditions and natural hydrosols.

Observe that the two ratios $r_N(y)$ and Q(y) are related to the downward reflectance function $R_-(y) \equiv H_+(y)/H_-(y)$ by

$$Q(y)\ r_N(y) = R_-(y). \tag{8.31}$$

Hence knowledge of any two of these three factors determines the third.

k. Contrast Transmittance of the Air-Water Surface

When visual searches are made from above the hydrosol for submerged objects, a key determinant of the visibility of the object is the optical state of the air-water surface. If the surface is agitated by capillary waves and the sky light is brightly reflected in the surface, the visual signal is not too readily transmitted through the surface to the searching eye. The *contrast transmittance T* is an essential property of the air-water surface and its lighting environment when gauging the visibility of submerged objects (cf.

H.O., Vol. I, p. 96 and H.O., Vol. VI, p. 42). The form of T for vertically upward photon flow is given by

$$T \equiv \frac{N^0 t/n^2}{(N^0 t/n^2) + N_o r} \tag{8.32}$$

where in the context of the Natural Hydrosol Model we have written

$$N^0 t/n^2 \equiv N^+(x;m,\cdot)\ t(x,a;m,\cdot|m,\cdot)$$

and (8.33)

$$N_0 r \equiv \sum_r \sum_s N^-(a;r,s)\ r(a,x;r,s|m,\cdot)$$

Here $N^+(x;m,\cdot)$ is the upward quad-averaged radiance at level x just below the air-water surface, and $t(x,a;m,\cdot|m,\cdot)$ is the quad-averaged vertically upward radiance transmittance for the air-water surface (recall the notation convention in (3.2)). $N_0 r$ is the average vertically upward reflected sky and sun light in the air-water surface, while $N^0 t/n^2$ is the radiance transmitted upward through the surface. Observe that the smaller $N_0 r$ is, relative to $N^0 t/n^2$, the closer T will be to 1, and hence the better the chance of seeing a submerged object.

9. COMPUTATION OF THE AIR-WATER SURFACE REFLECTANCE AND TRANSMITTANCE FUNCTIONS

We consider next the details of construction of the air-water surface boundary reflectance and transmittance functions. These functions are essential to determining realistic light fields within the water column, and it is now time to discuss how the needed quad-averaged reflectance and transmittance arrays are obtained in practice.

The defining equation for the quad-averaged reflectance and transmittance arrays is (3.19):

$$f(r,s|u,v) \equiv \frac{1}{\Omega_{uv}} \iint_{Q_{uv}} d\mu d\phi \iint_{Q_{rs}} d\mu' d\phi' \; f(\mu',\phi';\mu,\phi) \;, \tag{9.1}$$

where $f(\mu',\phi';\mu,\phi)$ stands for any of $t(a,x;\mu',\phi';\mu,\phi)$, $t(x,a;\mu',\phi';\mu,\phi)$, $r(a,x;\mu',\phi';\mu,\phi)$, or $r(x,a;\mu',\phi';\mu,\phi)$, and $f(r,s|u,v)$ denotes the corresponding quad-averaged quantity $t(a,x;r,s|u,v)$, etc. If the point reflectances and transmittances $f(\mu',\phi';\mu,\phi)$ are known in analytic form, then (9.1) can be analytically or numerically integrated to find the associated quad-averaged quantities. This procedure was illustrated in §3g for the case of a matte reflectance. For the anisotropic upper boundary, however, the analytic form of $f(\mu',\phi';\mu,\phi)$ is not available except for the case of a calm, level sea surface, for which the point reflectance can be related to the Fresnel reflectance formula. For the general case of a wind-ruffled sea surface, no adequate analytic treatment of the optical properties of the sea surface has yet been made.

a. A Ray-Tracing Model

However, a model does exist for the numerical computation of the needed optical properties. This model (Preisendorfer and Mobley, 1985 and 1986) uses Monte Carlo simulation to trace individual unpolarized light rays through their interactions with the wave facets of a simulated sea surface. The possibility of multiple scattering of light rays and of shadowing of waves by other waves is included, and the results are obtained as a function of wind speed. In this section we will show how the ray-tracing model can be used to compute the quad-averaged quantity $f(r,s|u,v)$. Only a cursory description of the model will be made; the details can be found in the above references.

The ray-tracing model works as follows.

(1) A finite region of the mean water surface is resolved by a hexagonal grid of triangles, as shown in Fig. 8. At each triangle vertex the sea surface elevation is defined, so that the waves are represented by a set of triangular facets. These facets are contained in the hexagonal domain (the cylindrical region of space) defined by the hexagonal grid. Four such facets are shown in Fig. 8. The sea surface elevations are determined by randomly drawing the elevations from a normal distribution of zero mean and variance σ^2. This variance σ^2 is a function of the wind speed (see discussion below (3.22)), and is so constructed that the resulting wave facets obey the same wave-slope wind-speed statistics as the actual sea surface. Drawing an elevation at each triangle vertex of the hexagonal grid generates one realization of the random sea surface.

(2) After a particular surface realization has been generated in stage (1), a light ray of unpolarized unit radiant flux is aimed toward the surface from any chosen direction. Figure 8 shows such a ray entering the hexagonal domain at point A. Every such initial ray eventually strikes a surface wave

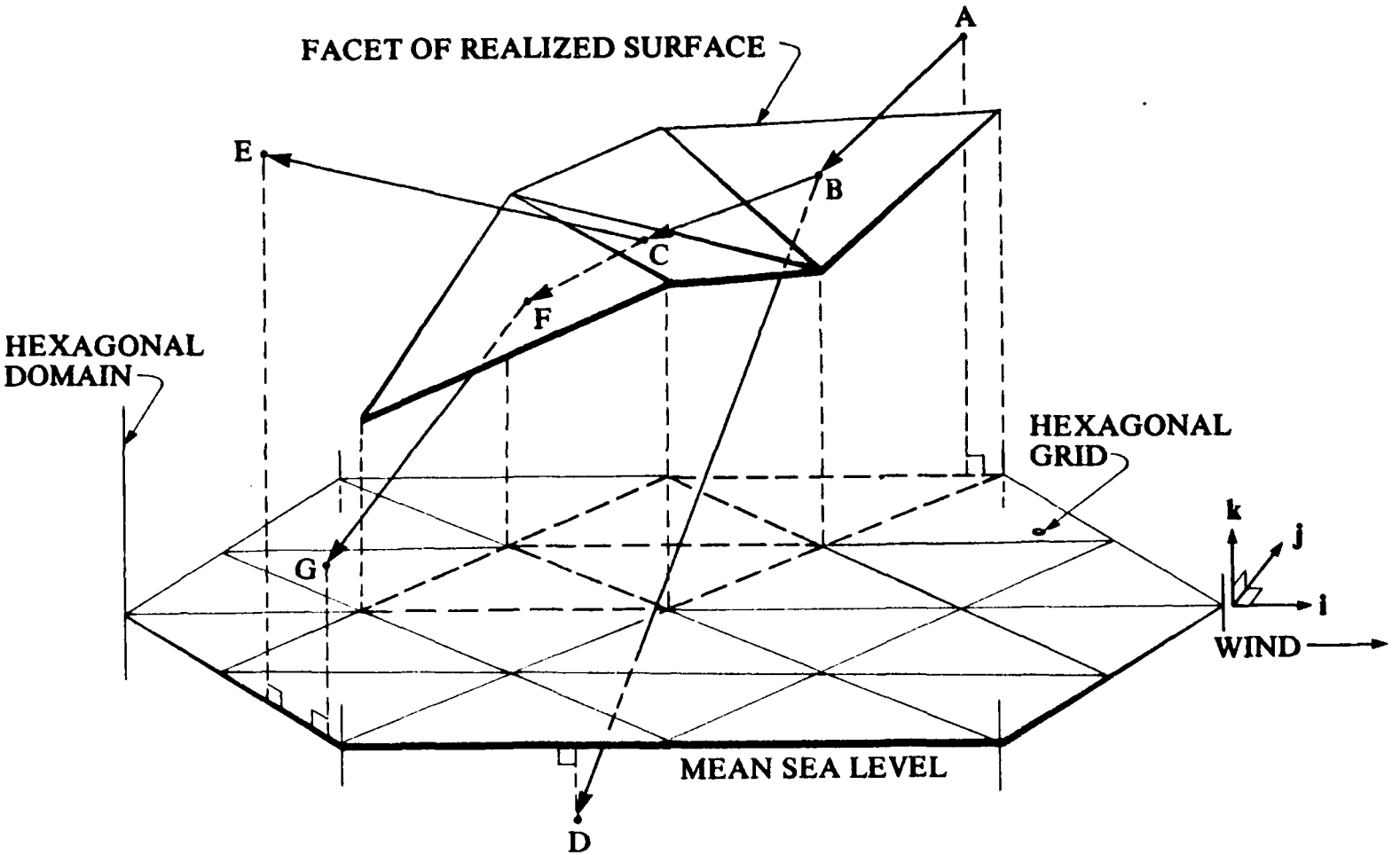

Figure 8.--Illustration of the hexagonal domain with a particular surface realization and ray tracing.

facet, as at B. In general, each encounter of a ray with a wave facet generates both a reflected and refracted daughter ray, whose directions are determined by the law of reflection and Snell's law, respectively. The radiant flux contents of these daughter rays are determined by Fresnel's formula. The daughter rays may undergo further encounters with other wave facets. As illustrated in Fig. 8, the first refracted ray at B, heading downward through the water, leaves the hexagonal domain at D without further scattering. The first reflected ray at B, however, intercepts another facet at C, generating two more rays. The reflected ray starting from C leaves the domain at E. The refracted ray starting from C encounters yet another facet at F and undergoes a total internal reflection before leaving the domain at G. Thus the initial ray finally results in one reflected and two refracted rays emerging from the hexagonal domain.

By tracing thousands of rays through their interactions with thousands of realized surfaces, a statistically stable pattern of reflected and transmitted rays can be established for a given wind speed and incident ray direction. The radiant fluxes of the daughter rays can be tallied in order to compute estimates of various optical properties of the random sea surface. The errors in these estimates, due to statistical fluctuations in the Monte Carlo simulations, can be made as small as desired by performing a sufficiently large number of simulations.

The previous applications (in the above two cited references) of this ray-tracing model have been to the calculation of the irradiance reflectance, or albedo, of the sea surface, and to the simulation of sea surface glitter patterns. However, the ray-tracing technique is ideally suited to the computation of the quad-averaged r and t arrays needed in the present Natural Hydrosol Model. We can proceed as follows.

b. Radiant-Flux Transfer Functions

Let us consider a Monte Carlo experiment in which S air-water surface realizations are generated. For each surface realization ω, $\omega = 1,2,\ldots,S$, one unpolarized parent ray is aimed toward the surface along a randomly chosen direction in some selected input quad Q_{rs}. Let $\underline{\xi}'_{rs}$ denote such a ray. This ray interacts with the ω^{th} surface realization, as illustrated in Fig. 8, and generates $\kappa(\underline{\xi}'_{rs},\omega)$ final daughter rays emerging from the hexagonal domain ($\kappa = 3$ in Fig. 8). The parent ray $\underline{\xi}'_{rs}$ is assigned a unit amount of unpolarized radiant flux, $P = 1$. At each interaction of a ray with a wave facet, the radiant flux of the incident ray is apportioned to the daughter rays according to Fresnel's formula. Thus when the parent ray intercepts a wave facet, the reflected daughter ray is assigned a radiant flux of magnitude Pr_1, where r_1 is the computed Fresnel reflectance, and the transmitted ray is assigned a flux of $P(1-r_1)$. If the reflected daughter ray then intercepts another wave facet, as in Fig. 8, the reflected ray receives a flux Pr_1r_2 and the transmitted ray receives $Pr_1(1-r_2)$, where r_2 is the Fresnel reflectance for the second ray-facet intersection. In this way it is possible to build up arbitrarily long products of Fresnel reflectances and transmittances. Let $\Pi(\underline{\xi}'_{rs},\underline{\xi}_j(\underline{\xi}'_{rs},\omega))$ be the product of the Fresnel reflectances and transmittances of all the daughter rays along a single unbroken path through space which connects the parent ray $\underline{\xi}'_{rs}$ with the j^{th} final daughter ray $\underline{\xi}_j(\underline{\xi}'_{rs},\omega)$ emerging from the hexagonal domain. The daughter rays $\underline{\xi}_j$, $j = 1,2,\ldots,\kappa$, as the notation indicates, of course depend on the direction $\underline{\xi}'_{rs}$ of the initial ray and upon the wave facet orientations of the ω^{th} random surface realization. The Fresnel product is dimensionless and satisfies $0 < \Pi(\underline{\xi}'_{rs};\underline{\xi}_j(\underline{\xi}'_{rs},\omega)) \leq 1$. (The product Π is 1 only in the case of $\underline{\xi}'_{rs}$ incident on the surface from the

water side and undergoing a total internal reflection to generate one final daughter ray $\underline{\xi}$).

Now define a *radiant-flux transfer function* P_{-+} by

$$P_{-+}(r,s|u,v) \equiv \frac{1}{S} \sum_{\omega=1}^{S} \sum_{j=1}^{\kappa} \Pi(\underline{\xi}'_{rs}, \underline{\xi}_j(\underline{\xi}'_{rs},\omega)) \; \chi_{uv}(\underline{\xi}_j(\underline{\xi}'_{rs},\omega)) \;, \qquad (9.1a)$$

when Q_{rs} in Ξ_- and Q_{uv} in Ξ_+

where Q_{rs} in Ξ_- and Q_{uv} in Ξ_+. As in (3.4), $\chi_{uv}(\underline{\xi}_j) = 1$ if $\underline{\xi}_j$ is in quad Q_{uv}, and $\chi_{uv}(\underline{\xi}_j) = 0$ otherwise. The "-" in P_{-+} denotes downward incidence (Q_{rs} in Ξ_-) and the "+" denotes upward reflection (Q_{uv} in Ξ_+). The sum over j adds up the κ Fresnel products for all those generated ray paths in space around a single surface realization which connect the input quad Q_{rs} and the output quad Q_{uv}; this result is then averaged over the ensemble of S surface realizations. $P_{-+}(r,s|u,v)$ is therefore a sample estimate of the fraction of the radiant flux incident down on the sea surface toward Q_{rs} that is reflected up into Q_{uv}. This fraction P_{-+} can be associated with a unit area of the mean sea surface and is therefore an *albedo* (irradiance reflectance) of the random sea surface for radiant flux from Q_{rs} in Ξ_- to Q_{uv} in Ξ_+. Three other transfer functions can be defined analogously to (9.1a), viz.:

$$P_{--}(r,s|u,v) \text{ when } Q_{rs} \text{ in } \Xi_- \text{ and } Q_{uv} \text{ in } \Xi_- \;, \qquad (9.1b)$$

$$P_{+-}(r,s|u,v) \text{ when } Q_{rs} \text{ in } \Xi_+ \text{ and } Q_{uv} \text{ in } \Xi_- \;, \qquad (9.1c)$$

and

$$P_{++}(r,s|u,v) \text{ when } Q_{rs} \text{ in } \Xi_+ \text{ and } Q_{uv} \text{ in } \Xi_+ \;. \qquad (9.1d)$$

Since the flux P = 1 of each parent ray ξ'_{rs} is apportioned without loss to the daughter rays, it is easy to see that

$$\sum_{u}\sum_{v} P_{-+}(r,s|u,v) + \sum_{u}\sum_{v} P_{--}(r,s|u,v) = 1, \text{ for every } Q_{rs} \text{ in } \Xi_{-} , \qquad (9.2)$$

Q_{uv} in Ξ_{+} $\qquad$ Q_{uv} in Ξ_{-}

and

$$\sum_{u}\sum_{v} P_{+-}(r,s|u,v) + \sum_{u}\sum_{v} P_{++}(r,s|u,v) = 1, \text{ for every } Q_{rs} \text{ in } \Xi_{+} . \qquad (9.3)$$

Q_{uv} in Ξ_{-} $\qquad$ Q_{uv} in Ξ_{+}

These equations merely state that radiant flux incident on the water surface is either reflected by the surface or transmitted through the surface without loss. A careful algebraic recording of the flux contents of the daughter rays shows that (9.2) and (9.3) are actually algebraic identities. We also note that the albedo (or irradiance reflectance) of the sea surface for flux incident toward Q_{rs} is given by

$$r_{-}(r,s) \equiv \sum_{u}\sum_{v} P_{-+}(r,s|u,v) .$$

Here the summation is over the hemisphere Ξ_{+}. Defining the associated irradiance transmittance $t_{-}(r,s)$ as

$$t_{-}(r,s) \equiv \sum_{u}\sum_{v} P_{--}(r,s|u,v) ,$$

where the summation is over Ξ_{-}, we can express (9.2) as

$$r_{-}(r,s) + t_{-}(r,s) = 1 \quad \text{for every } Q_{rs} \text{ in } \Xi_{-} .$$

A similar statement holds for the upward flux case in (9.3).

The four radiant flux transfer functions defined by (9.1), and computed by the ray-tracing model, form the core of the four quad-averaged r and t functions for radiance, as will now be seen.

c. Radiance Reflectance and Irradiance Reflectance

The upward (+) and downward (-) irradiances at any depth y are given by (8.7):

$$H_{\pm}(y) = \sum_u \sum_v N^{\pm}(y;u,v)|\mu_u|\Omega_{uv} \ , \ a \le x \le y \le z \le b$$

or

$$H_{\pm}(y) \equiv \sum_u \sum_v H_{\pm}(y;u,v),$$

where we have defined

$$H_{\pm}(y;u,v) \equiv N^{\pm}(y;u,v)|\mu_u|\Omega_{uv} \ , \text{ for } a \le x \le y \le z \le b \ . \qquad (9.4)$$

Evaluating the downward irradiance at y = a, contributed solely by flux in quad Q_{rs}, we can write the incident radiant flux per unit horizontal area of the sea surface (the irradiance) as

$$H_{-}(a;r,s) = N^{-}(a;r,s)|\mu_r|\Omega_{rs}.$$

The upward irradiance $H_{+}(a;u,v)$ generated when the sea surface reflects this incident irradiance is

$$H_{+}(a;u,v) = H_{-}(a;r,s)\ P_{-+}(r,s|u,v)$$

since, as we have seen, $P_{-+}(r,s|u,v)$ by construction is the irradiance reflectance connecting Q_{rs} and Q_{uv}. Using (9.4) this last equation can be written

$$N^+(a;u,v)|\mu_u|\Omega_{uv} = N^-(a;r,s)|\mu_r|\Omega_{rs}\ P_{-+}(r,s|u,v)$$

or

$$N^+(a;u,v) = N^-(a;r,s)\left[\frac{P_{-+}(r,s|u,v)|\mu_r|\Omega_{rs}}{|\mu_u|\Omega_{uv}}\right] . \qquad (9.5)$$

Now we recall the upper surface boundary condition (3.18):

$$N^+(a;u,v) = \sum_r \sum_s N^-(a;r,s)\ r(a,x;r,s|u,v) + \sum_r \sum_s N^+(x;r,s)\ t(x,a;r,s|u,v) .$$

This equation of course holds even if only one particular input quad Q_{rs} is illuminated and all others are dark, as we have postulated for the case of (9.5). In this case, (3.18) reduces to

$$N^+(a;u,v) = N^-(a;r,s)\ r(a,x;r,s|u,v) . \qquad (9.6)$$

Since the incident quad-averaged radiances are arbitrary, comparing (9.5) and (9.6) immediately yields (9.7a), below. Equation (9.7a) gives us the connection between the quad-averaged *radiance* reflectance $r(a,x;r,s|u,v)$ and the quad-averaged *irradiance* reflectance $P_{-+}(r,s|u,v)$ computed by ray-tracing. Corresponding analyses for the other terms of the boundary equations (3.17) and (3.18) give the results in (9.7b,c,d):

$$r(a,x;r,s|u,v) = P_{-+}(r,s|u,v)\,\frac{|\mu_r|\Omega_{rs}}{|\mu_u|\Omega_{uv}}\,, \tag{9.7a}$$

$$t(a,x;r,s|u,v) = P_{--}(r,s|u,v)\,\frac{|\mu_r|\Omega_{rs}}{|\mu_u|\Omega_{uv}}\,, \tag{9.7b}$$

$$r(x,a;r,s|u,v) = P_{+-}(r,s|u,v)\,\frac{|\mu_r|\Omega_{rs}}{|\mu_u|\Omega_{uv}}\,, \tag{9.7c}$$

$$t(x,a;r,s|u,v) = P_{++}(r,s|u,v)\,\frac{|\mu_r|\Omega_{rs}}{|\mu_u|\Omega_{uv}}\,. \tag{9.7d}$$

The two transmittances (9.7b,d) include the m^2 effect on radiance pencils crossing the air-water boundary, where m is the index of refraction. This follows on noting that, for narrow pencils of photons, we have* $m_a^2\mu_a\Omega_a = m_w^2\mu_w\Omega_w$, where the subscripts denote photons in air or water. We note that the quad-averaged r and t functions of (9.7) are non-dimensional, as required. Figure 9 summarizes the ray-tracing computations.

d. Irradiance Balance at the Surface

A requirement for the quad-averaged radiance reflectances and transmittances is that they conserve energy at the air-water surface. The irradiance balance at the surface for downward incident radiant flux is expressed as

$$\int_{\Xi_-} N(a;\mu,\phi)|\mu|d\Omega(\underline{\xi}) = \int_{\Xi_+} N(a;\mu,\phi)|\mu|d\Omega(\underline{\xi}) + \int_{\Xi_-} N(x;\mu,\phi)|\mu|d\Omega(\underline{\xi}) \tag{9.8}$$

* See, e.g., Preisendorfer (1965, p. 37). Note also that the present radiance transfer functions are compatible with the irradiance transfer functions derived in Preisendorfer and Mobley (1985, pp. 48-50).

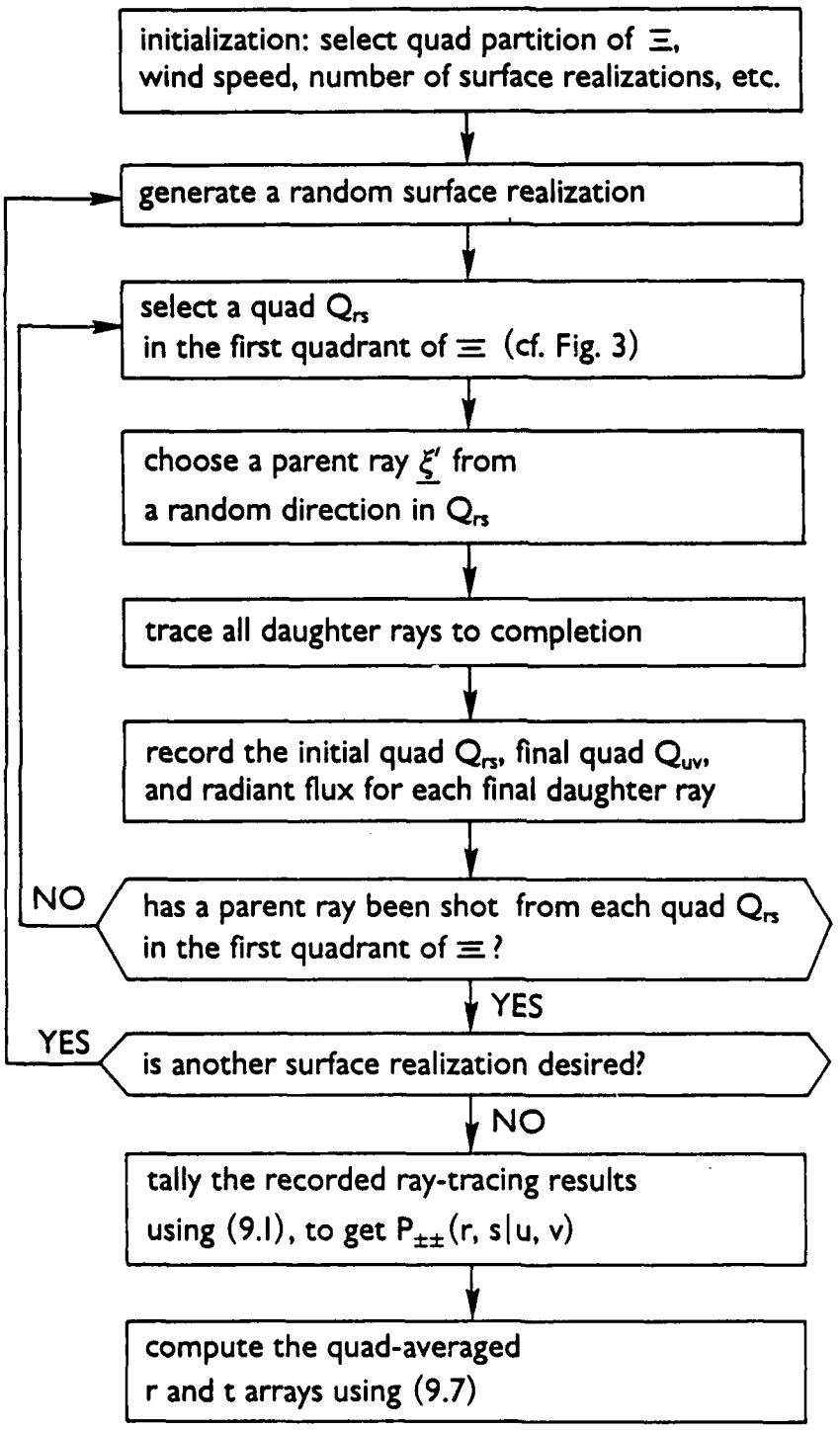

Figure 9.--Flow chart of the ray-tracing model used to compute the quad-averaged upper boundary reflectance and transmittance arrays.

The left side of (9.8) is the downward irradiance incident on the water surface from all directions above the surface. The first term on the right side of (9.8) is the upward irradiance at the surface induced by the incident downward radiance only, and the second term is the downward irradiance just below the surface also induced only by the incident downward radiance. Thus (9.8) states that the energy received from the sky alone by the surface is either reflected back to the sky or transmitted through to the water column. The quad-averaged form of (9.8) is

$$\sum_r \sum_s N^-(a;r,s)|\mu_r|\Omega_{rs} = \sum_u \sum_v N^+(a;u,v)|\mu_u|\Omega_{uv} + \sum_u \sum_v N^-(x;u,v)|\mu_u|\Omega_{uv} \quad .(9.9)$$

We will now show that (9.9) is an identity by virtue of (9.6), $N^+(a;u,v)$ can be rewritten in terms of $N^-(a;r,s)$, with a similar relation also possible for $N^-(x;u,v)$. If only one arbitrary input quad Q_{rs} of the unit sphere Ξ is illuminated, (9.9) then becomes

$$N^-(a;r,s)|\mu_r|\Omega_{rs} = \sum_u \sum_v N^-(a;r,s)\ r(a,x;r,s|u,v)|\mu_u|\Omega_{uv}$$

$$+ \sum_u \sum_v N^-(a;r,s)\ t(a,x;r,s|u,v)|\mu_u|\Omega_{uv} \ ,$$

or

$$1 = \frac{1}{|\mu_r|\Omega_{rs}} \sum_u \sum_v r(a,x;r,s|u,v)|\mu_u|\Omega_{uv}$$

$$+ \frac{1}{|\mu_r|\Omega_{rs}} \sum_u \sum_v t(a,x;r,s|u,v)|\mu_u|\Omega_{uv} \ . \qquad (9.10)$$

Substituting from (9.7a,b) for the quad-averaged reflectance and transmittance reduces (9.10) to (9.2), and an identity is obtained. Hence in the setting of quad-averaged radiative transfer, (9.9) is an identity. A corresponding

result is obtained for energy incident on the surface from below. Thus the ray-by-ray, or local, conservation of energy in the setting of the quad-averaged radiance reflectances and transmittances, guarantees the hemisphere-wide conservation of energy at the air-water boundary.

e. A Check on the Ray-Tracing Model

A direct check on $r(a,x;r,s|u,v)$ can be made for the case of a specular surface, i.e. when the wind speed is zero and the water surface is level. In this case the continuous reflectance function $r(a,x;\mu',\phi';\mu,\phi)$ depends only on the polar angle $\theta' = \cos^{-1}(\mu')$, since the angle of reflection θ equals the angle of incidence θ' and there is azimuthal symmetry. The Fresnel reflectance formula for unpolarized radiant flux is

$$r(a,x;\mu') \equiv r(a,x;\theta') = \tfrac{1}{2}\left\{\left[\frac{\sin(\theta'-\theta_t)}{\sin(\theta'+\theta_t)}\right]^2 + \left[\frac{\tan(\theta'-\theta_t)}{\tan(\theta'+\theta_t)}\right]^2\right\}, \tag{9.11}$$

where $\theta' = \cos^{-1}(\underline{\xi}'\cdot\underline{k}) = \cos^{-1}(\underline{\xi}\cdot\underline{k}) = \theta$, and the angle of the transmitted light is

$$\theta_t = \sin^{-1}\left(m_w^{-1}\sin\theta'\right) .$$

The direction $\underline{\xi}$ of a reflected beam is given in terms of the incident beam $\underline{\xi}'$ by

$$\underline{\xi} = \underline{\xi}' - 2(\underline{\xi}'\cdot\underline{k})\underline{k} = \underline{\xi}' - 2\mu'\underline{k} . \tag{9.12}$$

From (9.11) and (9.12), we can express the continuous reflectance function as

$$r(a,x;\mu',\phi';\mu,\phi) = r(a,x;\mu')\delta(\mu'+\mu)\delta(\phi'-\phi) \ , \tag{9.13}$$

where δ is the Dirac delta function. The delta functions select the allowed direction (μ,ϕ) of the reflected ray, given the direction (μ',ϕ') of the incident ray.

Substituting (9.13) into the defining equation (3.19) for $r(a,x;r,s|u,v)$ gives

$$r(a,x;r,s|u,v) = \frac{1}{\Omega_{uv}} \iint\limits_{Q_{uv}} d\mu d\phi \iint\limits_{Q_{rs}} d\mu' d\phi' \ r(a,x;\mu')\delta(\mu'+\mu)\delta(\phi'-\phi) \ ,$$

which can be rearranged to become

$$r(a,x;r,s|u,v) = \frac{1}{\Omega_{uv}} \int\limits_{\Delta\mu_u} d\mu \int\limits_{\Delta\phi_v} d\phi \left[\int\limits_{\Delta\mu_r} d\mu' \ r(a,x;\mu') \ \delta(\mu'+\mu)\right]\left[\int\limits_{\Delta\phi_s} d\phi' \ \delta(\phi'-\phi)\right] .$$

The integrals are zero unless $\Delta\phi_s$ coincides with $\Delta\phi_v$, i.e. unless $s = v$; and unless $\Delta\mu_u$ and $\Delta\mu_r$ are corresponding μ-bands in opposite hemispheres (which is by definition the case for a reflectance function), i.e. unless $r = u$. The last equation thus reduces to

$$r(a,x;r,s|u,v) = \frac{\Delta\phi_v \ \delta_{r-u} \ \delta_{s-v}}{\Omega_{uv}} \int\limits_{\Delta\mu_u} d\mu \ r(a,x;\mu) \ ,$$

or upon setting $r = u$ and $s = v$, and evaluating the Kronecker delta symbols, we have for every Q_{rs} in Ξ_-,

$$r(a,x;r,s|r,s) = \frac{1}{\Delta\mu_r} \int\limits_{\Delta\mu_r} d\mu \ r(a,x;\mu) = \frac{1}{\Delta\mu_r} \int\limits_{\Delta\theta_r} r(a,x;\theta) \sin\theta d\theta \ . \tag{9.14}$$

The integral over θ in (9.14) can be numerically evaluated using (9.11) in the integrand. The values of $r(a,x;r,s|r,s)$ obtained from (9.14) then give a direct check on the values obtained from ray-tracing with zero wind speed. A similar check can be made for the specular $r(x,a;r,s|r,s)$ values. Checks on the transmittance functions for the specular case are not as simple, because incident rays in one quad Q_{rs} can be transmitted into two or more quads Q_{uv}, as a result of refraction changing the direction of the incident and final rays.

Comparison of the results from (9.7a) and (9.14) also gives a lower bound on the number of rays which need to be traced in order to achieve an accurate estimate of $r(a,x;r,s|u,v)$.

10. THE REFLECTANCE OF THE LOWER BOUNDARY ABOVE AN INFINITELY DEEP, HOMOGENEOUS LAYER

In the assumptions governing the Natural Hydrosol Model (§1a) we have allowed for two possible types of lower boundary of the hydrosol: either the physical bottom of an optically shallow water body, or a plane below which the water body is homogeneous and infinitely deep. The physical bottom, in the form of a matte reflecting surface for example, is considered in (5.53). In this section we consider the remaining case: we shall specify the construction of the matrix $\underline{\hat{r}}_p(z,b;\ell)$ in (5.52) for the case where X[z,b] is an infinitely deep homogeneous medium, so that $b = \infty$. The detailed presentation of the requisite theory, called the eigenmatrix method, leading to $\underline{\hat{r}}_p(z,\infty;\ell)$ would be out of place in the present study, since the eigenmatrix method forms an alternate and independent approach to the problem of computing the light fields in natural hydrosols. However, there is one result of the theory which we find convenient to adopt in the present NHM, namely the form of $\underline{\hat{r}}_p(z,\infty;\ell)$ given by the eigenmatrix method. We shall present only the minimum directions needed to implement the construction of $\underline{\hat{r}}_p(z,\infty;\ell)$. A detailed description of the eigenmatrix theory can be found in Preisendorfer (1988).

Consider an infinitely deep hydrosol $X[z,\infty]$ whose local reflectance matrix $\underline{\hat{\rho}}(y;\ell)$ and local transmittance matrix $\underline{\hat{t}}(y;\ell)$, as defined in §5, are independent of depth y in $X[z,\infty]$. There are two cases to consider:

(i) The case of $\ell = 0$. $\underline{\hat{t}}(y;0)$ and $\underline{\hat{\rho}}(y;0)$ are given by (5.21). These matrices are m×m.

(ii) The case of $\ell = 1,\ldots,n$. $\underline{\hat{t}}(y;\ell)$ and $\underline{\hat{\rho}}(y;\ell)$ are given by (5.24). These matrices are $(m-1)\times(m-1)$.

These two distinct cases are necessary in the present context because we must form an invertible matrix, namely $\underline{E}^+$, below, in order to define $\hat{r}_p(z,\infty;\ell)$. Recall that we "padded" $\underline{\hat{\rho}}(y;\ell)$ and $\underline{\hat{t}}(y;\ell)$ in (5.29) to achieve a unified set

of formulas. This unification is satisfactory everywhere in this work except here, since the padding produces a singular $\underline{E}^+$ matrix. We must momentarily use the stripped-down matrices of (5.21) and (5.24) to find $\underline{E}^+(\ell)$ in (10.7).

Begin by defining the system matrix $\underline{K}(\ell)$ for each case:

$\underline{K}(0)$ is $2m\times 2m$ case (i)

$\underline{K}(\ell)$ is $2(m-1)\times 2(m-1)$ case (ii)

where (cf. (6.8)) in general, for the appropriate case at hand:

$$\underline{K}(\ell) = \begin{bmatrix} -\underline{\hat{\tau}}(\ell) & \underline{\hat{\rho}}(\ell) \\ -\underline{\hat{\rho}}(\ell) & \underline{\hat{\tau}}(\ell) \end{bmatrix} \quad , \quad \ell = 0,\ldots,n \tag{10.1}$$

Observe that we have dropped reference to depth y, as $\underline{K}(\ell)$ is now independent of depth.

Next, form and numerically solve the eigenvector problem

$$\underline{K}(\ell)\ \underline{E}(\ell) = \underline{E}(\ell)\ \underline{k}(\ell) \quad , \quad \ell = 0,\ldots,n \tag{10.2}$$

Here $\underline{E}(\ell)$ is a $2q\times 2q$ eigenmatrix, while the eigenvalues are in $\underline{k}(\ell) = \text{diag}[\underline{k}^+(\ell),\underline{k}^-(\ell)]$ and where, in turn, $\underline{k}^{\pm}(\ell) = \text{diag}[k_1^{\pm}(\ell),\ldots,k_q]$. Here $q = m$ or $(m-1)$, as the case may be.

It can be shown that $\underline{E}(\ell)$ may be written in block matrix form

$$\underline{E}(\ell) = \begin{bmatrix} \underline{E}^+(\ell) & \underline{E}^-(\ell) \\ \underline{E}^-(\ell) & \underline{E}^+(\ell) \end{bmatrix} \tag{10.3}$$

where $\underline{E}^{\pm}(\ell)$ are $q\times q$ matrices defined as follows. Thus, suppose the eigenvector subroutine returns $\underline{E}(\ell)$ in the form of a set of $2q\times 1$ eigenvectors $\underline{e}_j(\ell)$, where

$$\underline{E}(\ell) \equiv [\underline{e}_1(\ell) \cdots \underline{e}_q(\ell)\ \underline{e}_{q+1}(\ell) \cdots \underline{e}_{2q}(\ell)] \qquad (2q\times 2q) \tag{10.4}$$

and where (with "T" denoting matrix transpose) we have, for each $j = 1,\ldots,2q$:

$$\underline{e}_j(\ell) \equiv [e_j(1;\ell),\ldots,e_j(q;\ell),\ e_j(q+1;\ell),\ldots,e_j(2q;\ell)]^T. \tag{10.5}$$

Partition $\underline{e}_j(\ell)$ into two subvectors

$$\begin{aligned} \underline{e}_j^+(\ell) &\equiv [e_j(1;\ell),\ldots,e_j(q;\ell)]^T \\ \underline{e}_j^-(\ell) &\equiv [e_j(q+1;\ell),\ldots,e_j(2q;\ell)]^T. \end{aligned} \qquad , \ j = 1,\ldots,2q \tag{10.6}$$

Then the $\underline{E}^{\pm}(\ell)$ in (10.3) are defined as

$$\underline{E}^{\pm}(\ell) \equiv [\underline{e}_1^{\pm}(\ell) \cdots \underline{e}_q^{\pm}(\ell)] \qquad (q\times q) \tag{10.7}$$

The required reflectance $\hat{\underline{r}}_p(z,\infty;\ell)$ is then given by the following two cases:

case (i): For $\ell = 0$,

$$\hat{\underline{r}}_1(z,\infty;0) = -\underline{E}^-(0)[\underline{E}^+(0)]^{-1} \qquad m\times m \tag{10.8}$$

and

$$\hat{\underline{r}}_2(z,\infty;0) \equiv \underline{0} \ \text{ by (5.51).}$$

case (ii): For $\ell = 1,\ldots,n$

$$\left.\begin{aligned} &\hat{\underline{r}}_1(z,\infty;\ell) = -\underline{E}^-(\ell)[\underline{E}^+(\ell)]^{-1} \qquad (m-1)\times(m-1) \\ &\text{and} \\ &\hat{\underline{r}}_2(z,\infty;\ell) = \hat{\underline{r}}_1(z,\infty;\ell) \text{ for } \ell = 1,\ldots,n-1 \\ &\hat{r}_2(z,\infty;n) \equiv \underline{0} \ \text{ for } \ \ell = n. \end{aligned}\right\} \tag{10.9}$$

Therefore when we are integrating the Riccati equations ℓ-mode by ℓ-mode, as described in §7b, if we desire to have an optically infinitely deep homogeneous medium below the lower boundary, we must set up and solve the eigenvalue problem (10.2) for each ℓ-mode, in order to obtain the required $\underline{\hat{r}}_p(z,\infty;\ell)$ from (10.8) or (10.9). These $\underline{\hat{r}}_p(z,\infty;\ell)$ are then used as the initial conditions for the upward integration sweep of (6.48), as described in §7.b.4. At this point just prior to the sweep it is permissible to fill out the $\underline{\hat{r}}_p(z,b;\ell)$ matrices in (10.9), to become once again m×m, by adding zeros to make their m^{th} rows and m^{th} columns.

We note that, just as for the matte bottom (recall (5.50), (5.51) and (5.53)), we have $\underline{\hat{r}}_1(z,\infty;\ell) = \underline{\hat{r}}_2(z,\infty;\ell)$, $\ell = 1,\ldots,n-1$. (This equality does not hold when $\ell = 0$ or $\ell = n$ since we have defined $\underline{\hat{r}}_2(z,\infty;\ell)$ to be zero in these cases, consistent with our notationally convenient definition of $\underline{A}_2^{\pm}(y;\ell) \equiv 0$ for $\ell = 0$ and $\ell = n$.) However, unlike the matte bottom case, $\underline{\hat{r}}_1(z,\infty;\ell)$ is nontrivial for $\ell > 0$; therefore $\underline{R}_1(y_j,\infty;\ell)$ must be obtained for all $\ell = 0,\ldots,n$ by integration of (6.48) with $\underline{\hat{r}}_1(z,\infty;\ell)$ as the initial condition. (Recall the discussion in §7b4.) But since both $\underline{\hat{r}}_p(z,\infty;\ell)$, $\ell = 1,\ldots,n-1$ and equation (6.48) are independent of p = 1 or 2, it is necessary to actually integrate (6.48) only for the case of p = 1; the needed $\underline{R}_2(y_j,\infty;\ell)$ values follow from $\underline{R}_2(y_j,\infty;\ell) = \underline{R}_1(y_j,\infty;\ell)$, $\ell = 1,\ldots,n-1$.

11. COMPUTATION OF THE QUAD-AVERAGED PHASE FUNCTION

Given the continuous, geometric phase function $p(y;\mu',\phi';\mu,\phi)$, the quad-averaged phase function $p(y;r,s|u,v)$ can be computed by a numerical integration of the defining equation (3.11):

$$p(y;r,s|u,v) \equiv \frac{1}{\Omega_{uv}} \int_{Q_{uv}} \int d\mu d\phi \int_{Q_{rs}} \int d\mu' d\phi' \; p(y;\mu',\phi';\mu,\phi) \; . \tag{11.1}$$

The continuous function $p(y;\mu',\phi';\mu,\phi) \equiv p(y;\psi)$ (cf. (2.5)) for a fixed depth y may be available as an analytic function of ψ derived from scattering theory, or it may be obtained from measurements at a discrete set of ψ values, for example by a spline fit to the measured values. Since $p(y;\psi)$ for natural waters is an extremely peaked function of ψ near $\psi = 0$, great care must be taken in the evaluation of (11.1).

From the discussion of the symmetry of the phase function in §3d, we know that $p(y;\mu',\phi';\mu,\phi)$ depends not on ϕ' and ϕ separately, but only on $\phi'-\phi$ through $\cos(\phi'-\phi)$, and that $p(y;r,s|u,v)$ therefore depends on $|s-v|$. Thus it is not necessary to integrate (11.1) for all possible pairs of quads Q_{rs} and Q_{uv} in order to obtain all the possible values of $p(y;r,s|u,v)$. It is sufficient to fix Q_{rs} at Q_{r1} and then to evaluate (11.1) over the hemispheres containing Q_{uv} defined and for the range $v = 1,2,\ldots,n+1$. This is the discrete counterpart to setting $\phi' = 0$ and allowing ϕ to range over 0 to π in order to generate all possible values of $\cos(\phi'-\phi)$. Equation (11.1) thus can be written

$$p(y;r,1|u,v) = \frac{1}{\Omega_{uv}} \int_{\Delta\mu_u} d\mu \int_{\Delta\phi_v} d\phi \int_{\Delta\mu_r} d\mu' \int_{\Delta\phi_1} d\phi' \; p(y;\mu',\phi';\mu,\phi) \; . \tag{11.2}$$

In order to evaluate (11.2), each quad Q_{uv} is subdivided into a grid of n_μ by n_ϕ subquads of size $\delta\mu_u \equiv \Delta\mu_u/n_\mu$ by $\delta\phi_v \equiv \Delta\phi/n_\phi$. If Q_{uv} is a polar cap, $u = m$, then $\delta\phi_v \equiv 2\pi/n_\phi$, so that the entire cap is subdivided into sectors. Corresponding subdivisions are made for Q_{rs}. We then evaluate (11.2) as a summation over these subquads:

$$p(y;r,1|u,v) = \frac{1}{\Omega_{uv}} \sum_{i=1}^{n_\mu} \delta\mu_i \sum_{j=1}^{n_\phi} \delta\phi_j \sum_{k=1}^{n_\mu} \delta\mu'_k \sum_{\ell=1}^{n_\phi} \delta\phi'_\ell \; p(y;\mu'_k,\phi'_\ell;\mu_i,\phi_j) \; . \quad (11.3)$$

Here (μ_i,ϕ_j) is at the center of the (i,j) subquad of Q_{uv}, and (μ'_k,ϕ'_ℓ) is at the center of the (k,ℓ) subquad of Q_{r1}. The argument of the phase function is then ψ, defined by

$$\cos\psi = \mu'_k\mu_i + (1 - \mu'^2_k)^{\frac{1}{2}} (1 - \mu_i^2)^{\frac{1}{2}} \cos(\phi'_\ell - \phi_j) \; . \quad (11.4)$$

Note that even though we have set $s = 1$, we must still integrate ϕ' in (11.2) over the range $\Delta\phi'_1$ of the quad Q_{r1} centered at $\phi' = 0$.

The more subquads in Q_{r1} and Q_{uv}, that is the larger n_μ and n_ϕ, the more accurate is the numerical estimate of $p(y;r,1|u,v)$. Moreover, there is no requirement that all quads have the same number of subquads. Thus when Q_{r1} and Q_{uv} are the same or adjacent quads, so that the forward scattering angles (i.e. ψ near 0) are picked up in the integration, we can use more subquads in Q_{r1} and Q_{uv} in order to adequately resolve the highly peaked behavior of $p(y;\cos\psi)$ near $\cos\psi = 1$. The number of subquads needed to achieve the required accuracy in $p(y;r,1|u,v)$ also depends on the quad parameters m and n. If m and n are small, so that the quads Q_{r1} and Q_{uv} are large, then the phase function can vary significantly as the directions (μ',ϕ') and (μ,ϕ) range over the large quads. In this case we need many subdivisions in order

to pick up the variations in p. However, if m and n are large, so that Q_{rl} and Q_{uv} are small, then p varies less as (μ',ϕ') and (μ,ϕ) range over the small quads Q_{rl} and Q_{uv}. In this case we do not need as many subquads.

In the evaluation of (11.2), Q_{rl} and Q_{uv} can be in the same hemispheres, i.e., Q_{rl} in $\Xi_{\pm}$ and Q_{uv} in $\Xi_{\pm}$, or in opposite hemispheres, i.e. Q_{rl} in $\Xi_{\pm}$ and Q_{uv} in $\Xi_{\mp}$. From the symmetry relation (5.1), we see that when Q_{rl} and Q_{uv} are in the same hemisphere, Eq. (11.2) yields $p^{+}(y;r,s|u,v)$; when Q_{rl} and Q_{uv} are in opposite hemispheres we get $p^{-}(y;r,s|u,v)$.

a. Checks on the Quad-Averaged Phase Function

From (2.7) we know that the phase function must satisfy

$$\int_{-1}^{1}\int_{0}^{2\pi} p(y;\mu',\phi';\mu,\phi)\, d\mu d\phi = 1$$

for any depth y and direction (μ',ϕ') in Ξ. This equation is discretized in the usual manner by using (3.20) to write the continuous phase function $p(y;\mu',\phi';\mu,\phi)$ as a linear combination of discrete phase functions; the result is

$$\frac{1}{\Omega_{rs}}\sum_{u}\sum_{v} p(y;r,s|u,v)\,\Omega_{uv}$$

$$= \frac{1}{\Omega_{rs}}\sum_{u}\sum_{v} p^{+}(y;r,s|u,v)\Omega_{uv} + \frac{1}{\Omega_{rs}}\sum_{u}\sum_{v} p^{-}(y,r,s|u,v)\Omega_{uv} = 1 \qquad (11.5)$$

for all depths y and quads Q_{rs}. In the first form of (11.5) the sum is over all Q_{uv} in Ξ. The hemispherical summation ranges of the (u,v) in the expanded form of (11.5) are fixed once Q_{rs} is fixed (recall (3.2) and (5.1)). For example, if Q_{rs} is in Ξ_{+}, then in $\sum_{u}\sum_{v} p^{+}$, (u,v) is summed over Ξ_{+} while

in $\sum_u \sum_v p^-$, (u,v) is summed over Ξ_-. This equation can give a check on how accurately we have performed the integrations of (11.2). Conversely (11.5) can be used to define $p^+(y;r,s|r,s)$ in highly forward scattering media, after all other terms have been computed,* as will be discussed in paragraph b, below.

As an illustration of these results, consider the case of spherically symmetric scattering, for which

$$p(y;\mu',\phi';\mu,\phi) = \frac{1}{4\pi} , \tag{11.6}$$

for all (μ',ϕ'), (μ,ϕ) in Ξ. With (11.6) in (11.1) we get just

$$p^{\pm}(y;r,s|u,v) = \frac{\Omega_{rs}}{4\pi} ,$$

for all quads Q_{rs} and Q_{uv}. The check (11.5) then gives

$$\frac{1}{\Omega_{rs}} \cdot \frac{\Omega_{rs}}{4\pi} \cdot 2 \cdot \sum_u \sum_v \Omega_{uv} = 1 ,$$

as required.

b. Special Computation of the Forward Scatter Phase Function $p^+(y;r,s|r,s)$

Equation (11.5) can play a role even more important than that of checking the numerical accuracy of (11.3). In particular, (11.5) can be used to compute the quad-averaged phase function for forward scattering, thus eliminating the need for knowledge of $p(y;\psi)$ at $\psi = 0$ and reducing the

* In this way we can cut the Gordian knot of the forward scattering problem in phenomenological approaches to radiative transfer. See Preisendorfer (1965, p. 55).

numerical difficulties which arise from the extremely peaked nature of $p(y;\psi)$ for very small ψ values.

To justify the following reformulation, we note the following rules of thumb, which are based on extensive testing of the model with realistic phase functions. For partitions of the unit sphere such as those illustrated in Fig. 4, quad sub-divisions given by $n_\mu = n_\phi = 4$ give accurate results for quads which are not adjacent or identical (i.e., for those quads for which $\psi \geq 10°$), in the sense that further increasing n_μ or n_ϕ does not significantly change the computed values of $p^{\pm}(y;r,l|u,v)$. If adjacent quads are subdivided with ten times the resolution used for non-adjacent quads, i.e. with $n_\mu = n_\phi = 40$, then the associated values of $p^{\pm}(y;r,l|u,v)$ are also accurate, and the balance (11.5) holds to within a few percent. If a balance of (11.5) is required to within, say, 1 part in 1000, then it is necessary to make extremely fine subdivisions of the forward scattering quads whenever Q_{rl} and Q_{uv} coincide. The computations for the forward scattering quads alone thus take much more computer time than the computations for all other quads combined.

Since the forward scattering values $p^+(y;r,l|r,l)$ are clearly the last values to achieve numerical accuracy, it is reasonable to compute all other values $p^{\pm}(y;r,l|u,v)$ via (11.3) and then to use (11.5) to obtain $p^+(y;r,l|r,l)$:

$$p^+(y;r,l|r,l) = 1 - \frac{1}{\Omega_{rl}} \sum_u \sum_v p^+(y;r,l|u,v) \qquad (u,v)\neq(r,l)$$
$$- \frac{1}{\Omega_{rl}} \sum_u \sum_v p^-(y;r,l|u,v) \; . \qquad (11.7)$$

Note that when (11.7) is employed to obtain the forward scatter values, the subquad directions (μ_i,ϕ_j) and (μ'_k,ϕ'_ℓ) of (11.3) and (11.4) never coincide, and therefore we never require a value of $p(y;\psi)$ for $\psi = 0$. Indeed, there is always some angle ψ_0, determined by the quad partitioning and the quad subdivisions, such that $p(y;\psi)$ is not required for $0 \le \psi < \psi_0$. For quad partitions as in Fig. 4 and for $n_\mu = n_\phi = 40$ subdivisions for adjacent quads, $\psi_0 \approx 0.02°$. The smallest angles ψ for which phase functions have been empirically measured are about 0.1°. Analytic extrapolation can be used to extend $p(y;\psi)$ to the required ψ_0 value.

The discrete resolution of the Natural Hydrosol Model effectively frees the numerical model of any uncertainty owing to the unknown behavior of $p(y;\psi)$ for $0 \le \psi \le \psi_0$, provided that an independent estimate of the total scattering s is available.* If s must be obtained by numerical integration of the defining equation (2.6), then knowledge of $\sigma(y;\psi)$ is also required for $0 \le \psi < \psi_0$, even though this information is not needed for the discretization of the phase function. It can only be hoped that as computers become larger, thus permitting smaller quads and hence making ψ_0 smaller, that theory or experiment will also extend our knowledge of $\sigma(y;\psi)$ to the required smaller ψ_0 values.

---

* For example, the volume attenuation function $\alpha(y)$ is measureable with a beam transmissometer. The volume absorption function $a(y)$ can be determined from irradiance measurements via the divergence relation (8.9) rewritten as $a(y) = \alpha[h_+(y) + h_-(y)]^{-1} \frac{d}{dy}[H_+(y)-H_-(y)]$. The volume total scattering function $s(y)$ is then obtained from $s(y) = \alpha(y) - a(y)$. Here we are assuming that the beam transmissometer has been carefully constructed so as to correctly account for the forward scattering of photons. If this is not the case, then the quantity s is just as elusive as $p(y;0)$. See H.O. Vol. VI, sec. 13.5.

12. COMPUTER CONSIDERATIONS

The original code for the Natural Hydrosol Model was written (beginning in 1980) for a CDC 6600 computer. Storage on this machine was quite limited, and every effort was made to minimize the use of in-core memory, often at the expense of performing extra calculations. The most recent rewrite of the code (in 1986) was made so that it would run on a CDC 205 vector computer with virtual memory. Since available storage is essentially unlimited on a virtual memory machine, the special array packing and indexing routines used in the original code are no longer necessary. However, these features of the original code have been retained in the current version, in order to minimize the rewriting and debugging effort. Almost no effort has been made to rewrite the code so that it can take advantage of the vector processing on a pipeline computer; it remains essentially a scalar code. This section briefly describes the structure of the code, and documents the array storage and indexing techniques.

a. Computational Flow Structure

The various computations described in §7 to §11 are grouped into five separate programs, which are run in sequence to obtain the solution of a given problem. The first three programs compute the surface boundary reflectance and transmittance functions. The fourth program solves for the radiance amplitudes at all depths, and the fifth program then reconstitutes the radiances and analyzes the results. The specific tasks of these programs are charted in Fig. 10 and are described as follows.

Program I. This program does the ray-tracing described in §9a and charted in Fig. 9. To initialize the program we first select the quad resolution

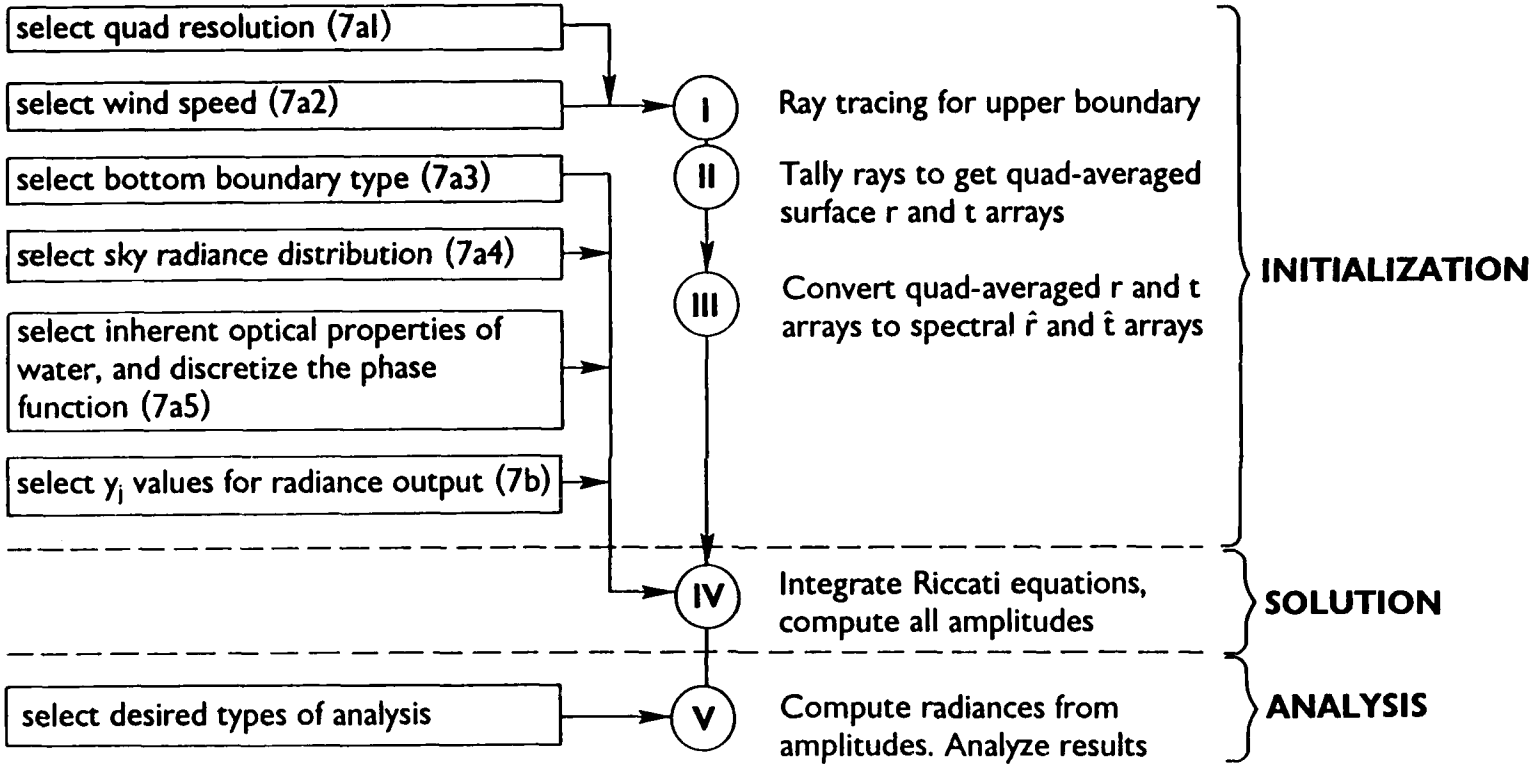

Figure 10.--Flow chart of the entire Natural Hydrosol Model solution procedure.

parameters m and n and a scheme for partitioning the unit sphere into the chosen number of quads, as described in §7a.1. We then select the desired wind speed at the water surface and the initial number of surface realizations to be made. The program then repeatedly generates a random surface realization, randomly selects a direction in Q_{rs}, and sends a parent ray toward Q_{rs} and the realized surface. All the reflected and refracted daughter rays are traced to completion, and the quads receiving the final daughter rays are determined. One parent ray is sent toward each quad Q_{rs} in the first quadrant (of the wind-based system shown in Fig. 1) for each surface realization, until the desired number of surface realizations has been made. For each (parent ray)-(daughter ray) pair, the program records the values of r,s,u,v, and the radiant flux of the daughter ray. These ray-tracing computations form a significant part of the entire work count of the NHM.

Program II. This program tallies the ray information from program I and computes the four quad-averaged reflectance and transmittance arrays using (9.1a-d) and (9.7a-d). The individual elements of the $f(r,s|u,v)$ arrays will approach their final values at differing rates as more and more rays are tabulated. For a given input quad Q_{rs}, the output quads Q_{uv} which are near the specular (still water) reflection or refraction directions of the parent rays in Q_{rs} will receive far more reflected or transmitted daughter rays than those quads which are in directions far from the specular directions. Thus after only a few hundred surface realizations, some elements of $f(r,s|u,v)$ may have achieved their final values with great accuracy, whereas other elements may not have had a single ray path connect the particular Q_{rs} and Q_{uv} quads. However, those elements which are largest in magnitude dominate the behavior of the light field in the sea, so it is not necessary to know all matrix

AD-A197 207 A NUMERICAL MODEL FOR THE COMPUTATION OF RADIANCE DISTRIBUTIONS IN NATURA..(U) WASHINGTON UNIV SEATTLE JOINT INST FOR STUDY OF ATMOSPHERE AN.. 3/3

UNCLASSIFIED C D MOBLEY ET AL. JAN 88 CONTRIB-40 F/G 8/8 NL

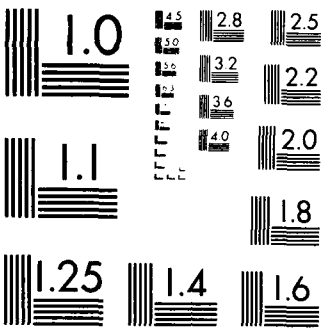

MICROCOPY RESOLUTION TEST CHART
NATIONAL BUREAU OF STANDARDS 1963 A

elements to the same degree of accuracy. The user of the NHM is thus faced with making a qualitative decision regarding the desired accuracy of the elements of the r and t arrays. The larger matrix elements can and must be determined with great accuracy, but the smaller matrix elements, which are many orders of magnitude smaller than the larger elements, cannot be accurately estimated unless a relatively large number of rays is traced.

Programs I and II can be run repeatedly to generate new batches of rays and to incorporate these new rays into a running, accumulating calculation of the r and t arrays. When the larger matrix elements have reached their final values, the r and t matrices can be deemed sufficiently accurate for the problem at hand, and the solution in the body of the hydrosol can proceed. How many rays need to be traced in order to reach this point depends on wind speed and quad partitioning and must, therefore, be determined by the researcher on a case-by-case basis.

Program III. This program computes the four spectral reflectance and transmittance arrays for the upper boundary, using (5.31c), (5.32), (5.34), (5.36) and the quad-averaged arrays from program II. At this point the air-water surface boundary conditions are known, and we can proceed with the solution for amplitudes.

Program IV. This program performs the remaining initialization steps of (7a.3)-(7a.5) and then assembles the solution amplitudes as described in §7b. The internal structure of Program IV is essentially that shown in Fig. 7. This program is the other main consumer of computer power in the NHM, owing to the discretization of the phase function.

Program V. This program first synthesizes the radiances from the amplitudes found in program IV. Then the results are analyzed and derived quantities are computed, as detailed in §8. Multiple runs of program V can be made for a given set of output from program IV. For example, one run can be made to check the balance of the radiative transfer equation, another run to compute the irradiances and other derived quantities, and then a run to generate graphical output, etc.

We note again, as discussed in §7a, that the expensive computations for the quad-averaged upper boundary r and t arrays need be done only once for a given wind speed and quad resolution. Likewise, the expensive discretization of the phase function is a one-time computation for a given phase function. The actual solution of the radiative transfer equation in programs IV and V is relatively inexpensive. Therefore, holding the wind speed and phase function fixed, it is possible to make many runs of programs IV and V in order to study the effects of varying the incident radiance distribution, the scattering-to-absorbtion ratio $s/a = \omega/(1-\omega)$, the bottom boundary type, etc.

b. Array Storage

In the NHM there are several occurrences of large sparse or symmetric matrices. Consider, for example, the quad-averaged upper boundary reflectance and transmittance arrays $s(r,s|u,v)$. These four-index arrays are stored (for reasons of FORTRAN limitations at the time the code was originally written) as two-dimensional arrays according to the layout of Table 3. As seen in Table 3, each row of the $m(2n) \times m(2n)$ array references a particular input quad Q_{rs}, and each column references a particular output quad Q_{uv}. The symmetries of these arrays as shown in (3.24) give the arrays the block structure

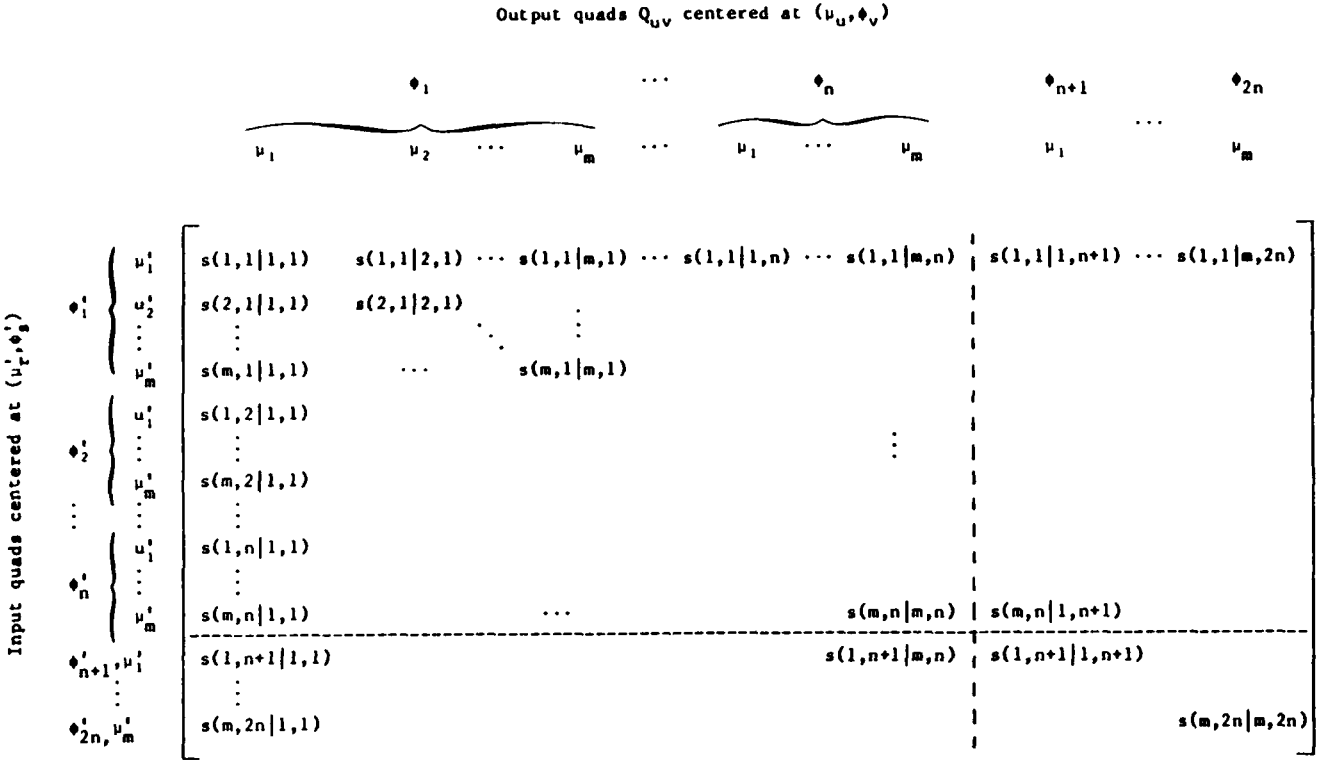

Table 3.--Array storage locations for the quad-averaged upper boundary reflectance and transmittance arrays $s(r,s|u,v)$.

$$\underline{s} = \left[\begin{array}{c|c} A & B \\ \hline B & A \end{array}\right],$$

where A and B are mn × mn blocks. (Note, for example, in Table 3 that $s(1,n+1|1,n+1) = s(1,1|1,1)$ by (3.24c) and $s(1,1|1,n+1) = s(1,n+1|1,1)$ by (3.24b).) Thus it is necessary to store only one-half of $\underline{s}$, say the "top-half" [A B]. When an array element in the "bottom-half" [B A] of $\underline{s}$ is needed, simple indexing calculations can be used to obtain the corresponding element from the stored top-half.

We note that the ray tracing of program I fills all m(2n) *columns* comprising the elements of *rows* $1,2,\ldots,m(\frac{n}{2}+1)$ of Table 3 as Q_{rs} sweeps over the first quadrant of Ξ (as defined by the wind-based coordinate system of Fig. 1), and all Q_{uv} throughout Ξ receive reflected and transmitted daughter rays. The remaining rows $m(\frac{n}{2}+1)+1,\ldots,mn$ of the "top-half" of $\underline{s}$ are then defined by symmetry.

We also note that since the polar caps have no azimuthal dependence, a parent light ray going toward anywhere in the polar cap $Q_{rs} \equiv Q_m$ and a daughter ray going to the non-polar quad Q_{uv} can be assigned the storage location $s(m,1|u,v)$. Locations $s(m,2|u,v),\ldots,s(m,n|u,v)$ then remain unused. Likewise, a parent ray going toward a non-polar quad Q_{rs} and a daughter ray going to the polar cap $Q_{uv} \equiv Q_m$ can be assigned to $s(r,s|m,1)$; then $s(r,s|m,2),\ldots,s(r,s|m,n)$ are unused. All light rays connecting one polar cap to the other are assigned to location $s(m,1|m,1)$. With the exception of this special storage for elements involving polar caps, the four-index matrix element $s(r,s|u,v)$ is stored at location (I,J) of the two-dimensional array $\underline{s}$ of Table 3, where

$$I = r + m(s-1)$$
$$J = u + m(v-1) \ . \tag{12.1}$$

I and J follow FORTRAN conventions with I labeling the rows from top to bottom in Table 3 and with J labeling the columns from left to right. Since only the top half of the full array is stored, the (I,J) location given by (12.1) may need modification:

$$\begin{aligned} &\text{if } I \le mn, \text{ element } (I,J) \text{ is stored at location } (I,J) \\ &\text{if } I > mn \text{ and } J \le mn, \text{ element } (I,J) \text{ is stored at } (I - mn,\ J + mn) \\ &\text{if } I > mn \text{ and } J > mn, \text{ element } (I,J) \text{ is stored at } (I - mn,\ J - mn). \end{aligned} \tag{12.2}$$

The values of (r,s,u,v) corresponding to location (I,J) are given by

$$\begin{aligned} r &= I_{\text{mod } m} \ , \text{ with } r \equiv m \text{ when } I_{\text{mod } m} = 0 \\ s &= 1 + \left[\frac{I-1}{m}\right] \ , \\ u &= J_{\text{mod } m} \ , \text{ with } u \equiv m \text{ when } J_{\text{mod } m} = 0 \\ v &= 1 + \left[\frac{J-1}{m}\right] \ . \end{aligned} \tag{12.3}$$

Here [x] is defined as the largest integer less than or equal to x.

The associated spectral upper boundary reflectance and transmittance functions $\hat{s}_p(r,k|u,\ell)$ have a matrix structure like that shown in (5.41) and (5.43) and in Tables 1 and 2. There is no need to store the m×m blocks of zeros, which occur when $\underline{\hat{s}}_p(k|\ell)$ has $(k + \ell)$ odd. Thus a factor of two in storage can be saved by reducing the full $m(n+1) \times m(n+1)$ array $\hat{s}_p$ to

$$\underline{\hat{s}}_p = \begin{bmatrix} \underline{\hat{s}}_p(0|0) & \underline{\hat{s}}_p(0|2) & \underline{\hat{s}}_p(0|4) & \cdots & \underline{\hat{s}}_p(0|n) \\ \underline{\hat{s}}_p(1|1) & \underline{\hat{s}}_p(1|3) & \underline{\hat{s}}_p(1|5) & \cdots & \underline{\hat{s}}_p(1|n) \\ \underline{\hat{s}}_p(2|0) & \underline{\hat{s}}_p(2|2) & \cdots & & \underline{\hat{s}}_p(2|n) \\ \vdots & \vdots & & & \vdots \\ \underline{\hat{s}}_p(n|0) & \underline{\hat{s}}_p(n|2) & \cdots & & \underline{\hat{s}}_p(n|n) \end{bmatrix} . \qquad (12.4)$$

The exact form of the n^{th} row and n^{th} column is determined by our choice of n even.

Special matrix manipulation routines are easily written to handle the matrix operations, such as those of eqs. (6.55) or (7.3), which involve these compressed arrays. The four-index matrix element $\hat{s}_p(r,k|u,\ell)$ is stored at location (I,J) of the two-dimensional matrix of (12.4), where

$$\begin{aligned} I &= mk + r \\ J &= m\ell + u - m\left\{\frac{k+\ell}{2} - \left[\frac{k}{2}\right]\right\}, \end{aligned} \qquad (12.5)$$

with [x] as the largest integer less than or equal to x. Conversely we can retrieve (r,k,u,ℓ) from (I,J) via

$$\begin{aligned} r &= I_{\bmod m} \\ k &= \left[\frac{I}{M}\right] \\ u &= J+m\left[\frac{J}{M}\right] \bmod m \\ \ell &= \left[\frac{J+m\left[\frac{J}{M}\right]}{m}\right] . \end{aligned} \qquad (12.6)$$

As previously discussed (§3d), the symmetries of the phase functions $p^{\pm}(y;r,s|u,v)$ make possible a considerable savings in computer storage. Recall that in evaluating (11.3) we set $s = 1$ (with $\phi_1' \equiv 0$), so that as v ranged from 1 to n, $|\phi_s-\phi_v| = |\phi_1-\phi_v|$ ranged from 0 to π. Moreover, for any arbitrary pair of angles ϕ_s and ϕ_v, with $s = 1,\ldots,2n$ and $v = 1,\ldots,2n$ so that $0 \le \phi_s, \phi_v \le 2\pi$, the included angle $|\phi_s-\phi_v|$ between ϕ_s and ϕ_v lies in the range $0 \le |\phi_s-\phi_v| \le \pi$. Therefore the general isotropic phase functions $p^{\pm}(y;r,s|u,v)$ can be obtained from the computed arrays. The arrays $p^{\pm}(y;r,s|u,v)$ are stored as three-dimensional arrays indexed by (I,J,K) where

$$I = r$$

$$J = \begin{cases} u & \text{if } r = m \\ u+m|s-v| & \text{if } |s-v| \le n \text{ and } u \ne m \\ u+m(n-|s-v|_{\text{mod}n}) & \text{if } |s-v| > n \text{ and } u \ne m \\ m & \text{if } u = m \end{cases} \tag{12.7}$$

K = the depth index, with $y_1, y_2, \ldots, y_i, \ldots, y_{YOP}$ as in Fig. 6.

Since J runs from 1 to m(n+1) as s and v run from 1 to 2n, the isotropic phase functions can be stored in arrays of size $m \times m(n+1) \times YOP$. This is a considerable savings as compared to the size $m(2n) \times m(2n) \times YOP$ required if the isotropy of the phase function is not explicitly used.

13. REFERENCES

References marked with a * are available from
National Technical Information Service,
U.S. Dept. of Commerce, 5285 Port Royal Road,
Springfield, VA 22161

Ambarzumian, V.A., 1943. Diffuse reflection of light by a foggy medium. *Compt. Rend. (Doklady) Acad. Sci. U.R.S.S., 38*, 229.

Austin, R.W., 1980. Gulf of Mexico, ocean-color surface-truth measurements. *Boundary-Layer Meteorol., 18*, 269-285.

Chandrasekhar, S., 1950. *Radiative Transfer*. Oxford.

Coddington, E.A., and N. Levinson, 1955. *Theory of Ordinary Differential Equations*. McGraw-Hill, New York.

H.O. See Preisendorfer, R.W., 1976.

Jeans, J.H., 1917. The equations of radiative transfer of energy. *Mon. Not. Roy. Astron. Soc., 78*, 28.

Preisendorfer, R.W., 1958. Invariant imbedding relation for the principles of invariance. *Proc. Natl. Acad. Sci., 44*, 320.

Preisendorfer, R.W., 1961. Generalized invariant imbedding relation. *Proc. Natl. Acad. Sci., 47*, 591.

Preisendorfer, R.W., 1965. *Radiative Transfer on Discrete Spaces*. Pergamon Press, New York.

*Preisendorfer, R.W., 1973. *Classic Canal Theory*. Hawaii Institute of Geophysics HIG-73-14 (NOAA-JTRE-83). (NTIS # COM-74-10875/4).

*Preisendorfer, R.W., 1975. Multimode long surface waves in two-part basins. Hawaii Institute of Geophysics HIG-75-4 (NOAA-JTRE-125) (NTIS # COM-75-10903/3).

*Preisendorfer, R.W., 1976. *Hydrologic Optics*. Pacific Marine Environmental Laboratory, ERL/NOAA, Honolulu, HI [A six volume set: Vol. I, Introduction, NTIS # PB-259793/8ST; Vol. II, Foundations, NTIS #

PB-259794/6ST; Vol. III, Solutions, NTIS # PB-259795/3ST; Vol. IV, Imbeddings, NTIS # PB-259796/1ST; Vol. V, Properties, NTIS # PB-259797/9ST; Vol. VI, Surfaces, NTIS # PB-268704/4ST.

*Preisendorfer, R.W., 1977. Transport Theory of Long Surface Waves III. Analytics. Hawaii Institute of Geophysics HIG-77-7 (NAOA-JTRE-188). (NTIS # PB85-136489).

Preisendorfer, R.W., 1988. Eigenmatrix representations of radiance distributions in layered natural waters with wind-roughened surfaces. NOAA Tech. Memo. ERL PMEL-76, 93 pp.

Preisendorfer, R.W. and C.D. Mobley, 1984. Direct and inverse irradiance models in hydrologic optics. *Limnol. Oceanogr., 29*, 903-929.

*Preisendorfer, R.W., and C.D. Mobley, 1985. Unpolarized Irradiance Reflectances and Glitter Patterns of Random Capillary Waves on Lakes and Seas, by Monte Carlo Simulation. NOAA Tech. Memo. ERL PMEL-63. NTIS # PB86-123577.

Preisendorfer, R.W. and C.D. Mobley, 1986. Albedos and Glitter Patterns of a Wind-Roughened Sea Surface. *J. Phys. Oceanogr., 16*, 1293-1316.